

**UCSF**

**UC San Francisco Electronic Theses and Dissertations**

**Title**

Early events in the activation of rabbit lymphocytes

**Permalink**

<https://escholarship.org/uc/item/3qc7374j>

**Author**

Davis, C. Geoffrey

**Publication Date**

1982

Peer reviewed|Thesis/dissertation

EARLY EVENTS IN THE ACTIVATION  
OF RABBIT LYMPHOCYTES  
by

C. GEOFFREY DAVIS

DISSERTATION

Submitted in partial satisfaction of the requirements for the degree of

DOCTOR OF PHILOSOPHY

in

IMMUNOLOGY

in the

GRADUATE DIVISION

of the

UNIVERSITY OF CALIFORNIA

San Francisco



Date

University Librarian

DEC 31 1982

Degree Conferred: .....

1. 1. 1.

1. 1. 1.

1.

© 1983

CLAUDE GEOFFREY DAVIS

All Rights Reserved



To My Father,  
Claude G. Davis

## ACKNOWLEDGEMENTS

Without doubt, the greatest contributors to this work have been Ivan Diamond and Adrienne Gordon. In addition to providing space and funding for my research, they painstakingly directed my development in the many disciplines required of a scientist. Their wise counsel and friendship will be sorely missed.

Art Ammann and Mort Cowan set aside time each week to meet with me and discuss my progress. I am indebted to them for their advice on the immunological aspects of this study as well as for making me a part of their group in Pediatric Immunology.

Juan Korenbrot generously donated the use of the TPP electrode as well as his time and expertise. Collaborating with him was both an education and a pleasure.

I am grateful to Phil Coffino for chairing both my orals committee and my thesis committee. Also, a note of thanks to Jack Stobo for serving on both committees.

The lab personnel, all cherished friends, have each contributed to making the lab an unique and surprisingly productive working environment. The assistance of Dale Milfay, Evelyn Manies, Ed Cooper, and Gil Magilen deserve special recognition.

Lastly, in a category all her own, is my wife, Christine. Her efforts over the last few months have been nothing short of remarkable. While working at least a full-time job, and for four months a half-time job besides, she has taken over most of the responsibilities of maintaining a household. In her spare time, Christine has learned how to use the lab computer and typed this manuscript.

## ABSTRACT

Although the physiological mechanisms of lymphocyte activation have received considerable attention in recent years, the emphasis has been on relatively late events. Increases in the level of intracellular free calcium, which have been detected in lymphocytes within one minute after the addition of mitogenic lectins, constitute a notable exception. In many cell types, calcium mobilization is associated with changes in several plasma membrane properties, including phospholipid turnover, permeability, Na-K-ATPase activity, and electrical potential. The effect of Con A on each of these membrane properties was investigated in rabbit thymocytes.

The effect of Con A on both breakdown and resynthesis of phosphatidylinositol (PI) was measured. Stimulation of PI breakdown was found to be an early event, detectable by 30-60 seconds. A 10-fold increase in the rate of PI resynthesis, presumably a late response to the early breakdown, was observed after one hour. This response was specific for mitogenic lectins. PI was the only phospholipid that showed an altered metabolism in response to activation by Con A.

Membrane permeability to potassium was found to increase at about the same time as the onset of PI breakdown. This change in potassium permeability appeared to be a transient event in the activation process with a distinct maximum at two minutes. Con A was also tested for possible effects on sodium influx and Na-K-ATPase activity. Neither process was found to be stimulated in the first ten minutes of lymphocyte activation.

A lipophilic cation, tetraphenylphosphonium (TPP), was used as a probe in an effort to test the effect of Con A on thymocyte membrane potential. Con A consistently induced a transient increase in the rate of TPP uptake by thymocytes. This increase in rate had an onset of about one minute and returned to a basal level five minutes later. This effect was consistent with a change of membrane potential in the hyperpolarizing direction, as might be expected when the potassium permeability increases. However, in the course of this work, TPP was found to interfere with the activation process and to be generally unreliable as either a quantitative or qualitative probe of membrane potential. Therefore, elucidation of the role of membrane potential in thymocyte activation must await the application of more reliable probes.

## CONTENTS

ACKNOWLEDGEMENTS . . . . . ii

ABSTRACT . . . . . iv

Chapter

page

I. RATIONALE . . . . . 1

II. PHOSPHATIDYLINOSITOL METABOLISM . . . . . 4

Introduction . . . . . 4

Methods . . . . . 9

Materials . . . . . 9

Preparation of Cells . . . . . 9

Thymidine Incorporation . . . . . 10

Fluorescent Labelling . . . . . 10

Incorporation of <sup>32</sup>P-Orthophosphate . . . . . 11

Incorporation of <sup>3</sup>H-Inositol . . . . . 12

Extraction of Phospholipids . . . . . 13

Separation of Phospholipids . . . . . 13

Thin Layer Chromatography . . . . . 14

Phospholipid Phosphate Determination . . . . . 14

Results . . . . . 15

Effect of Con A on <sup>32</sup>P Incorporation in

Thymocytes . . . . . 15

Effects of Different Lectins on PI Metabolism

in Thymocytes . . . . . 18

Incorporation of <sup>32</sup>P into Sacculus Rotundus

Cells . . . . . 23

Phosphatidylinositol Breakdown in Thymocytes . 25

Phosphatidylinositol Breakdown in Sacculus

Rotundus Lymphocytes . . . . . 28

Discussion . . . . . 28

III. MONOVALENT CATIONS . . . . . 35

Introduction . . . . . 35

Methods . . . . . 38

Measurement of Sodium Influx . . . . . 38

Measurement of Potassium Influx . . . . . 39

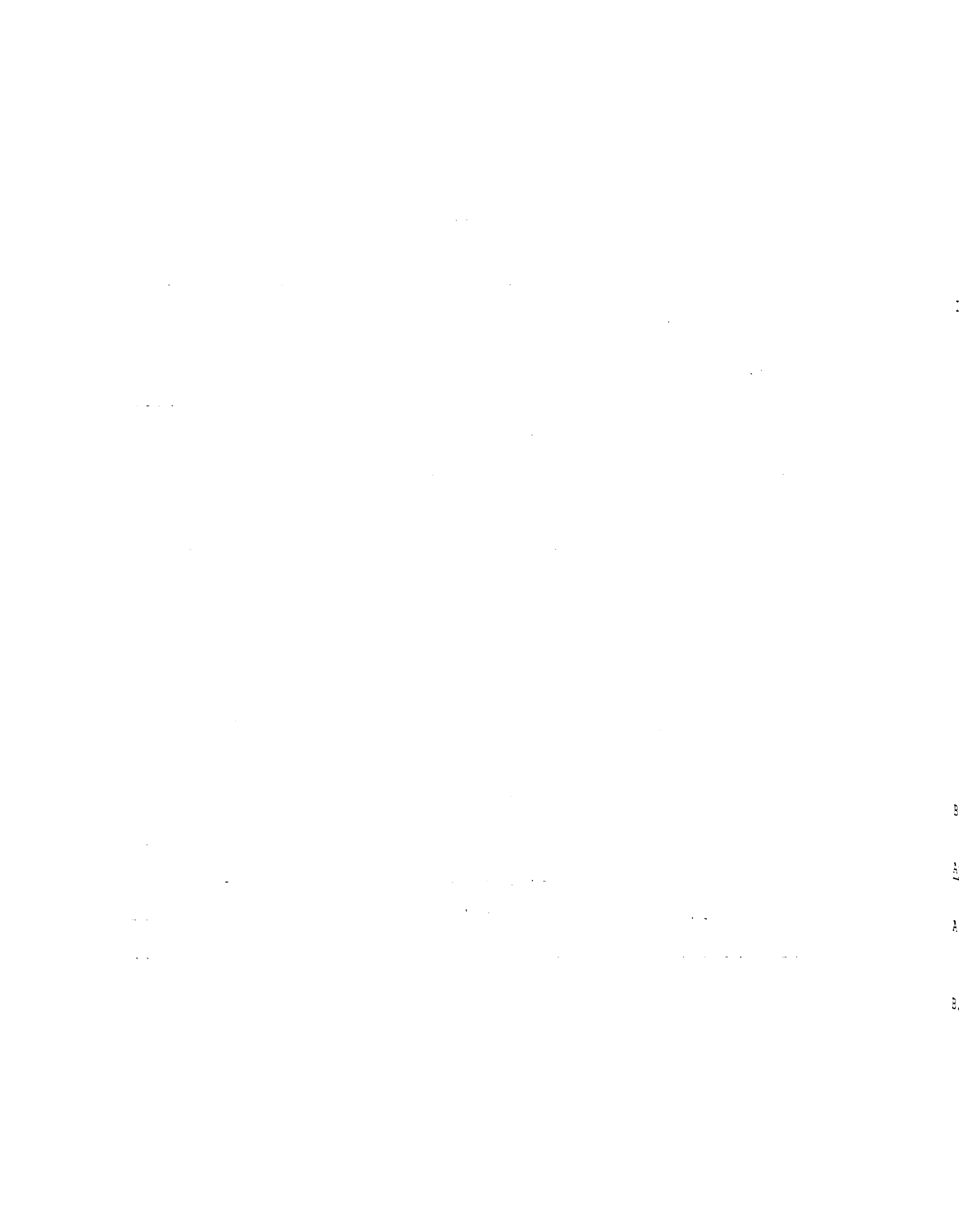
Results . . . . . 40

Effect of Activation on Potassium

Permeability . . . . . 40

Effect of Activation on Sodium Permeability . 42

Effects of Monensin on <sup>22</sup>Na and <sup>86</sup>Rb Fluxes . 43



Effects of Ion Flux Inhibitors on Thymidine	
Uptake . . . . .	46
Ouabain . . . . .	46
Amiloride . . . . .	48
Effect of Ouabain on Phosphatidylinositol	
Turnover . . . . .	51
Discussion . . . . .	51
<b>IV.    MEMBRANE POTENTIAL . . . . .</b>	<b>58</b>
Introduction . . . . .	58
Methods . . . . .	64
The TPP Electrode . . . . .	64
Assay of Radiolabelled TPP Uptake . . . . .	67
Measurement of Cell Water Volume . . . . .	67
Results . . . . .	68
Measurement of TPP Uptake with the TPP	
Electrode . . . . .	68
Effect of Con A on the Rate of TPP Uptake	69
Control Experiments . . . . .	71
Defining Optimal Conditions for Equilibrium	
TPP Uptake . . . . .	73
Effect of Temperature on TPP Uptake . . . . .	74
Effects of Tetraphenylboron . . . . .	74
TPP Uptake at Different Membrane Potentials . . . . .	76
Partitioning of TPP into Membranes	
Independent of Membrane Potential . . . . .	83
Effects of Stimulation on Steady-State TPP	
Distribution . . . . .	84
Effects of TPP on the Physiological Status of	
the Cell . . . . .	88
Discussion . . . . .	89
<b>BIBLIOGRAPHY . . . . .</b>	<b>99</b>

Appendix

	<u>page</u>
A.    ACTIVATION OF ACH RECEPTORS CAUSES THE PARTITION OF HYDROPHOBIC CATIONS INTO POST-SYNAPTIC MEMBRANE VESICLES . . . . .	108
B.    CALCULATIONS FOR TABLE 6 . . . . .	129



1. The first part of the document discusses the importance of maintaining accurate records of all transactions and activities. It emphasizes that this is crucial for ensuring transparency and accountability in the organization's operations.

2. The second part of the document outlines the various methods and tools used to collect and analyze data. It highlights the need for consistent data collection procedures and the use of advanced analytical techniques to derive meaningful insights from the data.

3. The third part of the document focuses on the role of technology in data management and analysis. It discusses how modern software solutions can streamline data collection, storage, and analysis processes, thereby improving efficiency and accuracy.

4. The fourth part of the document addresses the challenges associated with data management, such as data quality, security, and privacy. It provides strategies to mitigate these risks and ensure that the data remains reliable and secure throughout its lifecycle.

5. The fifth part of the document concludes by summarizing the key findings and recommendations. It stresses the importance of a data-driven approach in decision-making and the need for continuous monitoring and improvement of the data management process.

6. The sixth part of the document provides a detailed overview of the data management framework. It includes a description of the data sources, the data flow, and the various stages of data processing, from collection to analysis and reporting.

7. The seventh part of the document discusses the integration of data management with other organizational systems. It explains how data can be shared and used across different departments and functions to enhance collaboration and overall organizational performance.

8. The eighth part of the document focuses on the human element of data management. It discusses the importance of training and education in ensuring that staff members are equipped with the necessary skills to handle data effectively and responsibly.

9. The ninth part of the document provides a list of key performance indicators (KPIs) used to measure the success of the data management process. These KPIs include data accuracy, data completeness, data security, and data usage metrics.

10. The tenth part of the document concludes with a final summary and a call to action. It encourages the organization to embrace a data-driven culture and to continue to invest in data management capabilities to stay competitive in the market.

LIST OF TABLES

<u>Table</u>	<u>page</u>
1. Effects of Lectins on $^{32}\text{P}$ Incorporation into PI . . .	22
2. Effect of Con A and Anti-IgG on $^{32}\text{P}$ Incorporation into PI . . . . .	25
3. Effect of Con A on $^{22}\text{Na}$ Influx . . . . .	43
4. Reported Values of Lymphocyte Membrane Potentials . .	59
5. Effect of Con A on Uptake of $^3\text{H}$ -TPP . . . . .	87
6. Values for Thymocyte Membrane Potential Calculated from Different Models . . . . .	94

## LIST OF FIGURES

<u>Figure</u>	<u>page</u>
1. The PI Cycle . . . . .	5
2. Effect of Con A on $^{32}\text{P}$ Incorporation . . . . .	17
3. Effect of Con A on $^3\text{H}$ -Inositol Incorporation . . . . .	19
4. Effect of Lectins on Thymidine Uptake . . . . .	20
5. Concentration Effect of Con A and WGA on $^{32}\text{P}$ Incorporation . . . . .	23
6. Stimulation of Thymidine Uptake into SR Cells . . . . .	24
7. Con A Stimulation of PI Breakdown in Thymocytes . . . . .	27
8. Effect of Con A on $^{86}\text{Rb}$ Influx . . . . .	41
9. Effect of Monensin on $^{22}\text{Na}$ Influx . . . . .	45
10. Effect of Monensin on Na-K-ATPase Activity . . . . .	47
11. Effect of Ouabain on Thymidine Uptake . . . . .	48
12. Time Course of Ouabain Inhibition of Thymidine Uptake . . . . .	49
13. Effect of Amiloride on Thymidine Uptake . . . . .	50
14. The TPP Electrode . . . . .	65
15. Increased Rate of TPP Uptake Induced by Con A . . . . .	70
16. Cell Water Volume of Control and Con A-Stimulated Thymocytes . . . . .	72
17. The Effect of Temperature on TPP Uptake . . . . .	75
18. Effect of TPB on TPP Uptake . . . . .	77
19. The Effect of Membrane Potential on TPP Uptake . . . . .	81

20.	The Effect of Con A on TPP Uptake by Cells Equilibrated with TPP: The TPP Electrode . . . . .	87
21.	Effect of TPP on Thymidine Uptake . . . . .	89

## Chapter I

### RATIONALE

Under resting conditions, the primary function of a cell's plasma membrane is to maintain a permeability barrier between the cytoplasm and the external milieu. However, the nature of a cell is to function not in isolation but rather in a coordinated fashion with its environment. Therefore, the plasma membrane must also provide a means of transducing signals from outside to inside the cell. Although many of these signals, such as hormones and growth factors, are specific for certain cells and elicit an array of responses, the mechanisms evolved for their transduction appear to have been highly conserved.

A group of biochemical and biophysical membrane events have been found to occur concurrently in the first few minutes of activation of a number of types of cells. This group includes calcium mobilization, phosphatidylinositol turnover, monovalent cation fluxes, and changes in membrane potential (1). Although this general pattern has been observed in many cell types, the functional interrelationships of these events remains to be determined. Moreover, considerable variability is known to exist within this pattern. For example, calcium mobilization may involve either flux of

calcium through the membrane or release from internal binding sites. Turnover of phosphatidylinositol can involve several different biochemical pathways. Changes in either active transport or passive diffusion of potassium or sodium can occur. Finally, changes in membrane potential in both the hyperpolarizing and depolarizing directions have been observed.

This pattern of events is known to be utilized for signal transduction within the immune system. There is now substantial evidence that early changes in calcium mobilization, phosphatidylinositol turnover, ion flux, and membrane potential occur in both macrophages (2-4) and polymorphonuclear neutrophils (5-8). However, in lymphocytes the picture is considerably less clear. While changes in intracellular calcium concentration have been measured directly within one minute of activation by several laboratories (9-14), there have been very few attempts to determine whether changes in the other three processes also occur in the same time frame. The studies that have been reported have used different types of lymphocytes from different sources. For this reason, it has been difficult to formulate a cohesive view of the events involved in signal transduction in lymphocytes.

The goal of this study was to establish whether a pattern of events common to activation of many cell types was also involved in lymphocyte activation. The approach to this

question was to monitor each event directly within the first few minutes of activation of nontransformed lymphocytes from a single source. The source of cells selected for this study was the rabbit thymus. Rabbit thymocytes offer the advantages of being easily prepared in the large quantities needed for some of these studies and of constituting a relatively homogeneous population of cells.

## Chapter II

### PHOSPHATIDYLINOSITOL METABOLISM

#### 2.1 INTRODUCTION

The current widespread interest in the "phosphatidylinositol response" derives from a series of observations made by Hokin and Hokin nearly thirty years ago (15-17). In 1953, the Hokins reported that acetylcholine added to pancreas slices could induce a marked increase in the incorporation of  $^{32}\text{P}$  into phospholipids (15). In similar experiments, they examined the effect of acetylcholine on the incorporation of  $^{14}\text{C}$ -glycerol and found no stimulation (16). Therefore, they concluded that the observed incorporation of  $^{32}\text{P}$  reflected stimulated turnover of phospholipid phosphate and, presumably, the base attached to it. With the advent of chromatographic techniques for separating phospholipids, they found that phosphatidylinositol (PI), a quantitatively minor component of cell membranes, and, to a lesser extent, phosphatidic acid, accounted for most of the stimulated  $^{32}\text{P}$  incorporation (17).

In 1964, the Hokins advanced the scheme shown in Figure 1 to account for the observations accumulated at that time (18). In this scheme, the primary event is the hydrolysis of the glycerol-phosphate bond by phospholipase C. Incorporation



ration of phosphate ( $^{32}\text{P}$ ) then follows breakdown, perhaps much later, and represents resynthesis of PI.

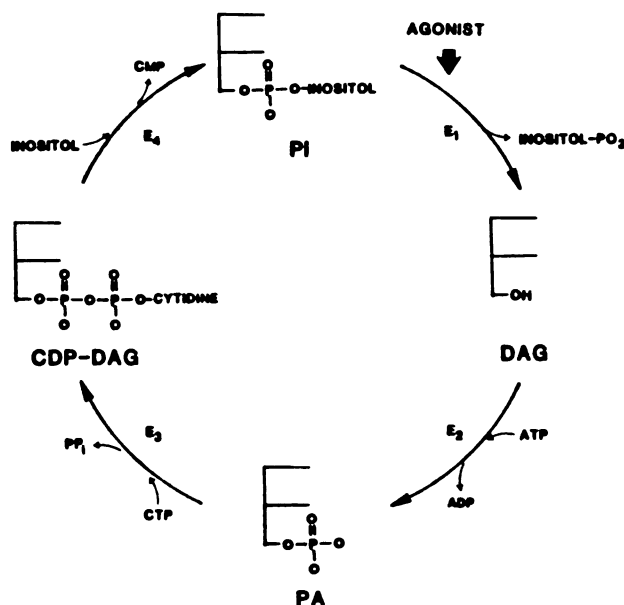


Figure 1: The PI Cycle

Receptor activation stimulates the hydrolysis of PI by phospholipase C (E<sub>1</sub>). The products of this reaction are inositol-phosphate and diacylglycerol (DAG). DAG is then phosphorylated by DAG kinase (E<sub>2</sub>) to form phosphatidic acid (PA). PA-CTP cytidyltransferase (E<sub>3</sub>) then mediates the conjugation of PA and CTP to form CDP-DAG. Resynthesis of PI is completed with the transfer of inositol by CDP-DAG inositol phosphatidyltransferase (E<sub>4</sub>).

Ligand-stimulated increases in incorporation of  $^{32}\text{P}$  into PI have now been reported in a large variety of cells (See 19 and 20 for reviews). In recent years, however, it has become clear that incorporation of  $^{32}\text{P}$  into PI is not necessarily the result of PI breakdown. Allan and Michell (21) showed that the calcium ionophore A23187 causes increased

incorporation of  $^{32}\text{P}$  into PI and PA with no effect on either PI breakdown or incorporation of  $^3\text{H}$ -glycerol. This effect appeared to be due to activation of triacylglycerol lipase which in turn increased the intracellular pool of diacylglycerol. Brindley et al. (22) have reported that certain cationic amphiphilic drugs can cause a rerouting of lipid metabolism such that PI is preferentially synthesized from PA. In addition, Abdel-Latif et al. (23) have found that increased labelling of PI can result from the breakdown of another phospholipid, triphosphoinositide. Taken together, these findings stress the importance of focussing future studies on the breakdown of PI rather than its resynthesis.

PI breakdown has now been shown to occur in a number of cells and tissues. These include mouse fibroblasts (24), blowfly salivary gland (25), rat parotid gland (26), guinea pig macrophages (2), rat hepatocytes (27), and platelets (28-30). In these studies, PI breakdown was determined by prelabelling the PI pool with radiolabelled phosphate, inositol, arachidonic acid, or glycerol and then measuring the stimulated disappearance of radioactivity in PI or by chemically assaying the PI concentration. In the few instances where both radiochemical and chemical assays have been used in the same cell type, the two approaches have yielded similar results (26,31). In most cases, the PI breakdown step has been found to be an early event occurring within a few seconds to several minutes after ligand binding.

The first indication that PI might play a role in activation of lymphocytes came from Fisher and Mueller in 1968 (32). They found that mitogenic concentrations of PHA selectively enhanced incorporation of  $^{32}\text{P}$  into PI in human peripheral blood lymphocytes after thirty minutes. Similar findings with T cell mitogens were subsequently reported for human tonsil lymphocytes (33), mouse spleen and thymus lymphocytes (34), pig lymph node lymphocytes (21,35), and rat lymph node lymphocytes (36).

Several attempts were made to determine whether PI also plays a role in B cell activation with as many answers as attempts. Masuzawa et al. (37) found that pokeweed mitogen, which stimulates both B and T lymphocytes, had only a minimal effect on incorporation of  $^{32}\text{P}$  into lipids extracted from human peripheral blood lymphocytes. They concluded that either pokeweed mitogen stimulates cells differently than other mitogens or PI does not play a role in B cell activation. The following year, Betel et al. (34) found no effect of lipopolysaccharide, a B cell mitogen, on  $^{32}\text{P}$  incorporation into PI in mouse spleen cells and concluded that B cells do not show an early increase in PI phosphate turnover. Finally, one year later, Maino et al. (35) reported that rabbit antibodies to pig immunoglobulin did in fact stimulate  $^{32}\text{P}$  incorporation into PI in pig lymphocytes. The issue has received no further attention.

In none of the above studies in lymphocytes was it established that the observed increase in  $^{32}\text{P}$  incorporation was a direct result of an early PI breakdown. Fisher and Mueller (38) found increased incorporation of  $^{32}\text{P}$  into phosphatidic acid in a membrane fraction prepared from stimulated lymphocytes and claimed that this suggested cyclic interconversion of PA and PI. In the same paper, they reported an increase in  $^3\text{H}$ -glycerol incorporation into PI but dismissed it as being relatively minor. Resch (39) has reviewed their results and calculated that on a mole per mole basis the stimulated incorporation of  $^3\text{H}$ -glycerol is actually greater than the incorporation of  $^{32}\text{P}$ . This suggests that the  $^{32}\text{P}$  incorporation into PI could reflect de novo synthesis independent of breakdown. Hasegawa-sasaki and Sasaki (36) have recently reexamined the question and confirmed that most of the PI synthesis in mitogen-stimulated human lymphocytes is via the de novo pathway rather than the turnover pathway. It should be pointed out that these results do not rule out the possibility of PI breakdown as an early event in lymphocyte activation. That is, the increase in de novo PI synthesis could be a response to breakdown.

In favor of PI breakdown in lymphocyte stimulation is the observation by Allan and Michell (40) that lymphocytes contain a higher concentration of phospholipase C than any other tissue examined. There was no direct evidence of PI breakdown in lymphocytes until a report by Hasegawa-sasaki

and Sasaki (41) published while this work was in progress. They prelabelled rat lymphocytes with radioactive arachidonic acid and found that Con A caused a small decrease in labelled PI. This decrease was first detectable at 1 minute (2%) and was maximal at 5 minutes (10%). They also observed concomitant increases in radiolabelled phosphatidic acid and diacylglycerol.

## 2.2 METHODS

### 2.2.1 Materials

$^{32}\text{P}$ -orthophosphate and myo-(2- $^3\text{H}$ )inositol were purchased from Amersham. Cell culture media and fetal calf serum were supplied by the Cell Culture Facility at UCSF. Lectins were purchased from Sigma Chemical Company (WGA & PWM), Burroughs-Wellcome (PHA), and Vector Laboratories Inc. (Con A, succinylated Con A, SBA, all biotinylated lectins). All antisera were purchased from Cappel Laboratories.

### 2.2.2 Preparation of Cells

The lymphocytes used for these studies were obtained from 8-12 weeks old male New Zealand White rabbits. The rabbits were anesthetized by i.v. injection of 1.5 ml sodium pentobarbital (65 ug/ml). They were then terminally bled by cardiac puncture in order to minimize red cell contamination of the cell preparation. The thymus and sacculus rotundus were rapidly removed and placed in Petri dishes containing Hanks

balanced salt solution (HBSS) warmed to 37° C. A cell suspension was obtained by gently teasing the organ apart. Connective tissue and cell aggregates were removed by straining the suspension through 45 um nylon mesh. The cells were washed once and resuspended to 5-10 x 10<sup>7</sup> cells/ml in HBSS. For most experiments, the cells were acclimated to HBSS for 2-4 hours at room temperature before use.

### 2.2.3 Thymidine Incorporation

Cells were cultured in RPMI supplemented with 500 units/ml Pen-Strep, 2 mM glutamine, and 15% heat-inactivated fetal calf serum in Linbro 96-well flat-bottom multiwell plates. Cell densities were 8 x 10<sup>6</sup> /ml for thymocytes and 2 x 10<sup>6</sup> /ml for sacculus rotundus cells. After 72 hours in culture, 0.5 uCi <sup>3</sup>H-thymidine was added to each well. After a further 4 hours of incubation, the cells were filtered and washed with a cell harvester. The amount of radioactivity retained on each filter was determined by liquid scintillation counting in Liquifluor (New England Nuclear).

### 2.2.4 Fluorescent Labelling

Binding of various ligands to the surface of lymphocytes was assayed by means of a biotin-avidin system. 2 x 10<sup>6</sup> cells were suspended in 100 ul labelling buffer (0.1% NaN<sub>3</sub>, 2% BSA in PBS). 5 ul of biotinylated ligand was then added

and the suspension was incubated for 1 hour on ice. Free ligand was removed by two washes in 3 ml of labelling buffer at 4° C. The cell pellet was then resuspended in 100 ul of labelling buffer and 5 ul of fluorescein-avidin was added for a further 1 hour on ice. The cells were then washed twice and resuspended in 200 ul of labelling buffer. Fluorescing cells were counted on a Zeiss fluorescent microscope.

Determination of the number of surface IgG-positive cells (B cells) by labelling with goat anti-rabbit IgG required an additional step. Binding of anti-IgG to IgG absorbed to non-B cells via Fc receptors can lead to an overestimation of the B cell population (42). Therefore, before adding biotinylated anti-IgG, the cells were preincubated in RPMI for 1 hour at 37° C., a procedure which facilitates endocytosis of surface-bound IgG.

#### 2.2.5 Incorporation of $^{32}\text{P}$ -Orthophosphate

$1.5 \times 10^7$  thymocytes or  $1 \times 10^7$  sacculus rotundus lymphocytes were incubated for 1 hour at 37° C in 1 ml of phosphate-free RPMI buffered with 25 mM HEPES in 10x75 mm glass test tubes. 30 uCi of  $^{32}\text{P}$ -orthophosphate was then added to each tube in a volume of 10 ul and the cells were returned to the incubator for a second 1 hour incubation. Mitogens, where indicated, were added in a volume of 5-25 ul, and the cells were incubated for an additional hour. At the end of this three hour incubation, each cell suspension was trans-

ferred to 1.5 ml microfuge tubes and spun at  $10,000 \times g$  in a Beckman microfuge for 10 sec. The cell pellet was washed once with 1 ml of cold phosphate-buffered saline. The cells were then resuspended in 1 ml of 10% tricarboxylic acid (TCA) and incubated on ice for 10 min. Cell protein and phospholipid was pelleted by centrifugation for 30 sec. The pellet was washed once with 1 ml 10% TCA and phospholipids were then extracted by the procedure described below.

#### 2.2.6 Incorporation of $^3\text{H}$ -Inositol

$1 \times 10^8$  thymocytes or  $2 \times 10^7$  sacculus rotundus lymphocytes were first incubated at  $37^\circ \text{C}$  for 1 hour in inositol-free RPMI. 15 uCi myo-(2- $^3\text{H}$ )inositol in a volume of 15 ul was then added and the cells were incubated for 2 hours. 10 ul of cold inositol was then added for 1 hour. After a total of 4 hours of incubation, the cells were transferred to 1.5 ml microfuge tubes, and the tubes were placed in a  $37^\circ \text{C}$  water bath. Mitogen (where indicated) was added and the reaction was rapidly stopped by the addition of 100 ul of 100% TCA at the specified time (0.5-5 min). For 0 time points, TCA was added without the addition of mitogen. The tubes were then incubated on ice for 10 min. Protein and phospholipid were pelleted by a 30 sec. centrifugation at  $10,000 \times g$ . After a wash with 1 ml of cold 10% TCA, the phospholipids were extracted.



### 2.2.7 Extraction of Phospholipids

Phospholipids were extracted with hexane:isopropanol (3:2, HIP). The cell pellet was resuspended in 1 ml HIP by vigorous vortexing. The capped microfuge tube was then placed in a Multi-Tube Vortexer (SMI) and vortexed for a further 10 min. The suspension was centrifuged for 2 min. The supernatant, containing extracted phospholipids, was transferred to a 16x100 mm glass screw cap culture tube. This procedure was repeated twice. The samples were then dried down under nitrogen and resuspended in 0.5 ml of mobile phase (hexane:isopropanol:water, 6:8:.75).

### 2.2.8 Separation of Phospholipids

Phospholipids were separated by HPLC on a Micropak Si-5 column (Varian). The solvent system consisted of two reservoirs, one containing hexane:isopropanol (3:4, solvent A) and the second containing 89.5% solvent A and 10.5% water (solvent B). Over the first 10 min., the mixture was changed from 55% solvent A and 45% solvent B to 1% solvent A and 99% solvent B and then held constant. The flow rate was 1 ml/min.

The column eluent was monitored for both UV absorption and radioactivity. Radioactivity was measured with a Radiomatic Model HP flow-through scintillation counter. The eluent was premixed with a scintillation fluid consisting of 2 liters toluene, 1 liter Triton X-100, 4 grams

2,5-Diphenyloxazole (PPO, Packard), and 0.2 grams 1,4-bis-2-(4-Methyl-5-Phenyloxazoyle)-Benzene (Dimethyl POPOP, Packard) which was pumped at 1.5 ml/min.

#### 2.2.9 Thin Layer Chromatography

Individual peaks from the HPLC were analyzed by two-dimensional thin layer chromatography on Silica Gel F plates (Analtech). The solvent for the first dimension was chloroform:methanol:sodium hydroxide (130:55:10), and the solvent for the second dimension was chloroform:methanol:water:acetic acid:acetone (150:30:15:30:60). 10 ug each of phosphatidylinositol, phosphatidylserine, phosphatidylcholine, phosphatidylethanolamine, and phosphatidic acid standards were spotted with the sample. Once the plate had dried, phospholipids were visualized with iodine vapor. In order to determine the distribution of radioactivity, the plate was marked off into a grid of 1x1.5 cm rectangles. Each rectangle was scraped into a vial containing 10 ml Liquiscint (National Diagnostics) for liquid scintillation counting.

#### 2.2.10 Phospholipid Phosphate Determination

The phospholipid fraction extracted from cells by the procedure described above was dried down and resuspended in 400 ul 10N H<sub>2</sub>SO<sub>4</sub> and heated at 170° C for 30 min. 100 ul of 10% H<sub>2</sub>O<sub>2</sub> was then added and the sample was again heated

at 170° C for 30 min. Once the sample had cooled, 4.6 ml of a solution of 1.8 mM ammonium molybdate in 250 mM sulfuric acid was added. After the addition of 200 ul of Fiske-Subbarow reagent (Sigma) the solution was boiled for 10 min. The OD was measured at wavelength 820 nm.

### 2.3 RESULTS

Incorporation of  $^{32}\text{P}$ -phosphate was measured as a first approach to determining whether PI played any role in activation of rabbit lymphocytes. Although stimulated incorporation of  $^{32}\text{P}$  would not necessarily imply an early PI breakdown, it would indicate some kind of alteration in PI metabolism. On the other hand, failure to detect a stimulation of  $^{32}\text{P}$  incorporation would strongly indicate that no PI breakdown had occurred. Since the methodology for measuring PI synthesis in lymphocytes had already been worked out by others it was decided to first measure the effects of mitogens on  $^{32}\text{P}$  incorporation and then, if the results were encouraging, to proceed to investigate the possibility of PI breakdown.

#### 2.3.1 Effect of Con A on $^{32}\text{P}$ Incorporation in Thymocytes

The technique for measuring  $^{32}\text{P}$  incorporation is described in Methods in detail. Briefly, it involves a three hour incubation at 37° C which is divided into three one-hour stages. In the first hour, the cells were depleted of

phosphate by incubation in phosphate-free media. At the beginning of the second hour,  $^{32}\text{P}$ -orthophosphate was added to radioactively label the ATP pools. At the beginning of the third hour, a lectin was added to stimulate the cells. At the end of the three hours, the phospholipids were extracted from the cells. Incorporation of radioactivity into specific phospholipids was assayed by means of an HPLC in series with a flow-through scintillation counter.

Using this approach, it was determined that the addition of the mitogenic lectin Con A to thymocytes for the third hour of the incubation produced a large increase of radioactivity in a single peak (see Figure 2). The column retention time of this peak was the same as that of PI standard. In some experiments, chromatograms of unstimulated cells showed a significant amount of label in a peak corresponding to phosphatidylcholine, the predominant phospholipid in cell membranes. However, phosphatidylcholine labelling was never altered by Con A over the one hour time course.

The retention time of the stimulated peak taken together with the fact that  $^{32}\text{P}$  incorporation into PI has been reported to result from activation of many cell types, including lymphocytes, strongly indicated that the peak was in fact PI. Two approaches were used to confirm the identity of the stimulated phospholipid. The first was to collect the peak from the HPLC column and to then rechromatograph it on silica gel plates using a two-dimensional thin layer

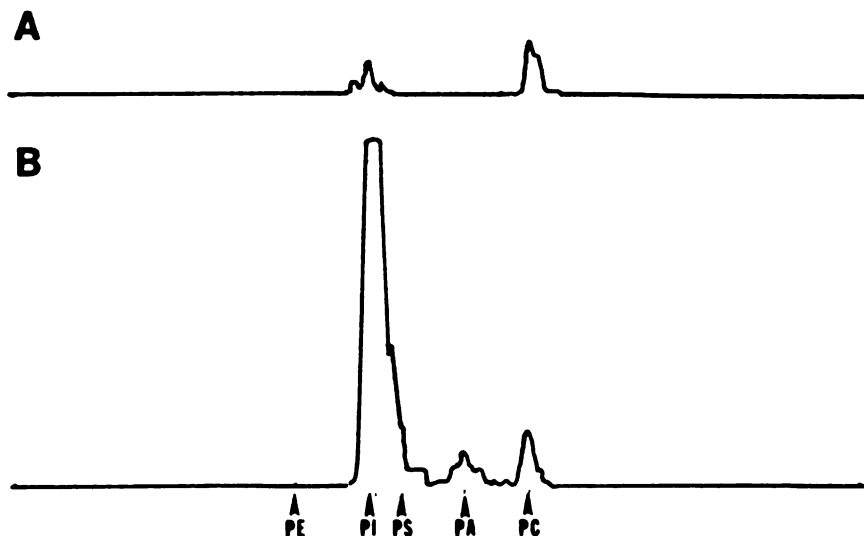


Figure 2: Effect of Con A on  $^{32}\text{P}$  Incorporation

HPLC elution profile of radioactivity in phospholipid fraction of thymocytes incubated for 1 hour with  $^{32}\text{P}$ -orthophosphate. (A) No additions (B) Con A (10 ug/ml) added. Arrows indicate retention times of major phospholipids: PE, phosphatidylethanolamine; PA, phosphatidic acid; PI, phosphatidylinositol; PS, phosphatidylserine; PC, phosphatidylcholine.

chromatography method. Results of this approach were consistent with the stimulated peak being PI but did not absolutely identify it. Several TLC systems were tested before one was found that gave good separation of PI and phosphatidylserine. In this system, the radioactivity migrated with the PI standard in the first dimension but tended to smear beyond it in the second dimension (not shown). There was no

radioactivity associated with any other phospholipid standard.

The second approach was to label cells with myo-(2-<sup>3</sup>H)inositol instead of <sup>32</sup>P-orthophosphate. The only phospholipids containing inositol are PI, diphosphoinositide (DPI), triphosphoinositide (TPI), and lysophosphatidylinositol (LPI). When DPI and TPI standards were applied to the column no UV peaks were detected. Both compounds are highly charged and may bind to the column irreversibly. LPI standard eluted from the column approximately 5 minutes after PI. Therefore, Con A stimulation of myo-(2-<sup>3</sup>H)inositol into a phospholipid with the same retention time as the <sup>32</sup>P peak would convincingly identify the peak as PI. Figure 3 shows a chromatogram from such an experiment. Con A clearly stimulated inositol incorporation into a peak with the same retention time as the <sup>32</sup>P peak. This result confirms that Con A stimulates PI metabolism in rabbit lymphocytes.

### 2.3.2 Effects of Different Lectins on PI Metabolism in Thymocytes

In the previous section it was shown that the addition of the mitogenic lectin Con A to thymocytes caused a dramatic increase in incorporation of <sup>32</sup>P into PI. If increased PI metabolism is relevant to the activation process, it would be predicted that mitogenic lectins would induce the effect while nonmitogenic lectins would not.

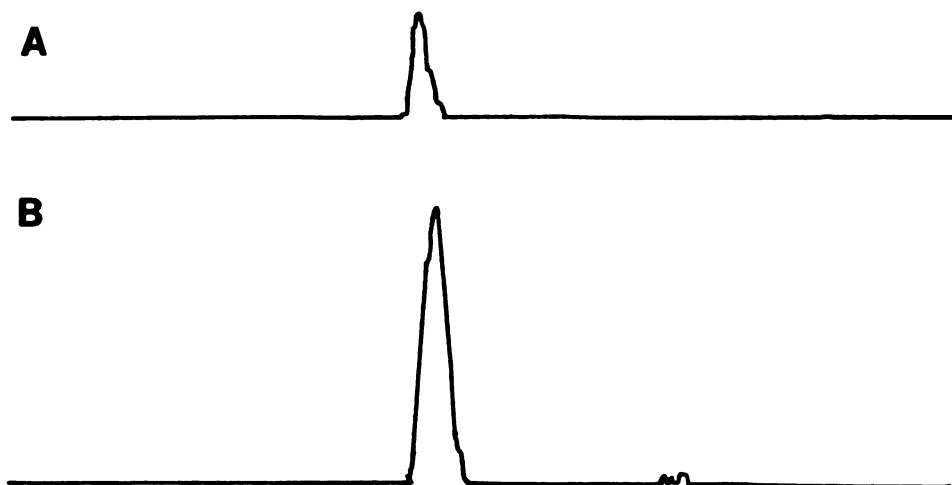


Figure 3: Effect of Con A on  $^3\text{H}$ -Inositol Incorporation

HPLC elution profile of radioactivity in phospholipid fraction of thymocytes incubated for 1 hour with  $^3\text{H}$ -inositol. (A) No additions (B) Con A (10 ug/ml) added. These chromatograms are typical of 4 different experiments.

Six lectins were tested for mitogenicity by the standard  $^3\text{H}$ -thymidine uptake assay. They included Con A, succinyl Con A, phytohemagglutinin (PHA), pokeweed mitogen (PWM), wheat germ agglutinin (WGA), and soybean agglutinin (SBA). Dose response curves for the effects of these six lectins on thymidine uptake are shown in Figure 4. It can be seen that four of the lectins, Con A, succinyl Con A, PHA, and PWM, stimulated thymidine uptake and are therefore mitogenic while WGA and SBA did not affect thymidine uptake at any of the concentrations tested.

It was possible that WGA and SBA failed to stimulate thymidine uptake because they did not bind to thymocytes.

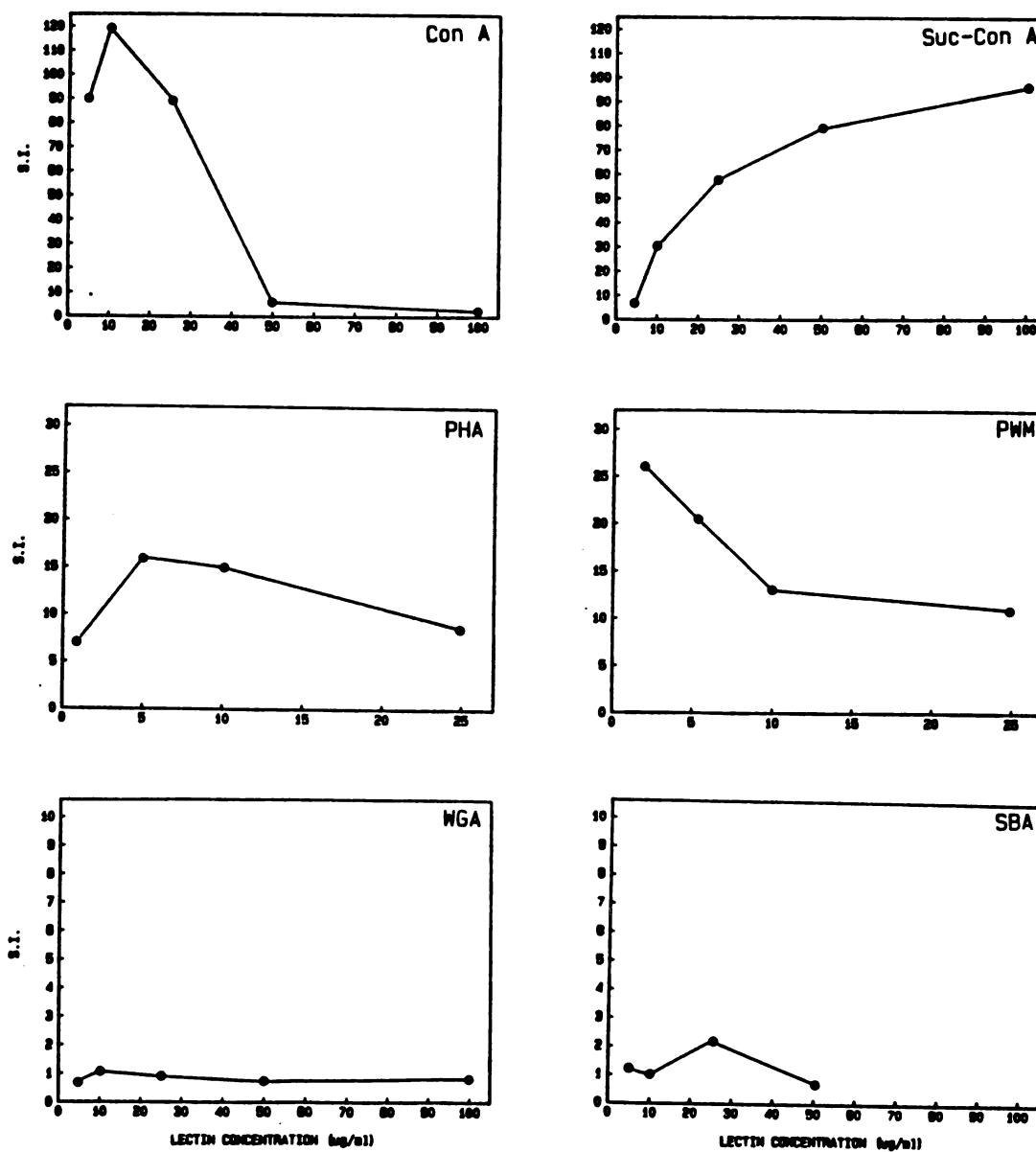


Figure 4: Effect of Lectins on Thymidine Uptake

Thymocytes were cultured with the indicated lectins for 72 hours and then pulsed with  $^3\text{H}$ -thymidine. S.I.=cpm in stimulated cells/cpm in resting cell. Each point is the mean of data pooled from 4-16 experiments done in triplicate.

Therefore, the binding of these two lectins was examined by



fluorescent microscopy and compared to Con A binding. Incubation of cells with WGA resulted in intense staining of all the cells indistinguishable from that seen with Con A. With SBA only about half the cells were stained and staining was considerably weaker. It can be concluded that WGA, at least, binds to cell membranes but does not activate the cell.

Each of the six lectins was tested for its effect on incorporation of  $^{32}\text{P}$  into PI. Optimal concentrations of the mitogenic lectins were determined from the data in Figure 4, and the concentrations of the nonmitogenic lectins were arbitrarily set at 10 ug/ml. The results of two representative experiments are shown in Table 1. For the sake of comparison, the mean stimulation index for thymidine uptake for each lectin at the same concentration is also shown. Although the absolute values varied from one experiment to the next, the order of potency of the lectins for their effect on  $^{32}\text{P}$  uptake was similar to that observed for thymidine uptake. PWM is the exception in that it was more potent in stimulating thymidine uptake than in stimulating PI synthesis. In three experiments, each done in duplicate, the mean stimulation index of  $^{32}\text{P}$  incorporation by PWM was 2.0.

The effects of different concentrations of WGA and Con A on  $^{32}\text{P}$  incorporation into PI were also tested. In Figure 5, it can be seen that WGA over the full range of concentrations tested for effects on thymidine uptake stimulated  $^{32}\text{P}$



TABLE 1  
Effects of Lectins on  $^{32}\text{P}$  Incorporation into PI

Lectin	Expt. 1	Expt. 2	Thymidine
Con A (10 ug/ml)	8.8	14.6	119
Suc-Con A (50 ug/ml)	4.3	6.2	79
PWM (5 ug/ml)	1.2	3.0	26
PHA (5 ug/ml)	4.1	4.8	16
WGA (10 ug/ml)	2.6	2.0	1.1
SBA (10 ug/ml)	0.7	1.5	1.0

Values shown are stimulation indices. Each  $^{32}\text{P}$  experiment was performed in duplicate. The values for thymidine uptake are the means of 6-22 experiments done in triplicate.

incorporation no more than 2-fold. Con A, on the other hand, stimulated  $^{32}\text{P}$  incorporation at all concentrations although less well at 100 ug/ml (S.I.=4-6) than at the lower concentrations (S.I.=10-11). This is similar to the effect of Con A concentration on thymidine uptake (Figure 4). The Con A concentration producing maximal stimulation is the same for both thymidine uptake and  $^{32}\text{P}$  incorporation.

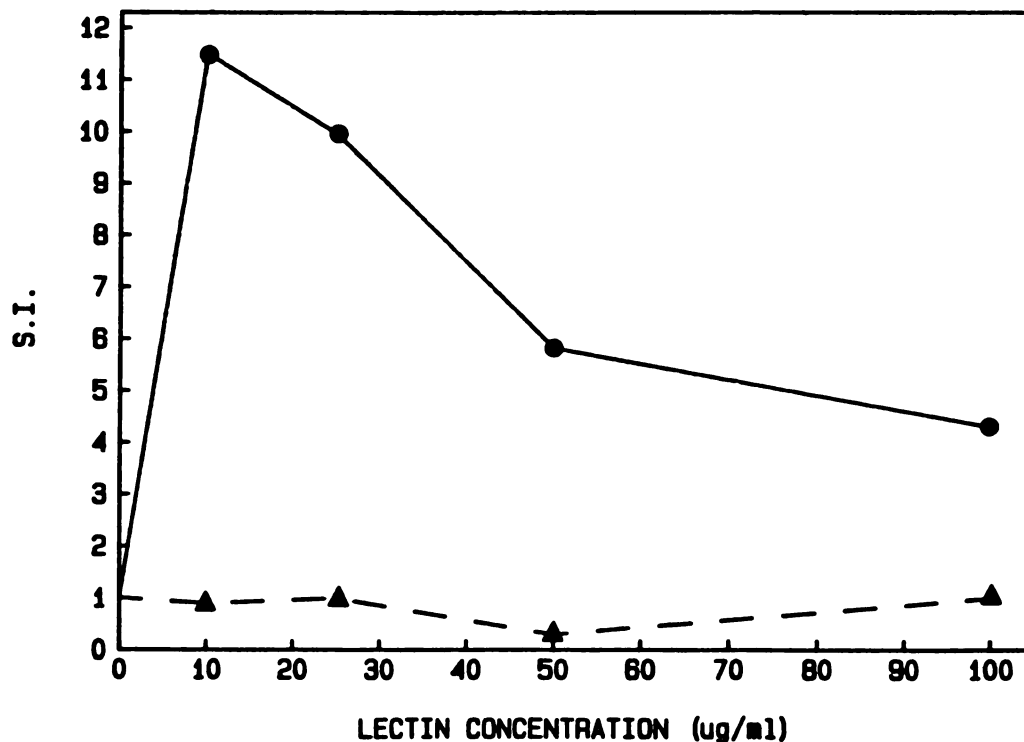


Figure 5: Concentration Effect of Con A and WGA on  $^{32}\text{P}$  Incorporation

Thymocytes were incubated with Con A (solid line) or WGA (broken line) at concentrations indicated on abscissa. All points are the means of duplicates.

### 2.3.3 Incorporation of $^{32}\text{P}$ into Sacculus Rotundus Cells

The sacculus rotundus (SR) is a rich source of B cells. By a fluorescent staining technique with anti-IgG it was determined that 55-60% of SR cells are B cells. This is in agreement with results reported by others (43). Wilson et al. (43) also used an anti-thymocyte antiserum to assay for

T cells and found that 30% of the SR cells bear T cell markers. The effects of a B cell mitogen, goat anti-rabbit IgG, and a T cell mitogen, Con A, on thymidine uptake into SR cells is shown in Figure 6.

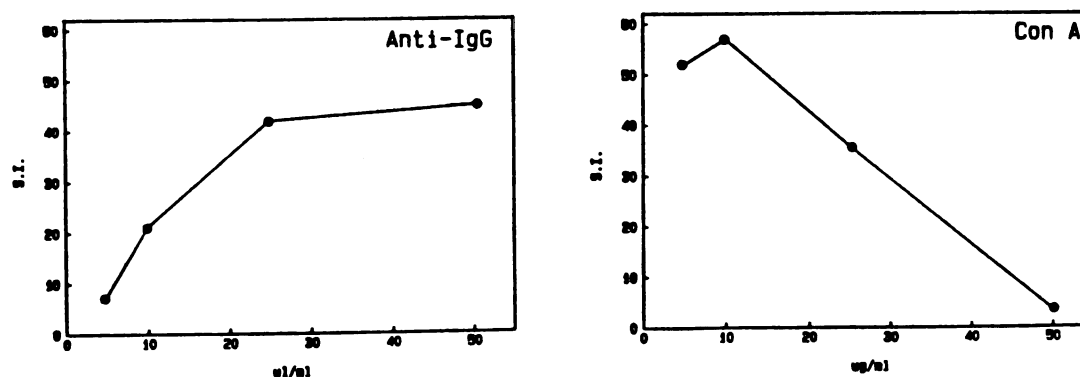


Figure 6: Stimulation of Thymidine Uptake into SR Cells

Each point is the mean of 7-8 experiments done in triplicate.

When  $^{32}\text{P}$  is added to resting SR cells, there is a high level of background incorporation. This is in striking contrast to the low levels of  $^{32}\text{P}$  incorporated into unstimulated thymocytes.  $^{32}\text{P}$  incorporation into both PI and phosphatidylcholine was 7-8 fold greater in SR cells than in thymocytes on a per cell basis. This result is only partially explained by the greater size of SR cells. Measurements of total phosphate in the two types of cells indicate that SR cells have approximately 50% more phospholipid per cell than thymocytes.

A second striking difference between SR cells and thymocytes is that mitogenic lectins fail to stimulate  $^{32}\text{P}$  incorporation into PI in SR cells. Both the T cell mitogen Con A and the B cell mitogen anti-IgG enhanced thymidine uptake, but neither showed a detectable effect on PI metabolism (Table 2). It should be noted that anti-IgM and Fab<sub>2</sub> fragments of anti-IgG were tested for their effect on thymidine uptake in SR cells. Their effect from 10-100 ul/ml was identical to that of anti-IgG (data not shown).

TABLE 2

Effect of Con A and Anti-IgG on  $^{32}\text{P}$  Incorporation into PI

Additions	$^{32}\text{P}$	Thymidine
Con A (10 ug/ml)	1.0 .5	57
Anti-IgG (25 ul/ml)	1.1 .3	42

Values for  $^{32}\text{P}$  incorporation into PI are from 4 experiments performed in duplicate (mean S.I. S.D.). Values for thymidine uptake are the mean S.I. from 18 (Con A) and 12 (Anti-IgG) experiments performed in triplicate.

#### 2.3.4 Phosphatidylinositol Breakdown in Thymocytes

The finding that mitogenic lectins stimulated incorporation of  $^{32}\text{P}$  into PI in thymocytes indicated that there was some alteration in PI metabolism associated with activation

of these cells. It remained to be determined whether the observed increase in phosphate incorporation reflected stimulation of the PI cycle or only of de novo synthesis. To distinguish between these two possibilities, methods were developed to measure PI breakdown directly.

Whereas in the above experiments activation caused a net increase in radioactivity in PI, the object now was to measure a decrease in radioactivity. This required raising the basal level of radioactivity in PI in unstimulated cells. To accomplish this, the cell concentration was increased from  $1.5 \times 10^7$  /ml to  $1 \times 10^8$  /ml and the incubation with the radioactive label was increased from one hour to two hours. In order to ensure that only PI metabolism was being measured, myo-(2-<sup>3</sup>H)inositol was used in place of <sup>32</sup>P-orthophosphate. After labelling the cells for two hours with the isotope, cold inositol was added in excess for one hour so that PI breakdown would not be rapidly obscured by reincorporation of label. Using this procedure, a basal level of radioactivity of 1500-4500 cpm in PI was routinely obtained.

The results of a typical experiment are shown in Figure 7. In seven out of seven experiments, Con A caused an early decrease in labelled PI. The onset of PI breakdown was observed by 30 seconds in four experiments and by one minute in the other three. The maximum reduction in labelled PI occurred from 30 seconds to 2 minutes and ranged from 25-68%

of the labelled PI at time 0. The mean and standard deviation of the decrease in labelled PI was  $45\% \pm 17\%$ .

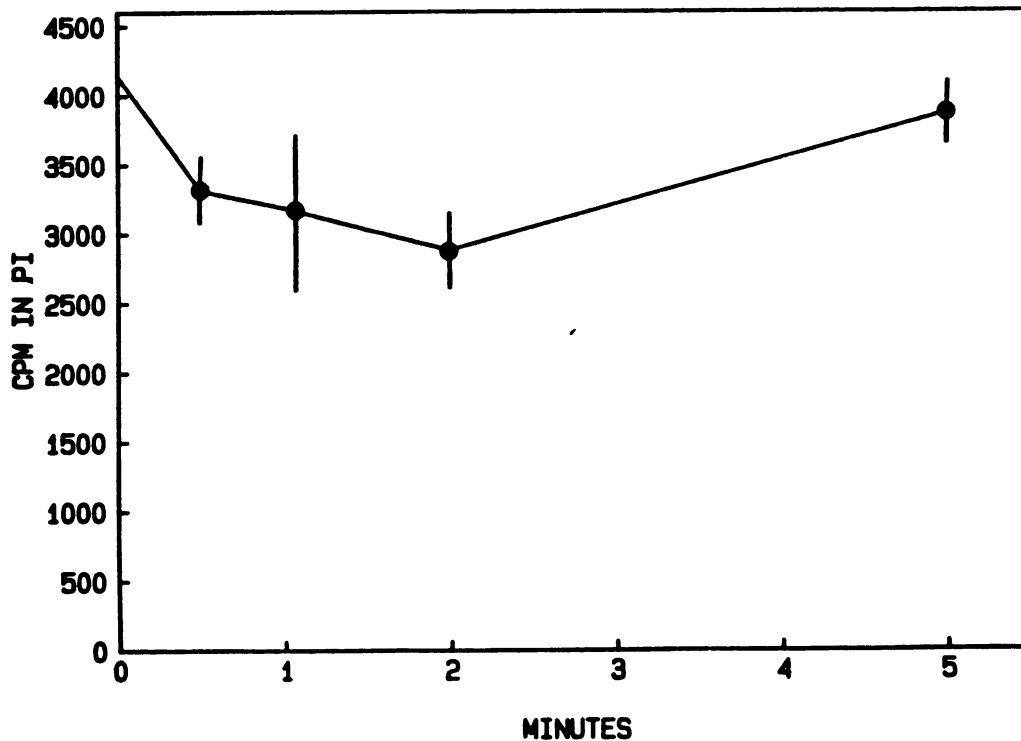


Figure 7: Con A Stimulation of PI Breakdown in Thymocytes

Thymocytes were incubated with  $^3\text{H}$ -inositol before stimulation with Con A. (ordinate) cpm in PI. (abscissa) Time after addition of 20 ug/ml Con A. Results are from a representative experiment. Each point is the mean of triplicates. Bars indicate standard deviations.

The tendency of PI labelling to increase again by 5 minutes, as seen in Figure 7, was consistently observed. Possible reasons for this effect will be discussed. Whatever



the reason, the relabelling of PI may obscure the duration and full magnitude of PI breakdown.

#### 2.3.5 Phosphatidylinositol Breakdown in Sacculus Rotundus Lymphocytes

The effect of anti-IgG on PI breakdown in sacculus rotundus lymphocytes was tested in two experiments. The protocol was similar to that for thymocytes, with each time point done in triplicate. As would have been predicted from the results with  $^{32}\text{P}$  uptake, anti-IgG at 25 ul/ml had no effect on PI breakdown (data not shown).

#### 2.4 DISCUSSION

Two different aspects of phosphatidylinositol metabolism, breakdown and synthesis, have been studied in rabbit thymocytes. Both processes were stimulated by mitogenic lectins. The data supports the hypothesis that PI plays a role in the early stages of lymphocyte activation.

PI breakdown was found to be a very early event in thymocyte activation, occurring as rapidly as thirty seconds after the addition of Con A. Although substantial early decreases in radioactively labelled PI were consistently measured, the onset time and magnitude of the decrease was somewhat variable. Undoubtedly, this is in large part due to the considerable variability observed between individual rabbits. A second factor contributing to variability was the consistently observed reappearance of  $^3\text{H}$ -PI by 5 min-

utes. Reincorporation of  $^3\text{H}$ -inositol into PI after a one hour chase with excess cold inositol is surprising. However, other investigators have made similar observations (2,28,41,44-46). Tolbert et al. (44) have suggested that the cleaved  $^3\text{H}$ -inositol might be compartmentalized and preferentially reincorporated into PI. Alternatively, the increase in labelled PI might be a result of conversion of di- and triphosphoinositide to PI (23).

In contrast to PI breakdown, PI synthesis, as measured by incorporation of  $^{32}\text{P}$ -orthophosphate, is a later event in thymocyte activation not detectable until approximately 15 minutes after addition of Con A. Despite the fact that PI is a relatively minor phospholipid, constituting only 2-12% of the total phospholipid in eucaryotic cells (19), this stimulation of  $^{32}\text{P}$  incorporation was specific for PI. Correlation of increased PI synthesis with cell activation was established by comparing the effects of mitogenic and nonmitogenic lectins. While three of the four mitogenic lectins (lectins which enhanced thymidine uptake) stimulated PI synthesis, the nonmitogenic lectins did not. In control experiments, it was determined that the failure of nonmitogenic lectins to stimulate was not due to a lack of cell receptors or the use of a suboptimal concentration.

The one mitogenic lectin that failed to stimulate PI synthesis was pokeweed mitogen (PWM). This observation is in accord with an earlier report that PWM failed to stimu-

late PI synthesis in human peripheral blood lymphocytes (37). Resch et al. (47) have found that when rabbit lymphocytes are activated by PWM a number of events, including the onsets of protein, RNA, and DNA synthesis, are delayed as compared to lymphocytes activated with other mitogens. They suggest that PWM-induced lymphocyte activation may occur via a mechanism different from that induced by other mitogens.

While T cell mitogens stimulated both PI breakdown and PI synthesis in thymocytes, a B cell mitogen, anti-IgG, had no effect on PI metabolism in sacculus rotundus cells. Although the failure to detect an effect of anti-IgG on PI may in fact be due to the absence of a PI response in B cells, certain factors should be kept in mind: (1) The sacculus rotundus contains a mixed population of cells, only 60% of which are surface Ig positive. (2) Despite the preponderance of B cells, anti-IgG is less effective than Con A in stimulating thymidine uptake in sacculus rotundus cells, indicating that anti-IgG might not be a very potent mitogen for rabbit B cells. (3) On a per cell basis, there was a higher rate of PI turnover in sacculus rotundus cells than in thymocytes which might have tended to obscure any stimulatory effects of anti-IgG. It therefore seems premature to draw any conclusions concerning the role of PI in activation of rabbit B cells at this time.

The function of PI turnover in cell activation remains to be elucidated. However, there is no shortage of sugges-

tions. The most popular hypothesis was advanced by Michell in 1975 (19). Michell had observed that in nearly every cell in which calcium fluxes had been found to play a role in activation, PI turnover was also involved. He postulated that the function of PI turnover was to regulate the gating of calcium channels. Although the calcium gate hypothesis has recently come under attack (48,49), there is a large body of evidence supporting it (for review see 19,20,50-52). An increase in calcium flux has been shown to be an early event in activation of lymphocytes isolated from a variety of sources (9-14). Most investigators agree that the onset of this flux is within one or two minutes of activation, similar to the onset of PI breakdown reported here.

Recent evidence in cells (53) as well as liposomes (54) that phosphatidic acid and leukotriene B<sub>4</sub> (another product of the PI cycle; see below) are calcium ionophores has stimulated new interest in the possible relationship of PI turnover to calcium fluxes. It has also been suggested that PI turnover modulates the release of calcium from intracellular stores and that calcium flux across the plasma membrane is a secondary event. In this respect, it is interesting to note that Mikkelsen and Schmidt-Ullrich (13) found that Con A had no effect on calcium influx into rabbit thymocytes but did enhance calcium efflux. Moreover, they found that addition of Con A to thymocytes pretreated with chlortetracycline caused a decrease in fluorescence, which indicates a release

of calcium from cell membranes. This effect of Con A was detectable by two minutes and completed by five minutes.

More recently, Nishizuka and coworkers have suggested that the function of PI turnover may be to regulate the activity of a phospholipid- and calcium-dependent protein kinase, which they have named C kinase (55). C kinase is an ubiquitous enzyme which requires calcium, diacylglycerol, and either phosphatidylserine or phosphatidylethanolamine to be fully activated. The diacylglycerol must have an unsaturated fatty acid at the number two position. PI, which exhibits a marked preference for arachidonic acid at the two position, would then provide the required diacylglycerol when hydrolyzed by phospholipase C. To date, the only strong evidence for C kinase having a role in activation derives from studies of platelets, in which thrombin stimulation of serotonin release, PI turnover, and phosphorylation of a 40k protein by C kinase are all tightly linked (56). However, C kinase has been found in every mammalian tissue examined. The highest concentrations were found in brain and in lymphocytes (57) (30 times higher than most other tissues).

Still another proposed role of PI turnover is the regulation of arachidonic acid metabolism. Arachidonic acid, as the precursor for prostaglandins, prostacyclins, thromboxanes, and leukotrienes, is critical to cell function. Under normal circumstances, there is very little free arachidonic

acid in a cell. Free arachidonic acid is rapidly metabolized and the rate-limiting step in arachidonic acid metabolism is its release from its cell repositories. PI represents a major arachidonic acid repository. Studies in platelets have revealed that arachidonic acid can be released from PI at various points in the cell cycle. Phospholipase  $A_2$  can cleave arachidonic acid directly from PI, producing free arachidonic acid and lysophosphatidylinositol (28). Alternatively, PI can be hydrolyzed by phospholipase C to form diacylglycerol and diacylglycerol lipase can then release arachidonic acid to produce monoacylglycerol (58). Lastly, the diacylglycerol produced from PI can go on to phosphatidic acid at which point a different phospholipase  $A_2$  with specificity for phosphatidic acid can liberate arachidonic acid to form lysophosphatidic acid (59). Therefore, PI turnover provides a means of modulating the availability of substrate for these various enzymes and consequently the availability of arachidonic acid for synthesis of various macromolecules.

Finally, it has been suggested that PI turnover may regulate the activity of guanylate cyclase. There is clearly a link between the two processes since almost all receptors that stimulate PI turnover also stimulate guanylate cyclase. Lymphocyte receptors for Con A and PHA fall into this category (60). The link may be indirect since these receptors also stimulated calcium fluxes and guanylate cyclase is

known to be regulated by calcium (60). However, Nishizuka and Takai (61) have recently found that guanylate cyclase can be stimulated by polyunsaturated fatty acids. Therefore, liberation of arachidonic acid by the action of phospholipase A<sub>2</sub> or diacylglycerol lipase, as discussed above, could provide a direct link between PI turnover and cGMP production. In studies of human peripheral blood lymphocytes, Con A has been shown to cause a three-fold enhancement in the level of cGMP in two minutes. The role of this increase in cGMP concentration is not known. In a recent study of platelets (62), 8-bromo-cGMP was found to inhibit phospholipase C, suggesting that the increased level of cGMP could serve to feedback inhibit PI turnover.

In conclusion, although the role of PI turnover in lymphocyte activation remains to be determined, many cell processes proposed to be associated with PI turnover have been extensively characterized in lymphocytes. Therefore, integration of the findings presented in this chapter with the studies of these various cell processes may yield important information concerning both the mechanism of lymphocyte activation and the role of PI turnover in biological systems.

## Chapter III

### MONOVALENT CATIONS

#### 3.1 INTRODUCTION

Quastel and Kaplan (63) first proposed a role for cation fluxes in lymphocyte activation in 1968. They based their proposal on the finding that the addition of ouabain, a cardiac glycoside which inhibits Na-K-ATPase, to PHA-stimulated human lymphocytes caused reversible blockade of a number of processes associated with mitogenesis, including protein, RNA, and DNA synthesis (63,64). They subsequently found that lymphocytes showed an increased rate of  $^{42}\text{K}$  uptake after several hours of incubation with mitogen (65). This stimulated uptake was inhibited by ouabain. With these findings, Quastel and Kaplan offered a revised hypothesis; activation of human lymphocytes by PHA involved an "early" stimulation of the Na-K pump which in turn elevated the intracellular potassium concentration to levels required for protein synthesis. Averdunk and Lauf (66) subsequently reported ouabain-sensitive increases in potassium influx and sodium efflux in lymphocytes from other species stimulated by an array of mitogenic lectins. This suggested that stimulation of Na-K-ATPase was a general feature of lymphocyte activation.



The theory of Quastel and Kaplan stood unchallenged until 1975 when Segel and coworkers made two important observations: (1) addition of PHA to rat lymphocytes caused an increase in potassium permeability measured at 30 minutes (67) and (2) there is no change in the intracellular potassium concentration during the first 24 hours of activation (68). These findings led to the prediction that there was a potassium efflux equivalent to the ouabain-sensitive potassium influx. This prediction was rapidly confirmed by Segel and Lichtman (69), Iversen (70), and Hamilton and Kaplan (71). In addition, Segel et al. (72) reported that the addition of PHA to lymphocyte membrane vesicles had no direct effect on Na-K-ATPase activity. Therefore, it now seems that activation of Na-K-ATPase may be a compensatory mechanism for maintaining potassium homeostasis which is secondary to an increase in potassium leak fluxes. However, the kinetics of neither the leak flux nor the active transport have been resolved sufficiently to definitively establish the functional relationship of these two processes.

Recently, early sodium fluxes have also been implicated in lymphocyte activation. Averdunk (73) has measured an increase in sodium uptake in mouse lymphocytes detectable by five minutes. Segel, Simons, and Lichtman (74) have detected an increase in the intracellular sodium concentration of 6 mM in human lymphocytes treated for 4 hours with PHA. They suggested that this increase in Na concentration is re-

sponsible for stimulating the Na-K-ATPase. Deutsch, Price and Johannson (75) have found that exposing lymphocytes to low sodium for the first three hours of activation greatly inhibited mitogenesis. However, their effect appeared to be independent of ATPase activity (76).

To date, these early "leak" fluxes of potassium and sodium in lymphocytes have been treated as direct effects of receptor binding with no attempt at understanding the underlying molecular events. Although direct coupling of the receptor with the ionophore is possible (e.g. the acetylcholine receptor), potassium and perhaps sodium channels in most nonexcitable tissues are thought to be regulated by a second messenger. In many cases, this second messenger has been identified as calcium. The involvement of intracellular calcium in modulating potassium permeability was first established by Gardos in 1958 and is often referred to as the "Gardos effect" (77). Now there is evidence in some systems (e.g. pancreas (78) and fibroblasts (79)) that calcium may also regulate sodium flux.

The increase of intracellular free calcium can arise either from calcium influx through membrane channels or from release of calcium from intracellular binding sites. The possible role of phosphatidylinositol turnover in these processes was discussed in the preceding chapter. In the vast majority of the tissues in which calcium-gated potassium channels have been found to be present, PI turnover also occurs.

It was established in the preceding chapter that PI breakdown in rabbit thymocytes occurs within 30 seconds and may be maximal at two minutes. This is very similar to the time course of calcium release reported by Mikkelsen and Schmidt-Ullrich (13). The study presented in this chapter was undertaken to determine whether changes in membrane permeability to monovalent cations occurred in a similar time frame in these cells.

## 3.2 METHODS

### 3.2.1 Measurement of Sodium Influx

Thymocytes or sacculus rotundus cells were suspended in Hanks Balanced Salt Solution at concentrations of  $4 \times 10^7$ /ml or  $2 \times 10^7$ /ml respectively. HBSS was used instead of RPMI in order to avoid sodium/amino acid cotransport. 400 ul aliquots of the cell suspension were pipetted into 13 X 75 mm glass test tubes. The tubes were then placed in a 37° C water bath and incubated for 30 minutes. In order to inhibit  $^{22}\text{Na}$  efflux, 3 mM ouabain was added in a volume of 200 ul (final concentration 1 mM) 10 minutes before the addition of isotope. At the end of this preincubation period, 6 ul of 2 mg/ml Con A was added. At various times after the addition of the stimulus, 3 uCi of  $^{22}\text{Na}$  (Amersham, 1mCi/ml) in 75 ul of HBSS was added. Two minutes later, the reaction was terminated by layering three 200 ul aliquots of the suspension over 100 ul of an oil mixture (80% Dow Corning 540 Fluid,

20% heavy mineral oil) in 400 ul Beckman microfuge tubes. The tubes were spun at 10,000 x g x 1 min in a Beckman Microfuge. The supernatant and oil layer were aspirated. The tip of the tube containing the cell pellet was cut off and counted in a Beckman Gamma Counter, Model L5500. All values shown in Results are corrected for counts in extracellular water space, which ranged from 280-550 cpm.

### 3.2.2 Measurement of Potassium Influx

$^{86}\text{Rb}$  was used as a tracer for potassium flux. The method used was similar to that for measuring  $^{22}\text{Na}$  uptake. In these experiments, ouabain was added only where indicated. 200 ul of HBSS was added to the other tubes. 3 uCi of  $^{86}\text{Rb}$  (Amersham, 1 mCi/ml) was added at the indicated time for only 1 minute. In order to measure the radioactivity in the cell pellets, the pellets were dissolved by heating the tips of the centrifuge tubes at 55° C in 1 ml Soluene 350 (Packard) and 100 ul water overnight in glass scintillation vials with polyethylene-lined caps. The vials were then cooled to room temperature, and 10 ml of Dimilume scintillation cocktail (Packard) was added to each vial. Radioactivity was counted on a Beckman Model LS-233 Liquid Scintillation Counter.

### 3.3 RESULTS

The goal of the following studies was to determine whether changes in ion flux occurred during the interval in which PI turnover and calcium mobilization are stimulated. Since neither of these two processes has been established to play a role in activation of sacculus rotundus (SR) cells, these studies focussed on thymocytes. SR cells were occasionally used in control experiments.

#### 3.3.1 Effect of Activation on Potassium Permeability

Changes in the potassium permeability of the thymocyte plasma membrane were monitored by measuring the initial rate of uptake of the potassium analog,  $^{86}\text{Rb}$ , at fixed intervals over the first eleven minutes of activation. In four experiments, each performed in triplicate, thymocytes consistently exhibited an early increase in the rate of  $^{86}\text{Rb}$  influx in response to Con A. This increase in influx was a transient phenomenon detectable by one minute, maximal at 1-2 minutes, and greatly reduced by 10 minutes (see Figure 8). The maximal stimulation of  $^{86}\text{Rb}$  uptake, measured one to two minutes after the addition of Con A, had a range of 30-130%.

In order to determine whether the observed increase in the rate of  $^{86}\text{Rb}$  uptake was due to increased Na-K-ATPase activity, parallel time courses were run in every experiment in the presence of ouabain. The effect of ouabain was to consistently reduce the stimulated influx by the same amount

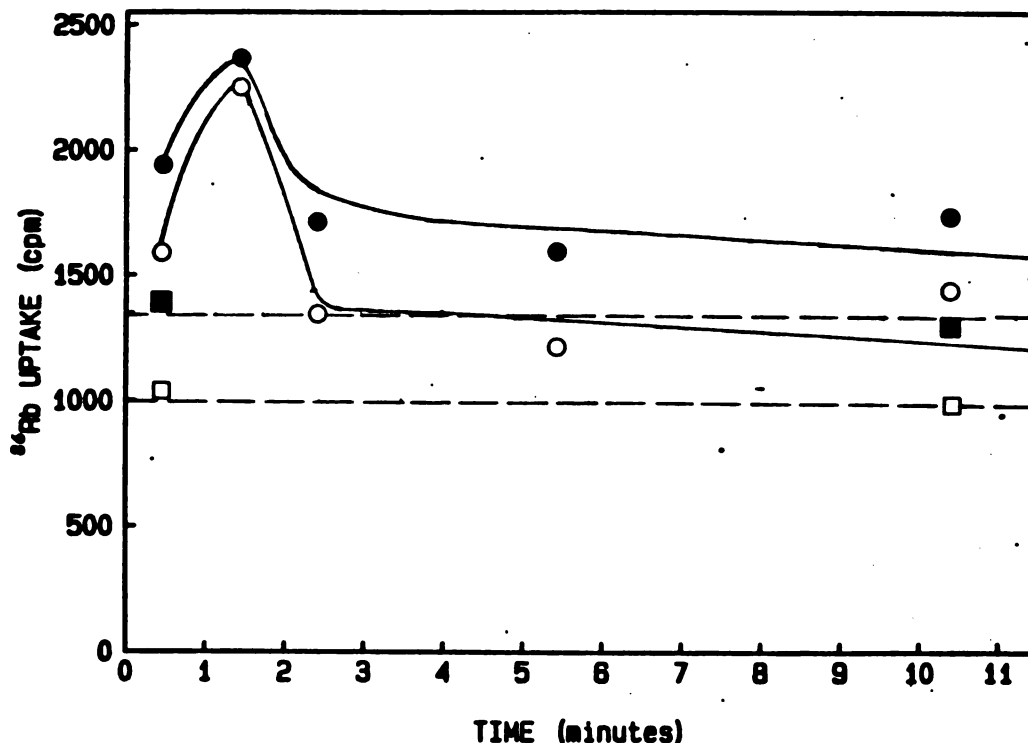


Figure 8: Effect of Con A on  $^{86}\text{Rb}$  Influx

Thymocytes were aliquotted and preincubated at  $37^{\circ}\text{C}$  as described in Methods. They were then subjected to one of the following treatments: (■) no additions, (●)  $10\ \mu\text{g}/\text{ml}$  Con A at time 0, (□)  $1\ \text{mM}$  ouabain, (○)  $10\ \mu\text{g}/\text{ml}$  Con A +  $1\ \text{mM}$  ouabain.  $^{86}\text{Rb}$  ( $3\ \mu\text{Ci}$ ) was added for 1 minute and the amount of  $^{86}\text{Rb}$  taken up is plotted at the middle of the 1 minute interval. Points represent the means of values determined from triplicate measurements of  $^{86}\text{Rb}$  uptake in three incubations at each time (SEM < 5%).

as it reduced the control influx. (Compare distance between solid lines to distance between broken lines in Figure 8.) If the Con A stimulation of  $^{86}\text{Rb}$  influx were due to increased ATPase activity, ouabain would be expected to reduce Con A-stimulated influx and control influx to the same level (i.e. open circles would be superimposed on open squares in

Figure 8). Therefore, these results strongly indicate that Con A caused an increase in  $^{86}\text{Rb}$  influx which was independent of the Na-K-ATPase pump.

### 3.3.2 Effect of Activation on Sodium Permeability

A rapid increase in the rate of Na entry has been determined to be an early response to mitogenic stimulation of several types of cells. Since the activity of the Na-K pump is known to be very sensitive to intracellular Na concentration (80), it has been proposed that an increase in the rate of Na entry would in turn cause an increase in pump activity. This has, in fact, been found to be the case for fibroblasts (81), neuroblastoma cells (82), and hepatocytes (83). A similar sequence of events has been proposed to occur in activation of human lymphocytes (74). However, nothing is known about sodium fluxes in rabbit lymphocytes. The results of the previous section indicated against an early increase in Na-K pump activity and, therefore, provided indirect evidence against an early increase in Na influx. In order to further investigate the role of Na in activation of rabbit thymocytes, the initial rate of Na influx was measured directly using  $^{22}\text{Na}$  as tracer. The technique used was very similar to that used for measuring  $^{86}\text{Rb}$  influx.

In three experiments, there was no significant effect of Con A on the rate of  $^{22}\text{Na}$  influx within the first five minutes of activation. The results from a representative experiment are shown in Table 3.

TABLE 3  
Effect of Con A on  $^{22}\text{Na}$  Influx

Additions	Time of Addition of $^{22}\text{Na}$ (minutes)	cpm
None	0	1193 (50)
Con A	0.5	1150 (18)
Con A	2	1223 (95)
Con A	5	1264 (42)
Con A	10	1388 (20)
Con A	30	1595 (22)
None	30	1421 (71)

Where indicated ("Additions"), thymocytes were stimulated with Con A at time 0.  $^{22}\text{Na}$  was added at the times indicated in the second column. Two minutes later,  $^{22}\text{Na}$  uptake was determined as described in Methods. Values for uptake are the means of values determined for three incubations.  $^{22}\text{Na}$  uptake in each incubation was measured in triplicate. Standard errors of the mean are in parentheses.

### 3.3.3 Effects of Monensin on $^{22}\text{Na}$ and $^{86}\text{Rb}$ Fluxes

Evidence has been presented that activation of rabbit thymocytes (1) involves an early increase in  $P_K$ , (2) does not involve an early increase in Na-K pump activity, and (3) does not involve an early increase in  $P_{\text{Na}}$ . The latter two conclusions, which are based on negative results, would clearly be strengthened if it could be shown, first, that the ouabain treatment was adequate for preventing the stimulation of Na-K pump activity and, second, that if the rate



of Na influx were increased it would in turn increase Na-K pump activity in these particular cells. To this end, monensin proved a useful tool.

Monensin is a carboxylic ionophore which mediates Na-H exchange. As a passive carrier, monensin transports sodium down a concentration gradient. Since the intracellular concentration of sodium is several fold lower than the extracellular concentration, the net effect of adding monensin to a cell suspension should be to increase the intracellular sodium concentration. When  $^{22}\text{Na}$  is used as tracer, an increase in intracellular sodium should be reflected by increased cell-associated radioactivity in a reliable assay system. When cell-associated radioactivity was measured up to 30 minutes after the addition of  $^{22}\text{Na}$  to thymocytes incubated with or without monensin, the results were as expected (Figure 9). At all time points assayed, monensin produced a 2-3 fold increase in cell-associated radioactivity.

In fibroblasts (81) and neuroblastoma cells (82) monensin has also had the effect of increasing Na-K-ATPase activity, presumably as a result of the increased intracellular sodium concentration. Therefore, monensin provided a means of asking whether rabbit lymphocytes would exhibit an accelerated Na-K-ATPase activity if the sodium permeability were in fact to increase during cell activation. If so, then it should be possible to measure an increase in the rate of  $^{86}\text{Rb}$  uptake in cells incubated with monensin as compared to control

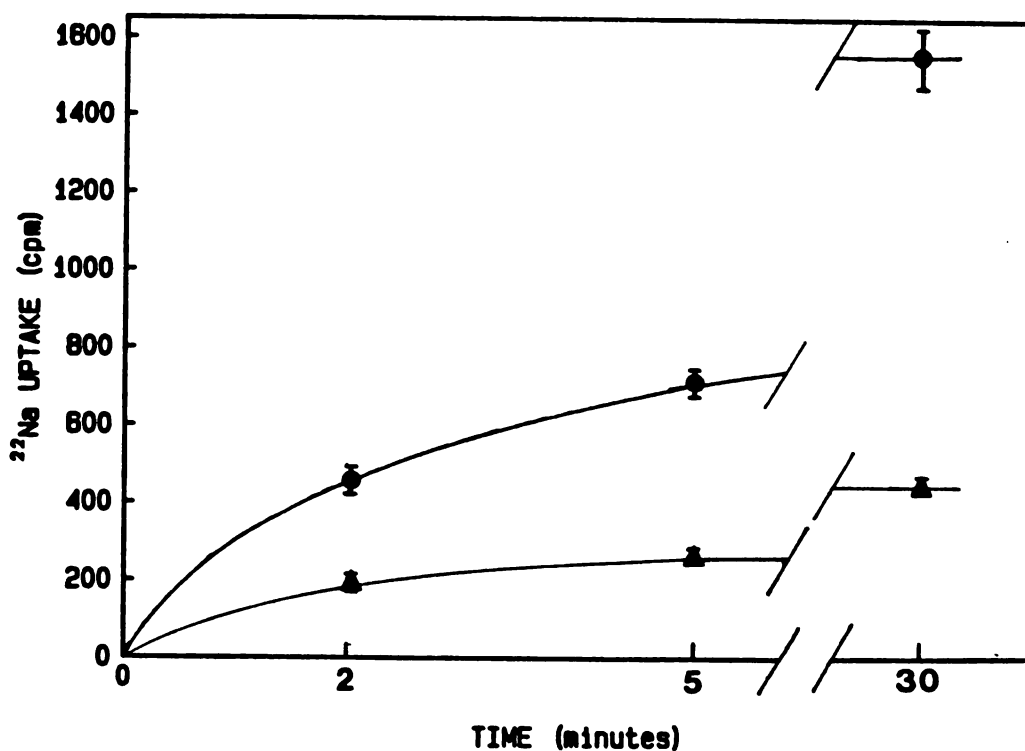


Figure 9: Effect of Monensin on  $^{22}\text{Na}$  Influx

(●) Monensin (3 ug/ml) was added 2 minutes before addition of  $^{22}\text{Na}$  at time 0. (▲) Control,  $^{22}\text{Na}$  only. Uptake was stopped at times indicated on abscissa by centrifuging cells through oil. Each point is the mean of values from three incubations measured in triplicate. Bars represent standard deviations (n=9).

cells. In the presence of ouabain, a specific inhibitor of Na-K-ATPase,  $^{86}\text{Rb}$  uptake in both cells exposed to monensin and control cells should be reduced to the same level. Figure 10 shows the effect of monensin on the initial rate of  $^{86}\text{Rb}$  uptake with or without ouabain in both thymocytes and SR cells. For the sake of comparison, initial rates of  $^{22}\text{Na}$  uptake are also shown. In both cell types, monensin stimulated  $^{22}\text{Na}$  uptake as well as  $^{86}\text{Rb}$  uptake. The basal rate of

$^{86}\text{Rb}$  uptake is reduced by ouabain, indicating that a portion of the  $^{86}\text{Rb}$  uptake is mediated by Na-K-ATPase pump activity. Ouabain also reduced the  $^{86}\text{Rb}$  uptake in cells stimulated with monensin and to the same level as control cells. Therefore, the increase in  $^{86}\text{Rb}$  uptake mediated by monensin in both thymocytes and SR cells was a result of an increase in Na-K-ATPase activity. Apparently, accelerated pump activity is a rapid response to elevation of intracellular sodium in both cell types.

### 3.3.4 Effects of Ion Flux Inhibitors on Thymidine Uptake

#### 3.3.4.1 Ouabain

The hypothesis that Na-K-ATPase plays an important role in the early stages of lymphocyte activation originated from the observation that ouabain inhibited thymidine uptake in PHA-stimulated human lymphocytes. This type of experiment was repeated with rabbit lymphocytes. In Figure 11, it can be seen that ouabain inhibited thymidine uptake of both thymocytes stimulated by Con A and SR cells stimulated by anti-IgG. 1  $\mu\text{M}$  ouabain partially inhibited both responses while 10  $\mu\text{M}$  ouabain inhibited totally. This result suggested that active transport of sodium and potassium by Na-K-ATPase might play a role at some point in activation of rabbit lymphocytes.

If Na-K-ATPase were involved in only the early stage of lymphocyte activation, it would be predicted that, while

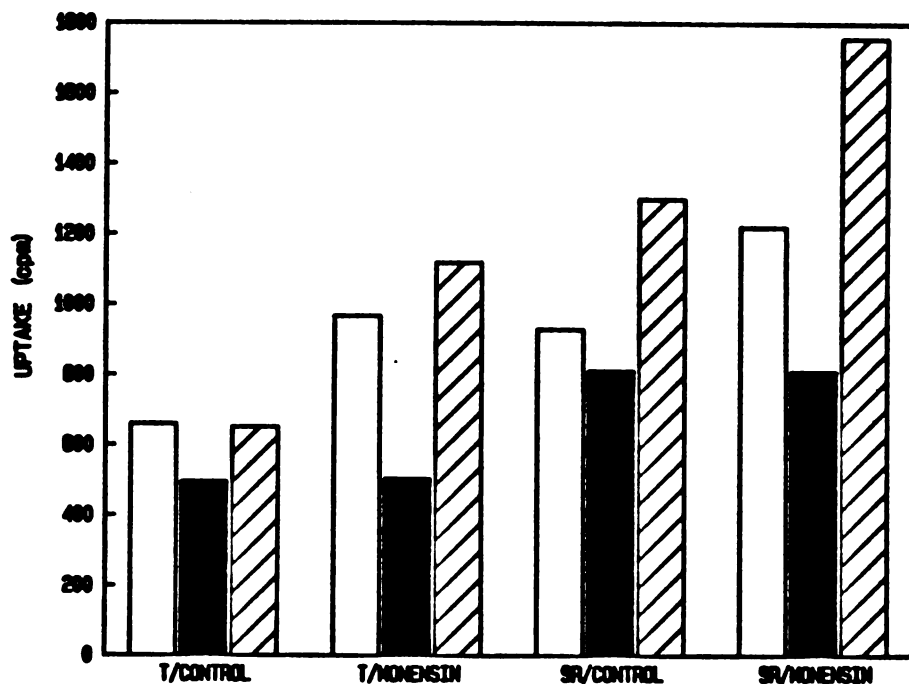


Figure 10: Effect of Monensin on Na-K-ATPase Activity

Where indicated (abscissa) cells were first incubated with monensin (3 ug/ml) for 2 minutes. The incubations were then pulsed for two minutes, either with <sup>86</sup>Rb in the absence (open bars) or presence (solid bars) of ouabain or with <sup>22</sup>Na (hatched bars). N=9, S.D. < 5%.

ouabain added at the same time as the stimulating ligand would totally inhibit thymidine uptake, ouabain added at later times would have little inhibitory effect. The results of an experiment testing this question in rabbit thymocytes are shown in Figure 12. As shown, the addition of ouabain as late as 48 hours totally inhibited thymidine uptake and ouabain added as late as 72 hours, i.e. at the same time as <sup>3</sup>H-thymidine, inhibited by 50%. Therefore, the in-

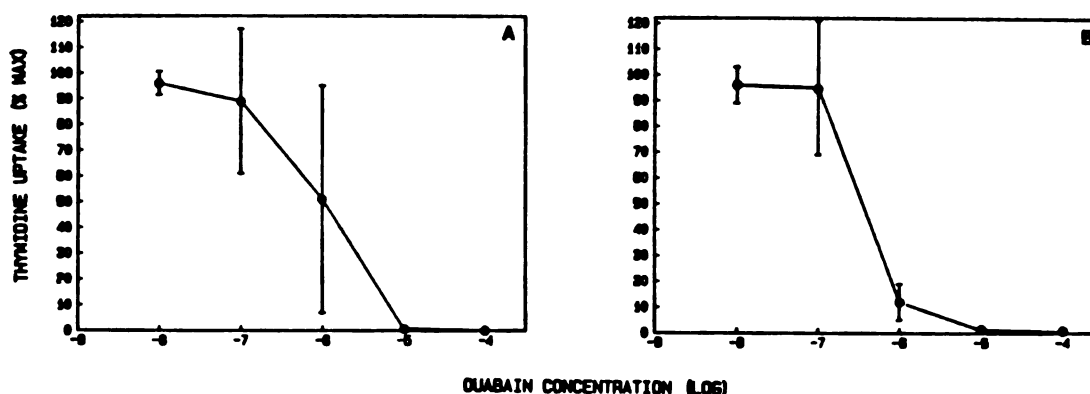


Figure 11: Effect of Ouabain on Thymidine Uptake

Ouabain, at concentrations indicated on abscissa, was added simultaneously with the addition of (A) 10 ug/ml Con A to thymocytes or (B) 25 ul/ml anti-IgG to SR cells. Each point is the mean of data from four experiments done in triplicate. Bars represent standard error of the mean.

Inhibitory effects of ouabain on lymphocyte mitogenesis could be the result of interference in a relatively late step in the activation process.

#### 3.3.4.2 Amiloride

The results of the <sup>22</sup>Na influx studies indicated that Na influx does not play a role in the first five minutes of thymocyte activation. The possible importance of Na fluxes in later stages of the activation process was investigated by testing the effect of amiloride on thymidine uptake. Amiloride inhibits passive sodium flux without affecting pas-

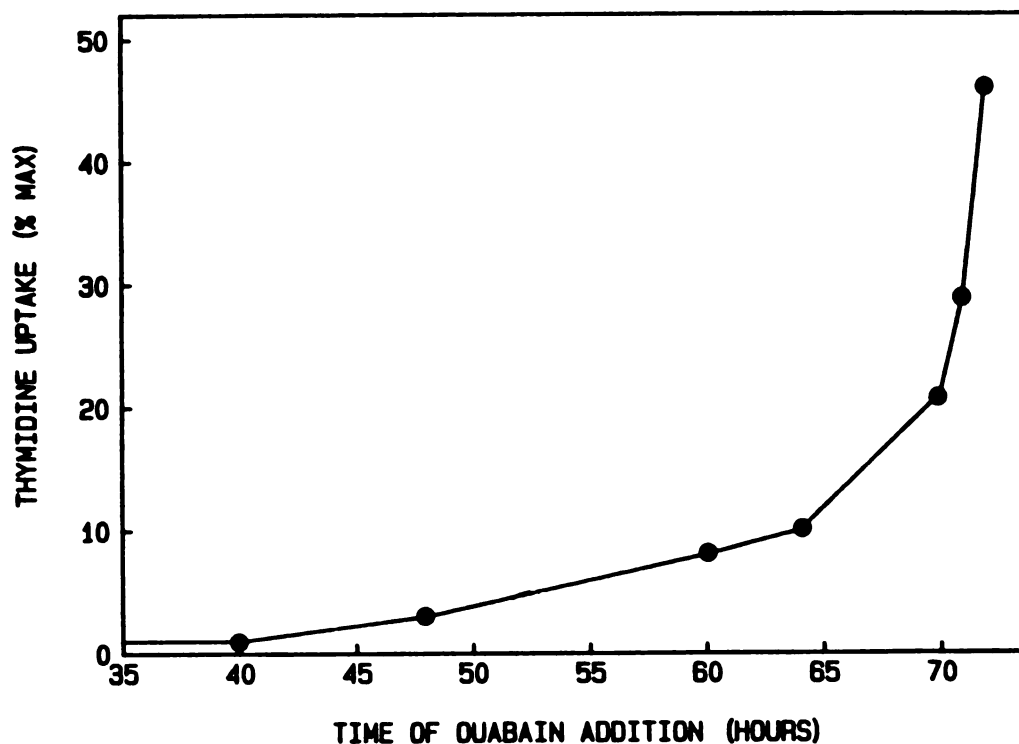


Figure 12: Time Course of Ouabain Inhibition of Thymidine Uptake

Thymocytes were stimulated at time 0 with 10 ug/ml Con A. 10 uM ouabain was added at times indicated on abscissa. Cells were pulsed with  $^3\text{H}$ -thymidine at 72 hours and harvested at 76 hours. Results are expressed as per cent of thymidine uptake observed in the absence of ouabain. Points are the means of triplicate determinations from a single experiment. The range of values was within 10% of the mean.

sive potassium fluxes or Na-K-ATPase activity (84). In non-excitabile cells in which sodium influx has been found to be an early event in cell activation, the influx has been shown to be totally inhibited by amiloride at concentrations of 10-400 uM (82,83,85). If sodium influx were an important step in lymphocyte mitogenesis, then it would be expected that mitogenesis would also be inhibited in the presence of

amiloride. In Figure 13 it can be seen that sodium uptake by SR cells stimulated with anti-IgG is inhibited by 45% in the presence of 100  $\mu$ M amiloride and by 90% in the presence of 400  $\mu$ M amiloride. In comparison, thymocytes were relatively insensitive to amiloride, their response to Con A being inhibited only 25% by 400  $\mu$ M amiloride. Therefore, while sodium influx may play a role in activation of SR cells, it seems less crucial to thymocyte activation.

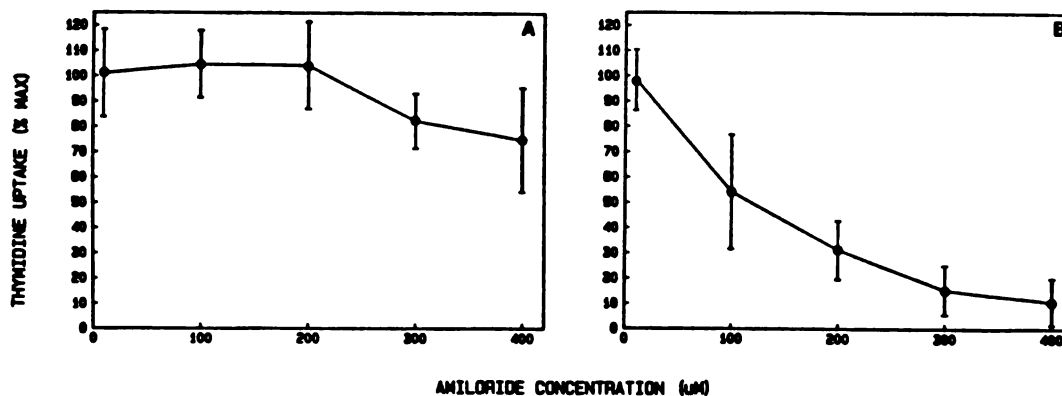


Figure 13: Effect of Amiloride on Thymidine Uptake

Amiloride, at concentrations indicated on the abscissa, was added at the same time as the addition of (A) 10  $\mu$ g/ml Con A or (B) 25  $\mu$ l/ml anti-IgG to SR cells. Each point represents the mean of data from 5 experiments done in triplicate. Error bars represent standard errors of the mean.

### 3.3.5 Effect of Ouabain on Phosphatidylinositol Turnover

Others have suggested that there might be a link between phosphatidylinositol turnover and Na-K-ATPase activity. In rabbit thymocytes, PI turnover has been found to be stimulated in the absence of any stimulation of Na-K-ATPase activity. The availability of a specific ATPase inhibitor made it possible to ask whether PI turnover required even basal Na-K-ATPase activity. In three experiments, 10  $\mu$ M ouabain had no effect on Con A-stimulated incorporation of  $^{32}$ P into PI (data not shown). It can be concluded that the early stimulation of PI turnover in rabbit thymocytes is independent of Na-K-ATPase activity.

## 3.4 DISCUSSION

In this chapter, a change in passive potassium flux has been detected within one minute after the addition of Con A to rabbit thymocytes. The observed increase in flux represents an increase in the permeability of the membrane to potassium which is transient in nature and has a distinct maximum at 1-2 minutes. There is only one other report of changes in potassium flux occurring in lymphocytes within 10 minutes of activation. In 1972, Averdunk (86) reported an increase in potassium influx within 30 seconds of the addition of PHA to human peripheral blood lymphocytes. He did not determine the ouabain sensitivity of this flux, but he claimed that it represented Na-K pump activity.



The first part of the paper is devoted to the study of the
 asymptotic behavior of the solutions of the system
 (1.1) as  $\epsilon \rightarrow 0$ . In the second part we study the
 asymptotic behavior of the solutions of the system
 (1.2) as  $\epsilon \rightarrow 0$ . In the third part we study the
 asymptotic behavior of the solutions of the system
 (1.3) as  $\epsilon \rightarrow 0$ . In the fourth part we study the
 asymptotic behavior of the solutions of the system
 (1.4) as  $\epsilon \rightarrow 0$ . In the fifth part we study the
 asymptotic behavior of the solutions of the system
 (1.5) as  $\epsilon \rightarrow 0$ . In the sixth part we study the
 asymptotic behavior of the solutions of the system
 (1.6) as  $\epsilon \rightarrow 0$ . In the seventh part we study the
 asymptotic behavior of the solutions of the system
 (1.7) as  $\epsilon \rightarrow 0$ . In the eighth part we study the
 asymptotic behavior of the solutions of the system
 (1.8) as  $\epsilon \rightarrow 0$ . In the ninth part we study the
 asymptotic behavior of the solutions of the system
 (1.9) as  $\epsilon \rightarrow 0$ . In the tenth part we study the
 asymptotic behavior of the solutions of the system
 (1.10) as  $\epsilon \rightarrow 0$ .

In the first part of the paper we study the asymptotic
 behavior of the solutions of the system (1.1) as
  $\epsilon \rightarrow 0$ . In the second part we study the
 asymptotic behavior of the solutions of the system
 (1.2) as  $\epsilon \rightarrow 0$ . In the third part we study the
 asymptotic behavior of the solutions of the system
 (1.3) as  $\epsilon \rightarrow 0$ . In the fourth part we study the
 asymptotic behavior of the solutions of the system
 (1.4) as  $\epsilon \rightarrow 0$ . In the fifth part we study the
 asymptotic behavior of the solutions of the system
 (1.5) as  $\epsilon \rightarrow 0$ . In the sixth part we study the
 asymptotic behavior of the solutions of the system
 (1.6) as  $\epsilon \rightarrow 0$ . In the seventh part we study the
 asymptotic behavior of the solutions of the system
 (1.7) as  $\epsilon \rightarrow 0$ . In the eighth part we study the
 asymptotic behavior of the solutions of the system
 (1.8) as  $\epsilon \rightarrow 0$ . In the ninth part we study the
 asymptotic behavior of the solutions of the system
 (1.9) as  $\epsilon \rightarrow 0$ . In the tenth part we study the
 asymptotic behavior of the solutions of the system
 (1.10) as  $\epsilon \rightarrow 0$ .

The absence of other reports of this early transient change in permeability may be a result of interspecies differences, although a number of other species, including several rodents, have been studied. More likely, the reason may be that no one has looked for very early changes. The bulk of the reports on fluxes in lymphocytes have described changes occurring from hours to days after stimulation, and only a very few describe changes as early as 15 minutes (69-71). No one to date has taken the approach of using initial rates to detect changes in permeability associated with lymphocyte activation. This is surprising in light of the valuable information gained by this approach in other cell types, including fibroblasts (85,87,88), neutrophils (89,90), neuroblastoma cells (82) and hepatocytes (83,91).

Ouabain had no effect on the Con A stimulation of potassium flux. A possible explanation might have been the known relatively low sensitivity to ouabain of Na-K-ATPase in rodents (92). However, the inhibitory effect of ouabain on monensin-induced  $^{86}\text{Rb}$  influx strongly indicated that the ouabain concentration and duration of exposure in these experiments were adequate to inhibit the Na-K pump. Therefore, it can be concluded that the Con A-stimulated potassium fluxes reported here were not the result of increased active transport via the Na-K pump.

Sodium fluxes were unaffected during the first ten minutes following the addition of Con A. The experiments with

monensin clearly demonstrated that the assay was sensitive to changes in sodium flux. The monensin experiments also showed that rabbit thymocytes, as expected, respond to an increase in intracellular sodium with increased Na-K pump activity. Therefore, the lack of any detectable stimulation of ouabain-sensitive  $^{86}\text{Rb}$  fluxes by Con A constitutes further evidence that no enhancement of sodium influx occurred during the 10 minute period.

Taken together, the increase in potassium permeability and absence of any change in either Na-K pump activity or sodium permeability suggest the early activation of potassium channels. In general, potassium channels in biological systems can be divided into two classes. In one class are channels which are gated by voltage-sensitive particles (93). These channels mediate the repolarization phase of action potentials and are probably restricted to nervous tissue. They can be selectively inhibited by application of tetraethylammonium (TEA).

A second class of potassium channels is voltage-insensitive and regulated by calcium. Since the discovery of the "Gardos effect" in 1958 (77), calcium-dependent potassium channels have been found to exist in many different tissues, both nervous and non-excitabile. In nervous tissue, these calcium-dependent channels generally mediate slow afterhyperpolarizations and are usually (94-96), but not always (97), distinguished pharmacologically from the fast channels

by their insensitivity to TEA. In non-excitabile tissues, opening of calcium-dependent channels has been established as an early event in receptor-mediated activation of parotid gland (98,99), lacrimal gland (100), liver (101,102) and polymorphonuclear neutrophils (103).

Activation of potassium channels as a result of increased concentration of intracellular calcium raises the question of what mediates the rise in calcium. In nervous tissue, calcium enters via voltage-dependent calcium channels which open late in the course of an action potential. Non-excitabile tissues, possessing neither voltage-sensitive calcium channels nor action potentials, must utilize other means for raising their intracellular calcium levels. This is probably accomplished by two mechanisms, release of bound calcium from intracellular sites and influx of external calcium. In parotid and lacrimal glands, there is direct evidence that both of these processes occur as a result of receptor binding (104-106). Potassium fluxes have been measured in both tissues and were found to be biphasic. In the first phase, there is a rapid efflux of potassium, lasting 2-6 minutes, which is unaffected by the removal of extracellular calcium. Direct measurements of increased intracellular calcium concentration, even in the absence of extracellular calcium, strongly indicate that this early phase of potassium efflux is a result of the release of bound calcium. In contrast, the second phase, in which potassium flux falls to a lower

level but remains above control for thirty minutes or more, does not occur in the absence of extracellular calcium. Therefore, this prolonged potassium flux is apparently mediated by influx of external calcium. It remains to be determined whether the biphasic nature of the potassium flux observed in rabbit thymocytes also reflects two different phases of calcium mobilization.

As noted in the preceding chapter, phosphatidylinositol (PI) turnover has been proposed by Michell (19) to mediate the increase in intracellular calcium in non-excitabile tissues. Recent evidence that two products of PI metabolism, phosphatidic acid and leukotriene B<sub>4</sub> (54), are calcium ionophores seems to increase the likelihood of PI playing a role in calcium influx. In opposition to Michell's proposal are the findings that PI turnover is both (1) inhibited by removal of extracellular calcium and (2) stimulated by the addition of A23187 in calcium-containing media in several cell types (49,107). In the studies in which extracellular calcium was removed, the amount of intracellular calcium was not measured and may have also been depleted. Therefore, the possibility still remains that calcium-sensitive PI breakdown, perhaps stimulated by the early release of bound calcium, mediates calcium influx.

Whatever the connection between PI breakdown and intracellular calcium, it cannot be denied that the two are tightly linked. In each of the non-excitabile tissues listed

above in which a stimulus has been found to trigger the opening of calcium-dependent potassium channels the same stimulus also activates PI turnover. Now, with the finding that calcium mobilization (13), PI turnover, and a biphasic potassium flux are activated by Con A within two minutes, it appears that rabbit thymocytes may be added to this list.

Is this triad of calcium mobilization, PI turnover, and potassium flux likely to be a feature common to activation of all lymphocytes? It would not be surprising if this turned out to be the case. Calcium influx has been reported to occur within one or two minutes of activation in lymphocytes from several species (10,108), and an increase in intracellular calcium has been measured in pig lymph node lymphocytes and mouse thymocytes (14). Also, the results of many studies in different types of lymphocytes indicate that PI metabolism and potassium permeability play a role at some point in lymphocyte activation.

As discussed in the introduction, there is also some evidence, although mostly indirect, that activation of sodium influx and/or Na-K-ATPase may be early events in human lymphocytes. If these processes were in fact found to occur early, their coexistence with activation of calcium-dependent potassium channels would be an arrangement with ample precedent. For example, an early stimulation of calcium-sensitive sodium fluxes has been found to occur at the same time as potassium fluxes in the exocrine glands (1). Recent

experiments with patch clamp techniques, in addition to confirming the existence of calcium-activated potassium-selective channels (109,110), have revealed the existence of calcium-activated channels equally permeable to potassium and sodium (111-113). There is also pharmacological evidence for calcium-sensitive channels selective for sodium in lacrimal glands (114). With regard to Na-K-ATPase, this enzyme may be activated as a result of either sodium influx (81), calcium mobilization (91), or membrane perturbation (91). Therefore, there are many mechanisms by which modulation of sodium flux and Na-K-ATPase activity, together or independently, might occur in concert with a calcium-sensitive increase in potassium permeability in activation of different types of lymphocytes.

In conclusion, the finding that Con A activation of rabbit thymocytes entails early changes in calcium mobilization, PI turnover, and potassium flux strongly indicates that the first step in transduction of an activating signal may involve the functional integration of this triad of cell processes. These same three processes have already been found to be closely connected in receptor-mediated activation of several other cell types. The functional interrelations of the processes, particularly the relationship of calcium to PI turnover, remain to be elucidated. It is suggested that rabbit thymocytes may now serve as a model system for further exploring these problems.

## Chapter IV

### MEMBRANE POTENTIAL

#### 4.1 INTRODUCTION

All cells, whether excitable or non-excitable, maintain transmembrane ionic gradients. As recognized by Bernstein in 1902, an ionic gradient across a semipermeable membrane gives rise to an electrical potential, the membrane potential ( $E_m$ ). The magnitude and sign of a cell's membrane potential depend upon both the ionic concentration differences between the inside and outside of the cell and the permeability properties of the membrane.

The values reported for the resting potential of mouse and human lymphocytes, measured by various techniques, are listed in Table 4. It can be seen that the values estimated by several different chemical probes are consistently larger than those estimated by direct electrical recordings. Although the reason for this discrepancy is not known, it has been suggested that, because lymphocytes are so small (less than 10  $\mu\text{m}$  in diameter), the microelectrodes used in these experiments may have caused extensive leaking and thereby disrupted the transmembrane ionic gradients. The use of the finer electrodes now available may resolve this issue. In lymphocytes, as in most cells, the intracellular potassium



concentration is higher than the extracellular concentration while the intracellular sodium concentration is lower. Various reports place the intracellular potassium concentration at 100-170 mM and the intracellular sodium concentration at 10-30 mM (70,73,115,116). The corresponding equilibrium potentials(1) for potassium and sodium,  $E_K$  and  $E_{Na}$ , are approximately -80 mV and +40 mV respectively.

TABLE 4

## Reported Values of Lymphocyte Membrane Potentials

$E_m$ (mV)	Source of Lymphocytes	Probe	Reference
-10	Human Blood	Microelectrode	117
-7	Human Blood	Microelectrode	118
-52	Human Blood	$^3\text{H-TPMP}$	119
-35	Human Blood	$^{14}\text{C-Thiocyanate}$	119
-60	Mouse Spleen	diS-C <sub>3</sub> -(5)	120
-65	Mouse Spleen	$^3\text{H-TPP}$	121
-50	Mouse Thymus	Oxanol	14

-----

(1) The equilibrium potential for ion X,  $E_x$ , is defined as the potential which would exist if the membrane were exclusively permeable to X. For any given intracellular and extracellular concentrations of the ion, the equilibrium potential is the potential at which electrical forces and diffusion forces are exactly balanced.

Ionic gradients and, consequently, membrane potentials are maintained by the Na-K pump at the expense of considerable metabolic energy. In excitable cells, the membrane potential is crucial to the conduction of nervous impulses and to muscle contraction. In non-excitable cells, the reason for this energy expenditure is less clear. It has been suggested that the membrane potential may regulate certain cell functions, such as solute transport across the membrane (122), the conformation and activity of membrane-bound enzymes (123), secretion (124) and intercellular communication (125). A corollary of this proposal is that changes in the membrane potential could serve to modulate and coordinate cell functions associated with cell activation.

There have been only a very few reports of early changes in membrane potential in lymphocyte activation. Taki (117) reported small depolarizations (about 2mV) in human and mouse lymphocytes detectable by intracellular recording within 10-30 minutes after stimulation. Utsumi et al. (126), using the cyanine dye diS-C<sub>3</sub>-(5), reported but did not quantitate a depolarization in mouse thymocytes detectable within three seconds and maximal at ten minutes. Most recently, Tsien (14) has used another fluorescent dye, oxanol, to measure membrane potential changes in mouse thymocytes and has reported very different results. He has recorded a transient hyperpolarization, the onset of which occurred after one minute. This hyperpolarization was ouabain-insensitive and calcium-dependent.

If a change in membrane potential occurs in activation of rabbit thymocytes, it might be predicted that its direction and time course would be similar to that observed by Tsien in mouse thymocytes. An increase in the permeability of the membrane to potassium with no change in the sodium permeability, as described in the previous chapter, would tend to shift the membrane potential closer to  $E_K$ , that is, to a more negative value. However, it is possible that the hyperpolarizing influence of an increase in  $P_K$  could be offset by changes in permeability to other ions, e.g. chloride or calcium. Alternatively, if the resting potential is already very close to  $E_K$ , an increase in  $P_K$  would have little effect. Therefore, the question of whether membrane potential plays a role in activation of rabbit thymocytes can be resolved only by direct measurement.

Cell membrane potentials can be monitored either by direct recording with intracellular microelectrodes or by the use of probe molecules. Of these two approaches, intracellular recording is generally more reliable but is not always technically feasible. In order to measure potentials in very small cells, investigators have resorted to the use of probe molecules.

The probe molecules can be divided into two classes, fluorescent dyes and lipophilic ions. The fluorescent dyes have been widely used to measure membrane potentials in many types of suspension cells. It has only recently been appre-

ciated that their use requires considerably more caution than originally supposed. Smith et al. (127) have reported that the dyes are toxic to cells and uncouple oxidative phosphorylation. Moreover, they can give erroneous estimates of  $E_m$  for a variety of reasons: they (1) can hyperpolarize cells by increasing  $P_K$  (128), (2) can depolarize cells by blocking calcium-activated potassium channels (129), (3) accumulate in mitochondria (130), and (4) are also responsive to pH changes (131).

In comparison to the fluorescent dyes, the lipophilic ions had received relatively little attention at the time this study was undertaken. Kaback and coworkers (132) had measured  $E_m$  in *E. coli* giant cells with both intracellular microelectrodes and radiolabelled tetraphenylphosphonium (TPP) distribution and found that the two methods yielded very similar values. Lichtshtein et al. (133) applied the same approach to neuroblastoma-glioma hybrid cells and again found close agreement. A closely related probe, triphenylmethylphosphonium (TPMP) had been used to measure hyperpolarization consequent to ligand-receptor interaction in human granulocytes (134) and bovine thyroid cells (135). Finally, Deutsch et al. (119) used both TPMP and a lipophilic anion, tetraphenylboron (TPB), together to measure the resting potential of human red cells and lymphocytes and, despite encountering some difficulty in calibration, concluded that the technique was generally applicable to suspension cells.

In this report, two different approaches have been taken to measuring TPP partitioning into rabbit thymocytes. One approach was the use of one of several techniques modelled after ligand-receptor binding assays. The standard procedure in this type of assay is to first incubate cells with a radiolabelled ligand, in this case  $^3\text{H}$ -TPP, and then to rapidly separate the cells from the external milieu. The amount of cell-associated ligand is then determined by scintillation counting.

The second approach was to use a newly developed TPP electrode, designed by Dr. Juan Korenbrot. The principle of this method is quite different from that of radioisotope methods. Rather than counting radioactivity associated with the cells, this technique monitors free extracellular TPP.

The TPP electrode offers two important advances over the conventional radioisotope techniques. First, changes in TPP uptake can be measured within 1 second of cell activation. The electrode has a rapid response time; the  $t_{1/2}$  for response to an instantaneous change in the free TPP concentration is approximately 300 milliseconds. In contrast, radioisotope methods require several seconds to separate the cells from the free TPP, either by centrifugation or by filtration. Second, the electrode allows continuous monitoring of TPP uptake in a cell suspension. To establish the time course of TPP uptake by the radioisotope method entails the cumbersome process of starting and stopping a series of reactions at precisely timed intervals.

The TPP electrode also has certain limitations. Care must be taken to control for possible interaction of some substances with the electrode itself rather than with the cells. For example, addition of ethanol at a final concentration of 1% v/v (a concentration thought to not adversely affect cells) to a solution containing 20  $\mu\text{M}$  TPP in the recording chamber caused a rapid voltage jump of 1 mV, corresponding to an apparent decrease in free TPP equal to .75  $\mu\text{M}$ . Ion carriers, such as valinomycin or monensin, cannot be used in the electrode since they alter its selectivity.

## 4.2 METHODS

### 4.2.1 The TPP Electrode

The TPP electrode is designed to measure the concentration of free TPP in a small volume. This is accomplished by means of electrical recording across a TPP-selective polyvinylchloride (PVC) membrane. The preparation and selectivity characteristics of the membrane are described by its creator, Dr. Juan Korenbrot, in Appendix A, page 121.

The construction of the TPP electrode is shown in Figure 14. A small circle (7 mm in diameter) of the TPP-selective membrane was glued to the top of a PVC cylinder (12 mm outside diameter, dark cylinder in Figure 14) with tetrahydrofuran containing 3% PVC (W/V). After overnight drying, the PVC cylinder was glued (with epoxy cement) to an acrylic cylinder (shaded cylinder in figure), thus creating a re-

recording chamber with a volume of 300  $\mu$ l. Finally, the PVC cylinder was attached to an acrylic U tube by means of a tight fit.

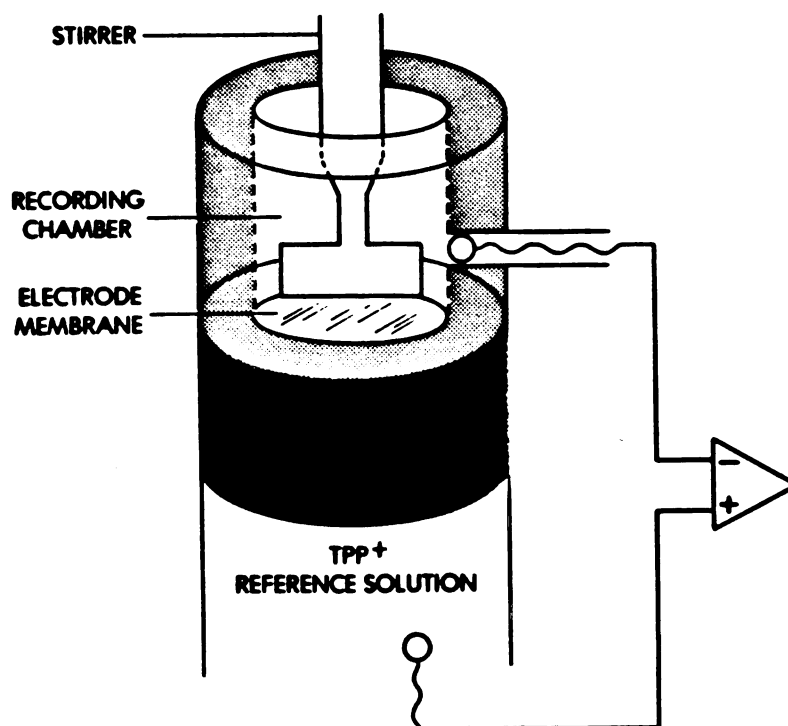


Figure 14: The TPP Electrode

In a typical experiment, the U tube was filled with a reference solution containing a fixed concentration of TPP





and cells suspended in 150  $\mu$ l of the same solution were placed in the recording chamber. The cell suspension was constantly stirred with a Teflon stirring rod driven by a low noise motor. Any uptake or release of TPP by the cell would cause a change in the concentration of free TPP in the recording chamber. The resulting gradient of free TPP concentration across the electrode membrane would generate an electrical potential which was detected by silver/silver chloride microelectrodes (IVM). The electrical signal was amplified 100-fold with a high input impedance (1000 Mohms), low noise differential amplifier with a recording bandwidth of DC to 100 Hz (PARC, Model 113) and recorded on a strip chart recorder (Gould, Brush 220) and a digital multimeter (Keithley, Model 179) wired in series. The TPP concentration in the recording chamber at any point in time was determined by fitting the corresponding value of the electrical potential measurement to a plot of E vs.  $\log$  [TPP] generated at the beginning of each experiment. In general, the response of the electrode was linear with the logarithm of the TPP concentration with a slope of 45-58 mV per decade concentration down to a limiting concentration of about 0.4  $\mu$ M.

#### 4.2.2 Assay of Radiolabelled TPP Uptake

Cells were suspended at the indicated densities in 1 ml of a TPP solution trace-labelled with .75 uCi  $^3\text{H}$ -TPP/ml (NEN, specific activity 4.3 mCi/mmol). Reactions were stopped by layering triplicate 200 ul aliquots over 100 ul of 80% silicon oil/20% mineral oil in Beckman 400 ul microfuge tubes and centrifuging for 30 seconds at 10,000 x g. The supernatant and oil layer were aspirated and the tips of the tubes were cut off. The cell pellets were solubilized by incubating each tip at 55° C overnight in 1 ml of Soluene 350 (Packard). Cell-associated radioactivity was measured by liquid scintillation counting in Dimilume (Packard). The values reported are corrected for radioactivity trapped in the extracellular space, which was less than 150 cpm.

#### 4.2.3 Measurement of Cell Water Volume

Thymocytes were suspended in 1.5 ml of HBSS to a density of  $3 \times 10^8$  cells/ml. 50 ug/ml Con A was added to half of the tubes and the cells were incubated for three minutes at 23° C. .3uCi of  $^3\text{H}$ -H<sub>2</sub>O (NEN) and .5 uCi of (1,2- $^{14}\text{C}$ )-polyethyleneglycol (PEG) (NEN, specific activity=0.7 mCi/gram, MW=4000) were then pipetted into each tube. Five aliquots of 250 ul each were layered over oil in microfuge tubes as rapidly as possible (about 30 seconds) and centrifuged for 2 minutes at 10,000 x g. In control experiments it was determined that the  $^3\text{H}$ -H<sub>2</sub>O completely equili-

brated with the intracellular water by 30 seconds. Cells were centrifuged as soon as possible after the addition of the radioactive markers in order to minimize adsorption of the extracellular marker,  $^{14}\text{C}$ -PEG, to the cell surface.

In order to determine the distribution of radioactivity, the cell pellets were dissolved by overnight incubation in 1 ml. of Soluene 350 (Packard) at  $55^{\circ}\text{C}$  and radioactivity in the pellet and supernatant was counted on two channels, 0-317 ( $^3\text{H}$  channel) and 397-655 ( $^{14}\text{C}$  channel), using library program 8 on a Beckman LS 7000 liquid scintillation counter. Counts per minute in the two channels were converted to disintegrations per minute of  $^3\text{H}$  and  $^{14}\text{C}$  by correcting for counting efficiencies and spillover of  $^{14}\text{C}$  counts into the  $^3\text{H}$  channel.

### 4.3 RESULTS

#### 4.3.1 Measurement of TPP Uptake with the TPP Electrode

As a first approach to determining whether Con A induces changes in membrane potential in rabbit thymocytes, the effect of Con A on the rate of TPP uptake was measured with the TPP electrode. The reason for looking at rates rather than equilibrium conditions was that equilibrium could not be attained within a reasonable span of time. The cells continued to take up TPP even after two hours of preincubation. It should be noted that the electrode was not equipped with a means of regulating the temperature at the time

of these experiments. All incubations were, therefore, at room temperature.

#### 4.3.1.1 Effect of Con A on the Rate of TPP Uptake

In these experiments, thymocytes were incubated with 25  $\mu$ M TPP in the recording chamber until a steady rate of TPP uptake was achieved (about one minute) before the addition of a stimulus. Using this approach, it was found that Con A caused a change in the rate of TPP uptake. Approximately 1.5 minutes after the addition of Con A, a marked increase in the rate of TPP partitioning into thymocytes (corresponding to an upward slope in Figure 15) was consistently observed. This increase in rate continued for about 3 minutes and then returned to control levels. The experimental conditions for the Con A effect on TPP uptake were as follows. First, it required a high cell density,  $10^9$  cells/ml. Second, it required a Con A concentration of 100  $\mu$ g/ml, 10 times higher than that found to be optimal for stimulation of mitogenesis (see Figure 4). This was not surprising since the cell concentration was over 100 fold higher than that used for the mitogenesis studies. Others have reported that working with higher cell densities requires working with higher mitogen concentrations (115). Third, the effect of Con A was observed only when the cells were stirred slowly, 60 rpm or less. At higher revolutions, no effect was observed even though the faster stirring did not affect viability.

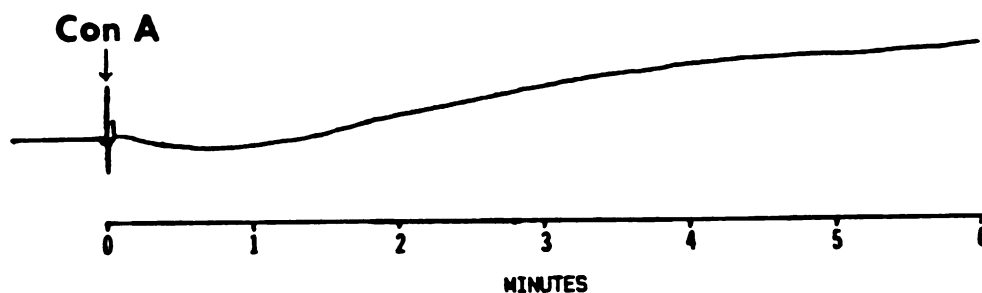


Figure 15: Increased Rate of TPP Uptake Induced by Con A

In a typical experiment, thymocytes ( $10^9$ /ml) were incubated with 25  $\mu$ M TPP in the electrode chamber until a steady rate of TPP uptake was achieved (about 1 minute). Con A (100  $\mu$ g/ml) was then added. In the electrical recording shown here, a ramp generator was used to produce an opposing signal so that the basal rate of TPP uptake is represented by a flat line. Therefore, the upward inflection at 1 minute reflects a Con A-stimulated increase in the rate of TPP uptake. The rate returned nearly to the basal level by 6 minutes.

The direction and time course of the observed electrical signal were consistent with an early transient hyperpolarization in thymocytes in response to Con A. Another observation provided further support for the existence of a hyperpolarizing response; when the cells were preincubated with 10  $\mu$ M ouabain for 10 minutes, there was no response to Con A. Since ouabain at low concentrations is thought to be a specific inhibitor of ATPase, inhibition of the response by ouabain strongly suggested that the electrical signal reflected a hyperpolarization which resulted from a transient increase in Na-K-ATPase activity. However, since this con-

flicted with results of the previous chapter, in which Con A was found to have no effect on Na-K-ATPase activity, alternative explanations were investigated.

#### 4.3.1.2 Control Experiments

Cell Volume. The first possibility considered was that Con A induced an early swelling of thymocytes. Such a swelling might be expected to cause an increase in the rate of TPP uptake either as a direct result of the larger surface area or as a result of distortions and concomitant permeability changes in the plasma membrane. To determine whether changes in cell volume occurred, the cell water volume of control cells and of cells exposed to Con A for 3 minutes were measured as described in Methods. As shown in Figure 16, Con A had no significant effect on the cell water volume.

Cell Aggregation. The second possibility tested was that the apparent decrease in extracellular TPP concentration was an artefact of cell aggregation. That is, it was possible that Con A caused the formation of large cell aggregates which could have settled on the TPP-selective membrane, thereby interfering with the function of the electrode. The fact that the Con A response was seen only with slow stirring could have been explained in this way, although it was difficult to understand why such a phenomenon would result in a transient signal. To address this question, the effects of Con A on both TPP uptake and cell aggregation were

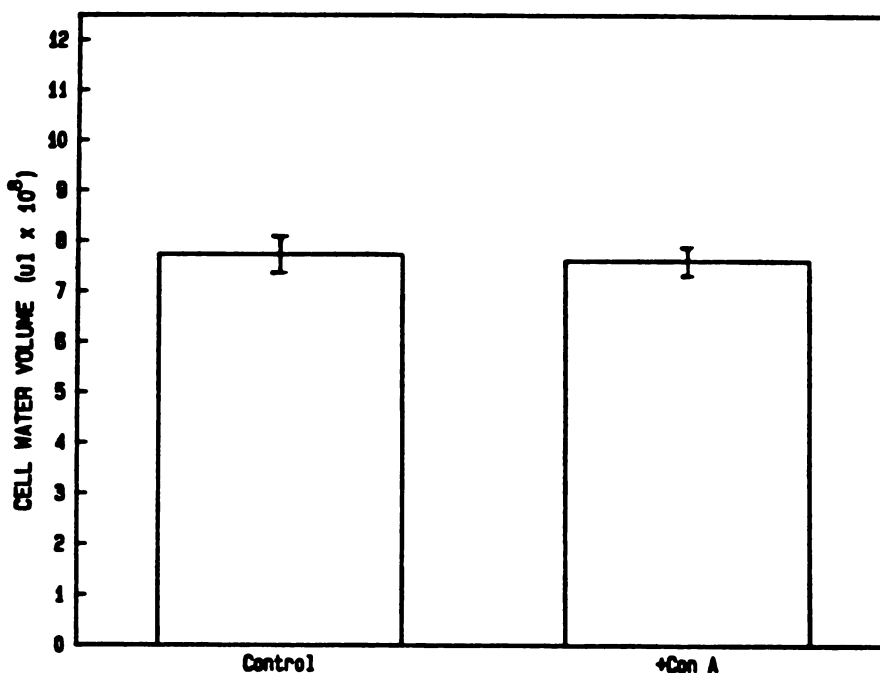


Figure 16: Cell Water Volume of Control and Con A-Stimulated Thymocytes

The cell water volumes of control cells and cells stimulated for 3 minutes with Con A were measured as described in Methods. Bars indicated standard deviations (n=8).

compared with the effects of WGA, a nonmitogenic lectin. In four trials, WGA was found to have no effect on TPP uptake. When cells were removed from the electrode and examined under the microscope, it was found that (1) no aggregates were observed in the absence of lectin, (2) many small aggregates (10-40 cells) were observed in the presence of 100 ug/ml Con A, and (3) many small aggregates as well as large aggregates (>100 cells) were observed in the presence of 100 ug/ml WGA. Although these results were not quantitated, it was clear

that WGA aggregated cells at least as much as Con A did and yet had no effect on TPP uptake. Therefore, it can be concluded that the effect of Con A on TPP uptake was independent of cell aggregation.

#### 4.3.2 Defining Optimal Conditions for Equilibrium TPP Uptake

The results of the various control experiments discussed above increased the likelihood that the observed change in the rate of TPP uptake was in fact due to a change in membrane potential. However, this putative change in potential could not be quantitated from a change in the rate of TPP uptake. This can only be accomplished by measuring steady-state distribution of the probe. Therefore, experiments were undertaken to define optimal conditions for establishing equilibrium between free and cell-associated TPP. Once this was accomplished, it would be possible to assess the quantitative relationship of TPP uptake to membrane potential in rabbit thymocytes.

For these studies, the more conventional radioisotope technique for measuring TPP uptake was used. This technique offered the capability of manipulating the incubation temperature and made possible the use of ionophores. Further, it was foreseen that the radioisotope technique would, at some point, be useful as a check on the TPP electrode. Accordingly, a method was adapted from the literature for measuring  $^3\text{H}$ -TPP uptake. Briefly, the method involves incu-



bating cells with TPP trace-labelled with  $^3\text{H}$ -TPP and at various times stopping the reaction by centrifuging aliquots of the cell suspension through a layer of silicon oil/mineral oil. In this way the cell-associated  $^3\text{H}$ -TPP could be efficiently separated from the free  $^3\text{H}$ -TPP. The method is described in detail in Methods.

#### 4.3.2.1 Effect of Temperature on TPP Uptake

As shown in Figure 17, the time course of TPP uptake by cells incubated at  $23^\circ\text{C}$  (solid lines) is distinctly different from that of cells incubated at  $37^\circ\text{C}$  (broken lines). The initial rate of TPP uptake is much greater in cells at  $37^\circ$  than in cells at  $23^\circ$ . The rate of TPP uptake into cells at  $37^\circ$  can be fit to a single exponential with a rate constant of  $.072\text{ min}^{-1}$  ( $t_{1/2} = 9.6\text{ min}$ ). TPP uptake in these cells reached equilibrium by 1 hour. In contrast, cells at  $23^\circ$  were still taking up TPP at 90 minutes and had by this time taken up approximately 20% more TPP than had cells at  $37^\circ$ .

#### 4.3.2.2 Effects of Tetraphenylboron

From the results in Figure 17 it can be seen that TPP uptake by rabbit thymocytes is a slow process which reaches equilibrium at  $37^\circ\text{C}$  by 60 minutes. Since the rate at which TPP fluxes across the cell membrane limits its usefulness in measuring rapid changes in membrane potential, efforts were

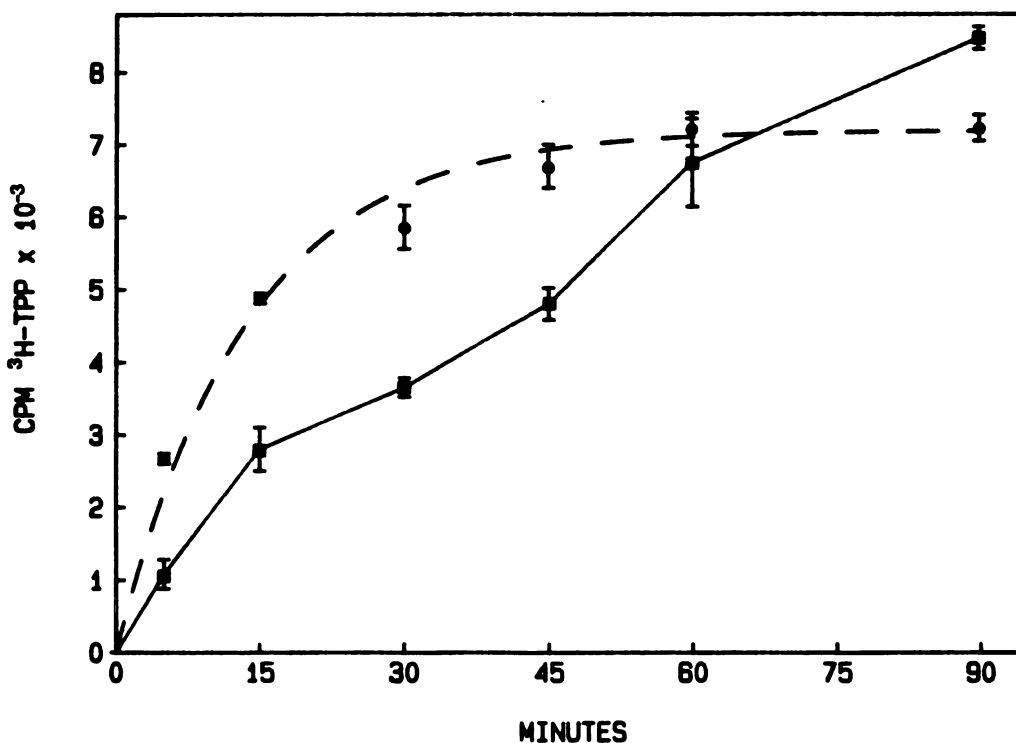


Figure 17: The Effect of Temperature on TPP Uptake

25  $\mu\text{M}$  TPP (.75  $\mu\text{Ci } ^3\text{H-TPP/ml}$ ) was added at time 0 to cells ( $1.5 \times 10^7/\text{ml}$ ) suspended in RPMI at  $23^\circ\text{C}$  (■) or  $37^\circ\text{C}$  (●). Cell-associated TPP (ordinate) was measured at various times (abscissa) as described in Methods. Points are the means of triplicate measurements (bars, S.D.). The time course at  $37^\circ\text{C}$  was fitted with a single exponential (broken line).

made to increase the rate of TPP uptake. As discussed above, tetraphenylboron increases the permeability of biological membranes to hydrophobic cations. Therefore, it might be expected that the time required for TPP uptake to reach equilibrium would be shortened by the addition of TPB to the incubation medium. The results of an experiment testing the

effect of TPB on the rate of TPP uptake are shown in Figure 18. In this experiment, the concentration of TPP was held constant at 25  $\mu\text{M}$ . TPP uptake was measured over a time course of 60 minutes in the absence of TPB and in the presence of 2 and 5  $\mu\text{M}$  TPB. Panel A shows the time course of uptake at 23 $^{\circ}$  C, and panel B shows the time course of uptake at 37 $^{\circ}$  C. It can be seen that TPB at all concentrations tested greatly enhanced the rate of TPP uptake at both temperatures. At 37 $^{\circ}$ , TPB at .5 and 2  $\mu\text{M}$  also had the effect of increasing the equilibrium level of TPP uptake by as much as 20%. The release of TPP in the presence of 5  $\mu\text{M}$  TPB by 60 minutes is probably due to the adverse effects of TPB on cell viability at concentrations greater than 2  $\mu\text{M}$  as reported by Cheng et al (136).

#### 4.3.3 TPP Uptake at Different Membrane Potentials

Membrane potential probes are generally used for one of two purposes; measuring the membrane potential in the steady state or detecting changes in membrane potential associated with cell activation. For measuring steady state potentials, it is important that there be an easily quantitated relationship between the signal and the membrane potential. Although not intuitively obvious, the importance of quantitation in detecting changes of membrane potential will become apparent (see Discussion). Since conditions had at this point been established for rapidly attaining steady-

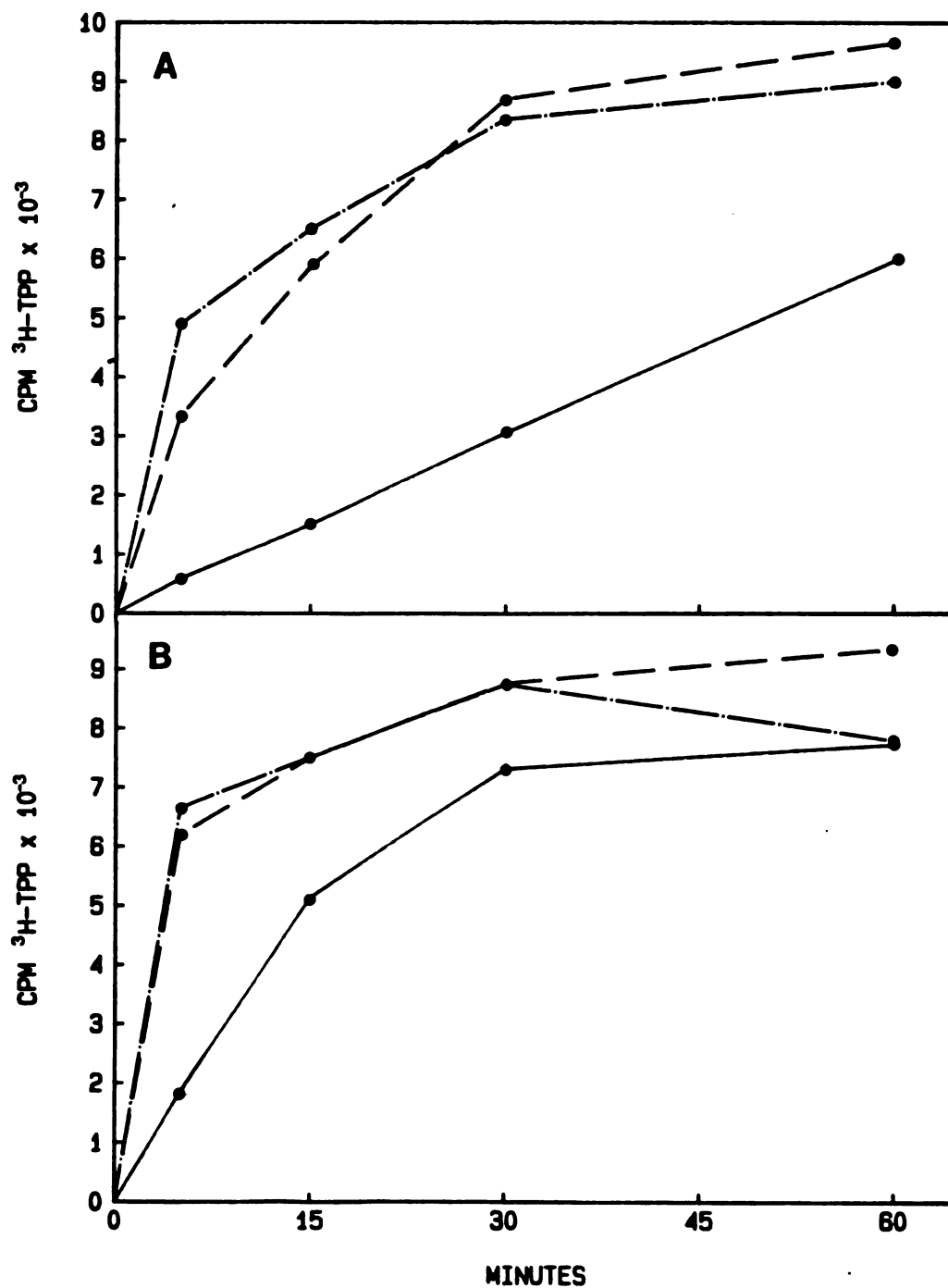


Figure 18: Effect of TPB on TPP Uptake

The following additions were made at time 0 to cell suspensions ( $1.5 \times 10^7$ /ml) incubated at  $23^\circ\text{C}$  (Panel A) or  $37^\circ\text{C}$  (Panel B): 25 uM TPP (solid line), 25 uM TPP + 2 uM TPB (dashed line), 25 uM TPP + 5 uM TPB (dash-dot line). TPP uptake (ordinate) was determined at times indicated

(abscissa). Points represent the means of triplicate measurements.

state TPP distribution, an assessment of the quantitative relationship of TPP uptake to cell membrane potential seemed possible. The approach to this problem was to manipulate the membrane potential by changing the composition of the suspension medium and then to measure TPP uptake under the various conditions.

If a cell in suspension can be treated as a simple two-compartment system in which compartment one, the cell, is separated from compartment two, the extracellular medium, by a semi-permeable membrane, the relationship between TPP uptake and membrane potential can be clearly defined. Assuming that TPP distributes passively across the plasma membrane (i.e.  $E_{\text{TPP}}=E_m$ ), at a given membrane potential ( $E_m$ ), TPP distribution between the two compartments will be described by the Nernst equation:

$$E_m = \frac{RT}{F} \ln \frac{[\text{TPP}]_e}{[\text{TPP}]_i}$$

In this equation R is the gas constant, T is temperature, and F is the Faraday constant. At 37° C the equation can be rewritten as:

$$E_m = 60 \log \frac{[\text{TPP}]_e}{[\text{TPP}]_i}$$

An approach to determining whether the assumption of a simple two compartment model is valid is to manipulate the membrane potential and measure TPP uptake at various potentials. In physiological solutions, a cell's membrane potential is a function of both the distribution and the relative permeabilities ( $P_x$ ) of the predominant ions, sodium, potassium, and chloride, as described by the Goldman-Hodgkin-Katz equation:

$$E_m = \frac{P_K [K]_e + P_{Na} [Na]_e + P_{Cl} [Cl]_i}{P_K [K]_i + P_{Na} [Na]_i + P_{Cl} [Cl]_e}$$

Although determining numerical values for all ionic permeabilities and intracellular concentrations in a single type of cell can be an arduous task, this equation can often be simplified for experimental purposes. For example, if sodium chloride in the medium is replaced with equimolar choline chloride, the terms containing Na drop out. (Biological membranes are essentially impermeable to choline.) Chloride is often assumed to be in or close to equilibrium so that chloride terms can also drop out, although this may not always be true. In addition, the dependence of membrane potential on K distribution can be enhanced by adding low concentrations of valinomycin to the medium. The effect of valinomycin, a potassium-specific carrier, is to increase the value of  $P_K$ . With these experimental manipulations and the assumption of chloride equilibrium, the Goldman-Hodgkin-Katz equation reduces to the Nernst equation:

$$E_m = \frac{RT}{F} \ln \frac{[K]_e}{[K]_i}$$

If [K] remains constant during the course of the experiment, the membrane potential ( $E_m$ ) will vary with the potassium concentration of the suspension medium. If the assumption of a simple two-compartment model is valid for describing TPP uptake into a cell, then it follows that (1) TPP uptake should also vary with the external potassium concentration and (2) TPP should distribute across the plasma membrane as according to the Nernst equation.

The effect of varying the external potassium concentration on TPP uptake in thymocytes is shown in Figure 19. At each potassium concentration, TPP uptake was measured in both the presence and absence of 2.2  $\mu$ M valinomycin. The effect of TPP concentration was also investigated; TPP uptake was measured at three different concentrations of TPP. It is evident from the figure that TPP uptake does in fact vary with external potassium concentration and is therefore related to the membrane potential. However, it is also evident, for reasons discussed below, that quantitation of the relationship is too complex to be fitted to a simple two-compartment model.

In the presence of valinomycin, when the extracellular potassium concentration is equal to the intracellular potassium concentration, the membrane potential should be equal to or very close to zero. Under these conditions, in the

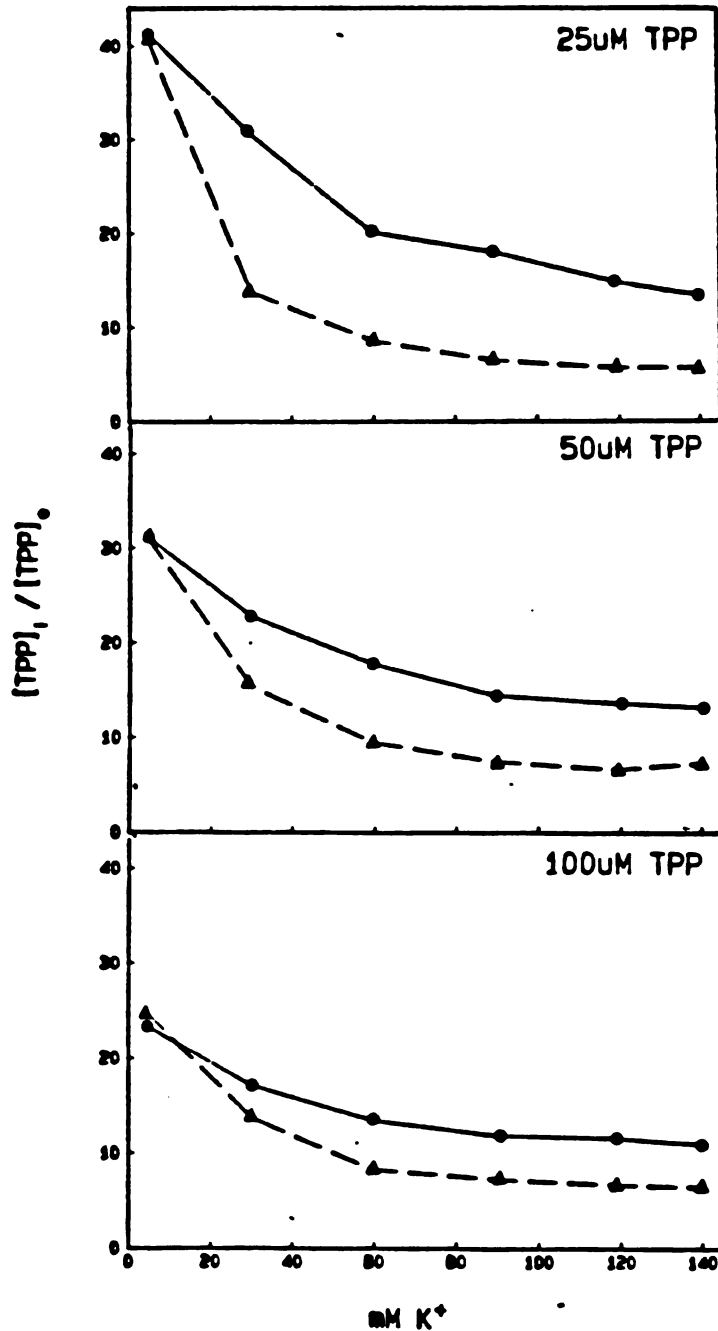


Figure 19: The Effect of Membrane Potential on TPP Uptake

The thymocyte membrane potential was varied by suspending cells ( $1.5 \times 10^7$ /ml) in medium containing different concentrations of potassium (abscissa). Sodium chloride was replaced with choline chloride and the combined concentration of potassium plus choline was equal to 150 mM. The TPP accumulation ratio (ordinate) was determined at three different TPP concentrations in the presence ( $\blacktriangle$ ) or absence ( $\bullet$ ) of 2.2 uM valinomycin by measuring  $^3H$ -TPP in the cell pellet and in the supernatant. All incubations were at 37°C for 45 minutes.



two compartment model, the ratio  $TPP_i/TPP_e$  should equal 1. The intracellular potassium concentration in lymphocytes is reported to be in the range of 110-150 mM. In this range of extracellular potassium concentrations, the cell-associated TPP in thymocytes is 5-7 fold more concentrated than the free TPP. Apparently, there is a third compartment in addition to the cytoplasm and the extracellular space. If TPP distribution is to be used as a measure of membrane potential, it now becomes necessary to quantitate TPP partitioning into this third compartment. Unfortunately, this becomes a complex problem, for the "third compartment" is likely to be composed of a number of compartments, including the various cell organelles and membranes. Quantitating the extent of TPP partitioning into these compartments at various membrane potentials is an imposing task. A number of approaches to this problem have been suggested and are reviewed in the Discussion.

Figure 19 also serves to illustrate a second problem in arriving at an estimate of  $E_m$  from TPP distribution. At a physiological potassium concentration, the TPP accumulation ratio is highly dependent on the extracellular free TPP concentration. This effect is probably the result of a combination of factors, including actual changes in  $E_m$  imposed by the TPP distribution itself (137), saturation of certain intracellular compartments, and changes in TPP conductance at higher concentrations (138). The relationship of TPP uptake

to concentration can be quite complicated. For example, Zaritsky et al. (137) have shown that the accumulation ratios of both TPP and TPMP in bacteria show discrete maxima at concentrations of 3 and 25  $\mu\text{M}$  respectively and decrease when the lipophilic ion concentration is shifted either higher or lower.

#### 4.3.4 Partitioning of TPP into Membranes Independent of Membrane Potential

In the course of this study, another observation was made which further complicates the use of TPP as a probe for membrane potential. It was found that TPP partitioning into membranes could be significantly increased under conditions at which the membrane potential remained at  $\emptyset$  (see Appendix 1 for details). This observation was made in acetylcholine receptor (AChR)-enriched membrane vesicles prepared from the electric organ of the marine ray Torpedo californica. The uptake was initiated by the addition of cholinergic ligands to the medium and was found to be a result of specific binding of the ligands to the AChR.

The extent of the ligand-induced TPP partitioning into the membranes was measured with the use of the TPP electrode. At maximum steady-state levels of TPP uptake, there was a reduction in the free TPP concentration of the medium equal to 1.6  $\mu\text{M}$ . The membrane protein concentration in this experiment was 2 mg/ml. The AChR constitutes approximately 50% of the total membrane protein. For the sake of compari-

son,  $2 \times 10^8$  thymocytes/ml represents an equivalent concentration of total cell protein.

The molecular nature of the ligand-induced change in the AChR-enriched membranes which in turn produced an increase in TPP partitioning is not fully understood. The partition coefficient for any ion is a function of the difference in free energy of the ion in the membrane and in the medium. For lipophilic ions, like TPP, the difference in free energy is determined by both the hydrophobic and electrostatic interactions of the ion with the solvating medium. Therefore, a change in either the hydrophobic or electrostatic properties of the membrane might cause a change in TPP partitioning. In these experiments, the change in the membrane was a result of binding of cholinergic ligands to the acetylcholine receptor. It seems reasonable to assume that binding of any ligand to a membrane receptor might cause similar changes. In such cases, measurements of TPP uptake would indicate changes in membrane potential where none may have occurred.

#### 4.3.5 Effects of Stimulation on Steady-State TPP Distribution

The results of the previous sections cast considerable doubt on the wisdom of attempting to use TPP as a quantitative probe of membrane potential in small lymphocytes. However, it still seemed reasonable to think that TPP could be used to detect and point the direction of a change in mem-

brane potential. If TPP partitioning is first allowed to reach equilibrium at the cell's resting potential, depolarization should then cause an overall release of TPP from the cell while hyperpolarization should result in a further uptake of TPP.

In order to make these measurements, both the  $^3\text{H}$ -TPP method and the TPP electrode method were used. A similar protocol for equilibrating the TPP was used for each method. This protocol was designed from information about the interaction of TPP and thymocytes which had been gained since the original observation of the Con A-induced change in the rate of TPP uptake. Accordingly, the preincubation was carried out at  $37^\circ\text{C}$  for 30 minutes in the presence of a low concentration of TPB. The continued presence of TPB, since it enhanced the rate of TPP partitioning, could also be expected to increase the rate of response of TPP to a membrane potential change.

Subsequent to the preincubation the cells were stimulated by the addition of Con A and TPP uptake was monitored over the course of the next ten minutes. In the case of the  $^3\text{H}$ -TPP method, this involved sampling of the cell suspension at fixed intervals. With the TPP electrode method, uptake was monitored continuously. In order to maintain the cells at  $37^\circ\text{C}$  on the electrode, the design of the electrode was modified to accommodate a  $37^\circ\text{C}$  water bath.

In the first set of experiments, the effect of Con A on steady-state TPP distribution was measured with the TPP electrode. Over the course of four separate experiments, a broad range of experimental parameters was tested. The cell density was varied from  $1.5 \times 10^7$ /ml to  $2.75 \times 10^8$ /ml. TPP concentrations from 15  $\mu$ M to 50  $\mu$ M were used with and without 2  $\mu$ M TPB. Cells were stimulated with 10 to 100  $\mu$ g/ml Con A. The stirring speed was varied from 20 to 120 rpm. The TPP uptake resulting from these various conditions generated recorded voltages of from 5 to 18 mV. The electrical noise in all experiments was less than 20  $\mu$ V. Con A, under all the conditions tested, had no effect on either release or uptake of TPP by rabbit thymocytes. A typical recording is shown in Figure 20.

In a second set of ten experiments, the effect of Con A on TPP uptake was measured with the radiolabelled TPP assay. In these experiments, cells were suspended at either  $6 \times 10^6$ /ml,  $1.5 \times 10^7$ /ml, or  $1 \times 10^8$ /ml. In six experiments, the TPP concentration was 25  $\mu$ M and the TPB concentration was 2  $\mu$ M. In the other four experiments, the concentration of TPP and TPB were reduced to 2 and .2  $\mu$ M respectively. Con A concentrations of 10 to 50  $\mu$ g/ml were tested. In agreement with the results from the TPP electrode measurements, Con A had no significant effect on TPP distribution in these experiments. The results of two experiments performed with different concentrations of TPP and TPB and different cell densities are shown in Table 5.

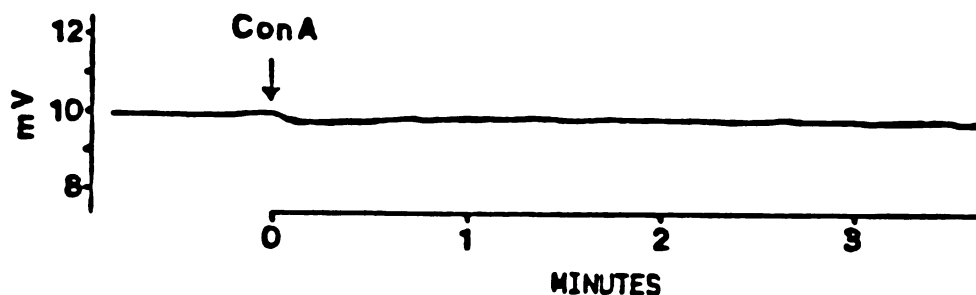


Figure 20: The Effect of Con A on TPP Uptake by Cells Equilibrated with TPP: The TPP Electrode

The electrical recording shown is from an experiment in which thymocytes at a density of  $5 \times 10^7$  /ml were preequilibrated with 15  $\mu$ M TPP in a 37 $^\circ$  C water bath. The cell suspension was then transferred to the TPP electrode chamber and stirred at 40 rpm. Con A was added to a final concentration of 20  $\mu$ g/ml (arrow).

TABLE 5

Effect of Con A on Uptake of  $^3$ H-TTP

[TPP]	Minutes After Addition of Con A					
	0	.5	1	2	5	10
	cpm					
25 $\mu$ M	5369 (150)	5308 (193)	N.D.	5305 (77)	5201 (359)	4955 (152)
2 $\mu$ M	15815 (826)	16378 (829)	16723 (558)	15778 (640)	15904 (469)	N.D.

Thymocytes were incubated at 37 $^\circ$  C for 30 minutes either at a density of  $1.5 \times 10^7$  cells/ml of RPMI containing 25  $\mu$ M TPP (.75  $\mu$ Ci  $^3$ H-TTP/ml) and 2  $\mu$ M TPB (top row) or at a density of  $6 \times 10^6$  cells/ml of RPMI containing 2  $\mu$ M TPP (2.5  $\mu$ Ci  $^3$ H-TTP/ml) and 0.2  $\mu$ M TPB (bottom row). Con A (10  $\mu$ g/ml) was then added and TPP uptake was measured at the indicated times as described in Methods. Values shown are the means (S.D. in parentheses) of triplicate points.

#### 4.3.6 Effects of TPP on the Physiological Status of the Cell

It has been well established that the fluorescent dyes disrupt certain cell functions. Similar deleterious effects of TPP might explain the results of the previous section in which Con A was found to have no effect on steady-state TPP distribution. Accordingly, the effect of TPP was first tested on thymidine incorporation. In Figure 21 it can be seen that TPP concentrations as low as 10  $\mu$ M inhibited the stimulation of thymidine uptake by Con A in thymocytes.

If the inhibitory effect of TPP on thymidine uptake were restricted to interference with the late stage of mitogenesis, TPP might still be a useful probe for detecting early membrane potential changes associated with activation. However, it was possible that TPP, as well as TPB, interfered with the very first steps in the activation process. This possibility was investigated by measuring the effects of TPP and TPB on two events reported herein to occur early in thymocyte activation -- phosphatidylinositol turnover and the early influx of potassium. The effect of the lipophilic ions on PI turnover was determined from the incorporation of  $^{32}$ P into PI in the presence of Con A. When 25  $\mu$ M TPP was added to thymocytes 1 minute before Con A, the Con A-induced increase in  $^{32}$ P incorporation was inhibited by 66%. 25  $\mu$ M TPP and 2  $\mu$ M TPB together inhibited incorporation by 94%. Similarly, when 25  $\mu$ M TPP and 2  $\mu$ M TPB were present during a 30 minute preincubation the stimulatory effect of Con A on  $^{86}$ Rb uptake was totally abolished.

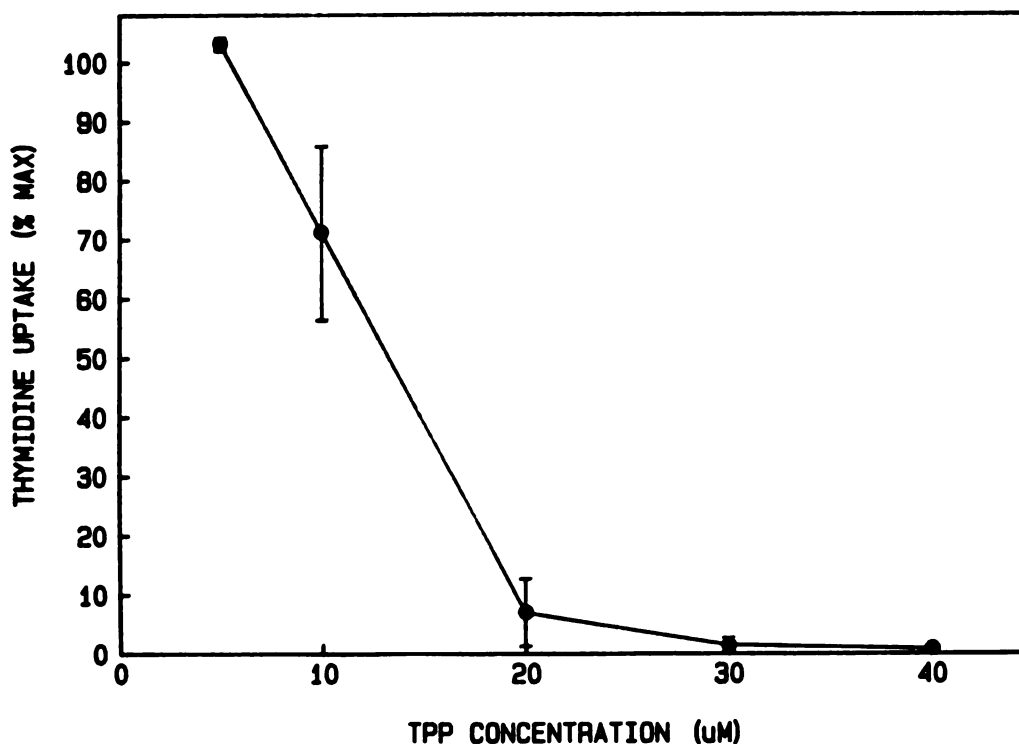


Figure 21: Effect of TPP on Thymidine Uptake

Thymocytes ( $8 \times 10^6$ /ml) were incubated with Con A ( $10 \mu\text{g}/\text{ml}$ ) for 72 hours with the indicated concentration of TPP (abscissa).  $^3\text{H}$ -thymidine was added for the last 4 hours of incubation. Thymidine uptake (ordinate) is expressed as the per cent of Con A-induced uptake measured in the absence of TPP. Points are the means of values from 4 experiments, each performed in triplicate. (Bars=S.E.M.)

#### 4.4 DISCUSSION

In the previous chapter it was reported that Con A caused an early transient increase in membrane permeability to potassium which was detectable by one minute and maximal at about two minutes. The experiments reported in this chapter were undertaken to determine whether the permeability change



was associated with a change in membrane potential. In the first experiments, Con A was found to cause a transient increase in the rate of TPP uptake which was detectable after about one minute and returned to baseline about five minutes later. This change in TPP uptake was consistent with the possibility that a membrane hyperpolarization occurred over the same time course as phosphatidylinositol turnover, calcium mobilization, and changes in potassium permeability. Control experiments indicated against several other explanations for the observed increase in the rate of TPP uptake. Surprisingly, however, in later experiments, Con A was found to have no effect on steady-state TPP distribution. Information gained in the course of this study as well as from recent reports from other laboratories concerning the use of lipophilic ions as membrane potential probes suggests some tentative solutions to these apparently paradoxical observations.

A major source of confusion in the use of lipophilic ions as membrane potential probes lies in the assumptions made in converting ion uptake to a quantitative estimate of  $E_m$ . As an example of the severity of this problem, three different laboratories have reported three widely disparate values of  $E_m$  for human neutrophils determined from the distribution of either TPMP or TPP: -26.7 mV (135), -45 mV (139), and -67 mV (140). Although some of this discrepancy undoubtedly derives from experimental technique, it is mostly due to the fact that each group used a different calculation.

The simplest assumption is that uptake of a lipophilic ion, e.g. TPP, into a cell is due solely to the cell's membrane potential. In this approach, the intracellular TPP concentration is calculated directly by dividing total cell-associated TPP by the total intracellular water volume (119,140).  $E_m$  is then calculated from the Nernst equation. The validity of this rather simplistic approach has been challenged by the observation that deenergized cells, in which the membrane potential should be equal to 0, concentrate TPP significantly higher (as much as 10-fold, see 141) than its free extracellular concentration (134,135,139,142, also Figure 19)..

The early model in which TPP was assumed to partition into a single potential-dependent intracellular compartment was then replaced by a two-compartment model. In this model, TPP partitioning into one compartment, the cytoplasm, was assumed to be potential-dependent while partitioning into a second compartment, the cell membranes, was assumed to be potential-independent. The potential-independent component was determined by measuring TPP uptake into cells incubated in a solution containing potassium at a concentration close to that of intracellular potassium with or without valinomycin.

Zaritsky et al. (137) have proposed a somewhat more elaborate version of the two-compartment model referred to as the "exponential mean model." This model takes into account the fact that one side of the plasma membrane is exposed to

the cytoplasm. Since the TPP concentration in the cytoplasm depends on the membrane potential, they suggest that TPP partitioning into the membrane would also assume a potential dependence and would be related to the exponential mean of the external and cytoplasmic concentrations.

It is now apparent that for most cells a two-compartment model is inadequate for quantitating TPP uptake since it ignores the contribution of cell organelles. Mitochondria in particular can be expected to constitute a significant TPP sink, even though the mitochondrial volume is only in the range of 4-12% of total cell volume. If TPP can be assumed to be an ideal lipophilic ion, the theoretical accumulation ratio of TPP into mitochondria is an exponential function of the mitochondrial membrane potential:

$$\frac{[\text{TPP}]_{\text{mi}}}{[\text{TPP}]_{\text{c}}} = e^{-E_{\text{mi}}/25}$$

where the subscripts mi and c refer to the mitochondria and cytoplasm respectively and  $E_{\text{mi}}$  is the mitochondrial membrane potential. Since  $E_{\text{mi}}$  has been determined to be in the range of -140 to -200 mV, TPP accumulated in mitochondria can be calculated to represent from 90% to 99% of the total intracellular free TPP. In fact, the potential-dependent partitioning of lipophilic cations into mitochondria is so great that several investigators have turned to using these probes to measure mitochondrial membrane potentials in whole cells (141,143,144). They have used  $^{86}\text{Rb}$  distribution to

ponent was determined by measuring TPP uptake into cells incubated in a solution containing potassium at a concentration close to that of intracellular potassium with or without valinomycin.

Zaritsky et al. (137) have proposed a somewhat more elaborate version of the two-compartment model referred to as the "exponential mean model." This model takes into account the fact that one side of the plasma membrane is exposed to the cytoplasm. Since the TPP concentration in the cytoplasm depends on the membrane potential, they suggest that TPP partitioning into the membrane would also assume a potential dependence and would be related to the exponential mean of the external and cytoplasmic concentrations.

It is now apparent that for most cells a two-compartment model is inadequate for quantitating TPP uptake since it ignores the contribution of cell organelles. Mitochondria in particular can be expected to constitute a significant TPP sink, even though the mitochondrial volume is only in the range of 4-12% of total cell volume. If TPP can be assumed to be an ideal lipophilic ion, the theoretical accumulation ratio of TPP into mitochondria is an exponential function of the mitochondrial membrane potential:

$$\frac{[TPP]_{mi}}{[TPP]_c} = e^{-E_{mi}/25}$$

where the subscripts  $mi$  and  $c$  refer to the mitochondria and cytoplasm respectively and  $E_{mi}$  is the mitochondrial membrane

make a rough estimate of the contribution of the cell membrane potential to total TPP uptake. Others have persisted in using lipophilic ions to measure cell membrane potentials by using a simultaneous equations approach (136,145). Inherent in this approach are the assumptions that TPP uptake into any subcellular compartment can be described by a partition coefficient and is not saturable.

A rather novel although decidedly less ambitious solution has been advanced in a recent report from Deutsch and Price (76). (It should be noted that Deutsch has published extensively in this field.) In that report, no attempt at correction of TPP uptake has been made. Instead, the authors "prefer to calculate a maximum possible upper limit of the potential." Table 6, which lists values for the membrane potential of rabbit thymocytes calculated from the data in the top panel of Figure 19 using several of the approaches described above, may serve to enhance the appeal of the Deutsch and Price solution. (See Appendix B for calculations.)

Implicit in all of the above models for quantitating TPP uptake is the assumption that TPP passively distributes across a cell membrane in such a way that the membrane potential is equal to the TPP equilibrium potential. The validity of this assumption has been challenged by the finding that yeasts are capable of actively taking up several lipophilic ions, including TPP, via the thiamine transport sys-

TABLE 6

Values for Thymocyte Membrane Potential Calculated from Different Models

$E_m$ (mV)	Model
-97	Single Compartment
-86	Two Compartments: High K
-93	Two Compartments: High K/Valinomycin
-69	Exponential Mean
-29	Simultaneous Equations: High K
-52	Simultaneous Equations: High K/Valinomycin

All calculations are based on the data obtained using 25  $\mu$ M TPP in the experiment shown in Figure 19 (top panel). In the 'Two Compartments' and 'Simultaneous Equations' models, the value for TPP uptake when  $E_m$  equals 0 was calculated from the amount of TPP taken up in either 140 mM K or 140 mM K plus valinomycin, as indicated. The calculations for the various models are in Appendix B.

tem (146). In addition, Ritchie (145) has presented evidence that two different species of giant-celled algae actively extrude TPMP against an electrochemical gradient, leading to a gross underestimate of the membrane potential. If similar transport systems are found to exist in other cell types, the use of lipophilic ions as quantitative probes of steady-state membrane potentials would be inappropriate for even the limited application suggested by Deutsch and Price (76).

If the lipophilic ions are not reliable as probes of the steady-state membrane potential, can they be used with confidence as qualitative indicators of the direction of a potential change? In the course of this study, it was found that the binding of ligand to the acetylcholine receptor stimulated TPP partitioning into membrane vesicles in the absence of any change in membrane potential. It was postulated that the ligand-induced redistribution of TPP was the result of charge movements within the membrane itself. Cheng et al. (136,147) saw a change in TPP distribution in the opposite direction, that is, TPP release, from hormone-stimulated rat adipocytes, and mistakenly concluded that a rapid depolarization of the membrane potential had occurred. After further investigation of this response, it has been found that the depolarization is localized to the mitochondria (148,149) while the plasma membrane potential may actually hyperpolarize (148). Therefore, the investigator must be aware that changes in the distribution of lipophilic probes can occur in the absence of any change in membrane potential and even in the presence of potential changes opposite to the direction indicated.

A second problem with using lipophilic ions to detect changes in membrane potential is that they may interfere with normal cell function. For example, glucose oxidation is inhibited in pancreatic islet cells suspended in solutions containing TPMP at concentrations of 1  $\mu$ M or greater

(142). 2  $\mu$ M TPP inhibits growth, macromolecular synthesis, and tumbling in bacteria (150). In the present study it was found that rabbit lymphocytes were adversely affected by prolonged incubation with TPP at concentrations of 10  $\mu$ M or greater as reflected by inhibition of thymidine uptake. Moreover, it was found that lipophilic ions had profound effects on two early events in thymocyte activation, phosphatidylinositol turnover and the stimulated increase in potassium permeability. Both of these events were inhibited in the presence of 25  $\mu$ M TPP. The addition of TPB caused an even greater inhibition of PI turnover. With regard to these findings, it should be noted that in the great majority of studies in which either TPP or TPMP has been used to measure membrane potentials of eucaryotic cells the probe concentration has been 10  $\mu$ M or higher, as high as 450  $\mu$ M (119).

In light of the above findings, what can be said about the role of membrane potential in rabbit thymocyte activation? Two different approaches to measuring Con A-induced changes in  $E_m$  have been taken in this study. With the first approach it was found that Con A caused an increase in the rate of TPP uptake. With the second approach Con A was found to have no effect on steady-state TPP distribution. If one assumes (1) that TPP distribution is governed solely by  $E_m$  and (2) that TPP does not affect cell function, the results of the two approaches lead to contradictory conclu-



sions concerning the effect of Con A on membrane potential, i.e. hyperpolarization vs. no change. However, the findings discussed above stress the need for reassessment of these basic assumptions and also suggest possible alternative explanations for the opposing observations. For example, the Con A-induced increase in the rate of TPP uptake (Figure 15) could have reflected stimulation of a transport system analogous to thiamine transport in yeast (146). Alternatively, Toyoshima and Osawa (151) have reported that mitogenic lectins cause a general increase in membrane fluidity. Resch (152) has provided evidence that this fluidity change is the result of an early stimulation of lysolecithin acyltransferase. Phenomena of this type could cause an increased rate of TPP uptake in the absence of any real change in membrane potential. It is interesting to speculate that the inhibitory effect of ouabain might be related to the close spatial and functional relationship of Na-K-ATPase and lysolecithin acyltransferase in lymphocyte membranes (153,154).

The results of the steady-state measurements (Figure 20 and Table 5), although in agreement with the observation by Deutsch and Price (76) that succinyl Con A had no effect on TPP distribution in human peripheral blood lymphocytes, can also be misleading. Changes in plasma membrane potential could have occurred but been obscured by opposing changes in mitochondrial membrane potential. TPP at equilibrium could

have reached intracellular concentrations sufficiently high to disrupt normal cell function. Finally, the limits of detection of these assays are difficult to assess since there is no clear way of determining how much of the TPP uptake is due to the membrane potential without an independent measurement.

In conclusion, since TPP appears to be such an unreliable probe, it is not possible at this time to say whether or not a change in membrane potential is an early event in activation of rabbit thymocytes. However, two other processes, phosphatidylinositol breakdown and an increase in the membrane permeability to potassium, have been found to be stimulated within one minute of activation. It is suggested that these changes may be related to the early calcium mobilization reported by others (1928). In contrast, no early change in either sodium permeability or Na-K-ATPase activity could be detected. Therefore, while the early stage in activation of rabbit thymocytes shares some striking similarities with a pattern of events frequently observed in other cell types, the differences are also noteworthy. It is hoped that the similarities will stimulate immunologists to take a broader view of lymphocyte activation and that the differences will be of interest to those studying cell activation in general.

## \_IBLIOGRAPHY

1. Putney, J.W., *Pharm. Rev.*, 30, 209-245 (1979).
2. Homma, Y., Onozaki, K., Hashimoto, T., Nagai, Y. and Takenawa, T., *J. Immunol.*, 129, 1619-1626, (1982).
3. Gallin, E.K., Wiederhold, M.L., Lipsky, P.E., and Rosenthal, A.S., *J. Cell. Physiol.*, 86, 653-662 (1975).
4. Gallin, E.K. and Gallin, J.I., *J. Cell Biol.*, 75, 277-289 (1977).
5. Naccache, P.H., Showell, H.J., Becker, E.L. and Shaafi, R.I., *J. Cell Biol.*, 73, 428-444 (1977).
6. Cockcroft, S., Bennett, J.P. and Gomperts, B.D., *FEBS Lett*, 110, 115-118 (1980).
7. Naccache, P.H., Showell, H.J., Becker, E.L. and Shaafi, R.I., *J. Cell Biol.*, 75, 635-649 (1977).
8. Korchak, H.M. and Weissman, G., *PNAS*, 75, 3818-3822 (1978).
9. Whitney, R.B. and Sutherland, R.M., *J. Cell. Physiol.*, 82, 9-20 (1974).
10. Freedman, M.H. and Raff, M.C., *Nature*, 255, 378-382 (1975).
11. Hesketh, T.R., Smith, G.A., Houslay, M.D., Warren, G.B. and Metcalfe, J.C., *Nature*, 267, 490-494 (1977).
12. Deutsch, C. and Price, M.A., *Biochim. Biophys. Acta*, 687, 211-218 (1982).
13. Mikkelsen, R.B. and Schmidt-Ullrich, R., *J. Biol. Chem.*, 255, 5177-5183 (1980).
14. Tsien, R.Y., Pozzan, T., and Rink, T.J., *Nature*, 295, 68-70 (1982).
15. Hokin, M. and Hokin, L.F., *J. Biol. Chem.*, 203, 967-977 (1953).

16. Hokin, M.R. and Hokin, L.E., J. Biol. Chem., 209, 549-558 (1954).
17. Hokin, L.E. and Hokin, M.R., Biochim. Biophys. Acta, 18, 102-110 (1955).
18. Hokin, M.R. and Hokin, L.F., Conference on Metabolism and Physiological Significance of Lipids, Ed. P.M.C. Dawson and Douglas N. Rhodes (1963).
19. Michell, R.H., Biochim. Biophys. Acta, 415, 81-147 (1975).
20. Berridge, M.J., Molec. Cell. Endocrin., 24, 115-140 (1981).
21. Allan, D. and Michell R.H., Biochem. J., 164, 389-397 (1977).
22. Brindley, D.N., Allan, D. and Michell R.H., J. Pharmaceut. Pharmacol., 27, 462-464 (1975).
23. Abdel-Latif, A.A., Akhtar, R.A. and Hawthorne, J.N., Biochem. J., 162, 61-73 (1977).
24. Habenicht, A.J.R., Glomset, J.A., King, W.C., Nist, C., Mitchell, C.D. and Ross, R., J. Biol. Chem., 256, 12329-12335 (1981).
25. Fain, J.N. and Berridge, M.J., Biochem. J., 178, 45-58 (1979).
26. Jones, L.M. and Michell, R.H., Biochem. J., 148, 477-485 (1975).
27. Prpic, V., Blackmore, P.F. and Exton, J.H., J. Biol. Chem., 257, 11323-11331 (1982).
28. Billah, M.M. and Lapetina, E.G., J. Biol. Chem., 257, 5196-5200 (1982).
29. Broekman, M.J., Ward, J.W. and Marcus, A.J., J. Clin. Invest., 66, 275-283 (1980).
30. Bell, R.L. and Majerus, P.W., J. Biol. Chem., 255, 1790-1792 (1980).
31. Kirk, C.J. and Michell, R.H., Biochem. J., 194, 155-165 (1981).
32. Fisher, D.B. and Mueller, G.C., PNAS, 60, 1396-1402 (1968).

33. Lucas, D.O., Shoehet, S.B. and Merler, E., J. Immun., 106, 768-772 (1971).
34. Betel, I., Martijnse, J. and van den Berg, K.J., Cell. Immun., 14, 429-434 (1974).
35. Maino, V.C., Hayman, M.J. and Crumpton, M.J., Biochem. J., 146, 247-252 (1975).
36. Hasegawa-Sasaki, H. and Sasaki, T., Biochim. Biophys. Acta, 666, 252-258 (1981).
37. Masuzawa, Y., Osawa, T., Inoue, K. and Nojima, S., Biochim. Biophys. Acta, 326, 339-344 (1973).
38. Fisher, D.B. and Mueller, G.C., Biochim. Biophys. Acta, 248, 434-438 (1971).
39. Resch, K., Receptors and Recognition, 1, 61-116 (1976).
40. Allan, D. and Michell, R.H., Biochem. J., 142, 591-597 (1974).
41. Hasegawa-Sasaki, H. and Sasaki, T., J. Biochemistry, 91, 463-468 (1982).
42. Jones, P.P., Cebra, J.J. and Herzenberg, L.A., J. Immun., 111, 1334-1347 (1973).
43. Wilson, B.S., Teodorescu, M. and Dray, S., J. Immun., 116, 1306-1312 (1976).
44. Tolbert, M.E.M., White, A.C., Aspry, K., Cutts, J. and Fain, J.N., J. Biol. Chem., 255, 4938-4944 (1980).
45. Lapetina, E.G., Billah, M.M. and Cuatrecasas, P., Nature, 292, 367-369 (1981).
46. Cockcroft, S., Bennett, J.P. and Gomperts, B.D., Nature, 288, 275-277 (1980).
47. Resch, K., Ferber, E., Prester, M. and Gelfand, F.W., Eur. J. Immun., 6, 168-173 (1976).
48. Hawthorne, J.N., Nature, 295, 281-282 (1982).
49. Cockcroft, S., Trends Pharm. Sci., 340-342 (1981).
50. Fain, J.N. and Garcia-Sainz, J.A., Life Sciences, 26, 1183-1194 (1980).
51. Berridge, M.J., Adv. Cyc. Nuc. Res., 14, 289-299 (1981).

52. Putney, J.W., *Life Sciences*, 29, 1183-1194 (1981).
53. Ohsako, S. and Deguchi, T., *J. Biol. Chem.*, 256, 10945-10948 (1981).
54. Serhan, C.N., Fridovich, J., Goetzl, E.J., Dunham, P.B. and Weissman, G., *J. Biol. Chem.*, 257, 4746-4752 (1982).
55. Kishimoto, A., Takai, Y., Mori, T., Kikkawa, U. and Nishizuka, Y., *J. Biol. Chem.*, 255, 2273-2276 (1980).
56. Takai, Y., Minakuchi, R., Kikkawa, U., Kaibuchi, K., Yu, B., Matsubara, T. and Nishizuka, Y., *Prog. Brain Res.*, 56, 287-301 (1982).
57. Ogawa, Y., Takai, Y., Kawahara, Y., Kamura, S. and Nishizuka, Y., *J. Immun.*, 127, 1369-1374 (1981).
58. Bell, R.L., Kennerly, D.A., Stanford, N. and Majerus, P.W., *PNAS*, 76, 3238-3241 (1979).
59. Billah, M.M., Lapetina, E.G. and Cuatrecasas, P., *J. Biol. Chem.*, 256, 5399-5403 (1981).
60. Coffey, R.G., Hadden, F.M. and Hadden, J.W., *J. Immun.*, 119, 1387-1394 (1977).
61. Takai, Y. and Nishizuka, Y., *Cold Spring Harbor Conf. Cell Prolif.*, 8, 237-249 (1981).
62. Takai, Y., Kibuchi, K., Matsubara, T. and Nishizuka, Y., *Biochem. Biophys. Res. Comm.*, 101, 61-67 (1981).
63. Quastel, M.R. and Kaplan, J.G., *Nature*, 219, 198-200 (1968).
64. Quastel, M.R. and Kaplan, J.G., *Exp. Cell Res.*, 62, 407-420 (1979).
65. Quastel, M.R. and Kaplan, J.G., *Exp. Cell Res.*, 63, 230-233 (1971).
66. Averdunk, R. and Lauf, P.K., *Exp. Cell Res.*, 93, 331-342 (1975).
67. Segel, G.B., Hollander, M.M., Gordon, B.R., Klemperer, M.R. and Lichtman, M.A., *J. Cell. Physiol.*, 80, 327-330 (1975).
68. Segel, G.B., Lichtman, M.A., Hollander, M.M., Gordon, B.R. and Klemperer, M.R., *J. Cell. Physiol.*, 88, 43-48 (1976).

69. Segel, G.B. and Lichtman, M.A., *J. Clin. Invest.*, 58, 1358-1369 (1976).
70. Iversen, J., *J. Cell. Physiol.*, 89, 267-276 (1976).
71. Hamilton, L.J. and Kaplan, J.G., *Can. J. Biochem.*, 55, 774-778 (1977).
72. Segel, G.B., Kovach, G. and Lichtman, M.A., *J. Cell. Physiol.*, 100, 109-118 (1979).
73. Averdunk, P., *Biochem. Biophys. Res. Comm.*, 70, 101-109 (1976).
74. Segel, G.B., Simon, W. and Lichtman, M.A., *J. Clin. Invest.*, 64, 834-841 (1979).
75. Deutsch, C., Price, M.A. and Johannson, C., *Exp. Cell Res.*, 136, 359-369 (1981).
76. Deutsch, C. and Price, M.A., *J. Cell. Physiol.*, 113, 73-79 (1982).
77. Gardos, G., *Biochim. Biophys. Acta*, 30, 653-654 (1958).
78. Poulsen, J.H. and Williams, J.A., *J. Physiol.*, 264, 323-329 (1977).
79. Owen, N.E. and Villereal, M.L., *PNAS*, 79, 3537-3541 (1982).
80. Skou, J.C., *Biochim. Biophys. Acta*, 23, 394-401 (1957).
81. Smith, J.V. and Rozengurt, E., *PNAS*, 75, 5560-5564 (1978).
82. Moolenaar, W.H., Mummery, C.L., van der Saag, P.T. and de Laat, S.W., *Cell*, 23, 789-798 (1981).
83. Koch, K.S. and Leffert, H.L., *Cell*, 18, 153-163 (1979).
84. Aceves, J. and Cereiido, M., *J. Physiol.*, 229, 709-718 (1973).
85. Villereal, M.L., *J. Cell. Physiol.*, 107, 359-369 (1981).
86. Averdunk, R., *Hoppe-Seyler's Z. Physiol. Chem.*, 353, 79-87 (1972).
87. Villereal, M.L., *J. Cell. Physiol.*, 108, 251-259 (1981).

88. Moolenaar, W.H., Yarden, Y., de Laat, S.W. and Schlessing, J., *J. Biol. Chem.*, 257, 8502-8506 (1982).
89. Naccache, P.H., Showell, H.J., Becker, F.L. and Shaafi, R.I., *J. Cell Biol.*, 73, 428-444 (1977).
90. Simchowitz, L., Spilberg, I. and de Weer, P., *J. Gen. Physiol.*, 79, 453-479 (1982).
91. Capiod, T., Berthon, B., Poggioli, J., Burgess, G.M. and Claret, M., *FEBS Lett.*, 141, 49-52 (1982).
92. Quastel, M.R. and Vogelfanger, I.J., *Cell. Immun.*, 2, 504-507 (1971).
93. Hodgkin, A.L. and Huxley, A.F., *J. Physiol.*, 117, 500-544 (1952).
94. Thompson, S.H., *J. Physiol.*, 265, 465-488 (1977).
95. Barrett, E.F. and Barrett, J.N., *J. Physiol.*, 255, 737-774 (1976).
96. Caroni, P. and Carafoli, E., *PNAS*, 79, 5763-5767 (1982).
97. Meech, R.W. and Standen, N.B., *J. Physiol.*, 249, 211-239 (1975).
98. Selinger, Z., Batzri, S., Eimerl, S. and Schramm, M., *J. Biol. Chem.*, 248, 369-372 (1973).
99. Selinger, Z., Eimerl, S. and Schramm, M., *PNAS*, 71, 128-131 (1974).
100. Parod, R.J. and Putney, J.W., *J. Physiol.*, 281, 371-381 (1978).
101. Burgess, G.M., Claret, M. and Jenkinson, D.H., *J. Physiol.*, 317, 67-90 (1981).
102. Weiss, S.J. and Putney, J.W., *J. Pharm. Exp. Ther.*, 207, 669-676 (1978).
103. Naccache, P.H., Showell, H.J., Becker, F.L. and Shaafi, R.I., *J. Cell Biol.*, 75, 635-649 (1977).
104. Putney, J.W., *J. Pharm. Exp. Ther.*, 198, 375-384 (1976).
105. Putney, J.W., *J. Physiol.*, 268, 139-149 (1977).



106. Meech, R.W. and Standen, N.B., *J. Physiol.*, 237, 43P-44P (1973).
107. Hawthorne, J.N., *Nature*, 295, 281-282 (1982).
108. Allwood, G., Asherson, G.L., Davey, M.J. and Goodford, P.J., *Immunology*, 21, 509-516 (1971).
109. Pallotta, B.S., Magleby, K.L. and Parrett, J.N., *Nature*, 293, 471-474 (1981).
110. Marty, A., *Nature*, 291, 497-500 (1981).
111. Yellen, G., *Nature*, 296, 357-359 (1982).
112. Maruyama, Y. and Petersen, O.H., *Nature*, 299, 159-161 (1982).
113. Colquhoun, D., Neher, E., Reuter, H. and Stevens, C.F., *Nature*, 294, 752-754 (1981).
114. Parod, R.J., Ph.D. Dissertation, Wayne State University (1979).
115. Holian, A., Deutsch, C.J., Holian, S.K., Daniele, R.P. and Wilson, D.F., *J. Cell. Physiol.*, 98, 137-144 (1979).
116. Cuff, J.M. and Lichtman, M.A., *J. Cell. Physiol.*, 85, 209-216 (1974).
117. Taki, M., *Mie Med. J.*, 19, 245-262 (1970).
118. Malofiejew, M., Kostrzewska, A. and Kowal, E., *Acta Haemat.*, 53, 138-144 (1975).
119. Deutsch, C.J., Holian, A., Holian, S.K., Daniele, R.P. and Wilson, D.F., *J. Cell. Physiol.*, 99, 79-94 (1979).
120. Rink, T.J., Montecucco, C., Hesketh, T.R. and Tsien, R.Y., *Biochim. Biophys. Acta*, 595, 15-30 (1980).
121. Kiefer, H., Blume, A.J. and Kaback, H.R., *PNAS*, 77, 2200-2204 (1980).
122. Mitchell, P., *Bioenergetics*, 4, 63-91 (1973).
123. Lantz, R.C., Elsas, L.G. and Dehaan, R.L., *PNAS*, 77, 3062-3066 (1980).
124. Douglas, W., Kanno, T. and Sampson, S., *J. Physiol.*, 188, 107-120 (1967).

125. Schneider, C., Gennaro, R., de Nicola, G. and Romeo, D., *Exp. Cell Res.*, 112, 249-256 (1978).
126. Utsumi, K., Miyahara, M., Okimasu, F., Sugiyama, K. and Inoue, M., *Physiol. Chem. Physics*, 11, 365-369 (1979).
127. Smith, T., Herlihy, J. and Robinson, S., *J. Biol. Chem.*, 256, 1108-1110 (1981).
128. Smith, T. and Robinson, S., *Biochem. Biophys. Res. Comm.*, 95, 722-727 (1980).
129. Simons, T., *Nature*, 264, 467-469 (1976).
130. Laris, P., Bahr, D. and Chaffee, R., *Biochem. Biophys. Acta*, 376, 415-425 (1975).
131. Hladky, S.B. and Rink, T.J., *J. Physiol.*, 263, 287-319 (1976).
132. Felle, H., Porter, J.S., Slayman, C.L. and Kaback, H.R., *Biochemistry*, 19, 3585-3590 (1980).
133. Lichtshtein, D., Kaback, H.R. and Blume, A.J., *PNAS*, 76, 650-654 (1979).
134. Korchak, H.M. and Weissman, G., *PNAS*, 75, 3818-3822 (1978).
135. Meldolesi, M.F., Aloj, S.M., Coon, H.G., Kaback, H.R., and Kohn, L.D., *PNAS*, 74, 2352-2356 (1977).
136. Cheng, K., Haspel, H.C., Vallano, M.L., Osotimehin, B. and Sonenberg, M., *J. Membrane Biol.*, 56, 191-201 (1980).
137. Zaritsky, A., Kihara, M. and Macnab, R.M., *J. Membrane Biol.*, 63, 215-231 (1981).
138. Ketterer, B., Neumcke, B. and Lauger, P., *J. Membrane Biol.*, 5, 225-245 (1971).
139. Seligmann, B.E. and Gallin, J.I., *J. Clin. Invest.*, 66, 493-503 (1980).
140. Mottola, C. and Romeo, D., *J. Cell Biol.*, 93, 129-134 (1982).
141. Deutsch, C., Erecinska, M., Werrlein, R. and Silver, I., *PNAS*, 76, 2175-2179 (1979).
142. Sehlin, J. and Taljedal, I., *Exp. Cell Res.*, 136, 147-156 (1981).

143. Scott, I. and Nicholls, D., *Biochem. J.*, 186, 21-33 (1980).
144. Hoek, J., Nicholls, D. and Williamson, J., *J. Biol. Chem.*, 255, 1458-1464 (1980).
145. Ritchie, R.J., *J. Membrane Biol.*, 69, 57-63 (1982).
146. Barts, P.W.J.A., Hoerberichts, J.A., Klaassen, A. and Borst-Pauwels, G.W.F.H., *Biochim. Biophys. Acta*, 597, 125-136 (1980).
147. Cheng, K., Groarke, J., Osotimehin, B., Haspel, H. and Sonenberg, M., *J. Biol. Chem.*, 256, 649-655 (1981).
148. Davis, R., Brand, M. and Martin, R., *Biochem. J.*, 196, 133-147 (1981).
149. Vallano, M.L. and Sonenberg, M., *J. Membrane Biol.*, 68, 57-66 (1982).
150. Zaritsky, A. and Macnab, R.M., *J. Bact.*, 14, 1054-1062 (1981).
151. Toyoshima, S. and Osawa, T., *J. Biol. Chem.*, 250, 1655-1660 (1975).
152. Ferber, E., Reilly, C.E. and Resch, K., *Biochim. Biophys. Acta*, 448, 143-154, 1976.
153. Szamel, M. and Resch, K., *Biochim. Biophys. Acta*, 647, 297-301 (1981).
154. Szamel, M., Schneider, S. and Resch, K., *J. Biol. Chem.*, 256, 9198-9204 (1981).

Appendix A

ACTIVATION OF ACH RECEPTORS CAUSES THE PARTITION  
OF HYDROPHOBIC CATIONS INTO POST-SYNAPTIC  
MEMBRANE VESICLES

ACTIVATION OF ACh RECEPTORS CAUSES THE PARTITION OF  
HYDROPHOBIC CATIONS INTO POST-SYNAPTIC MEMBRANE VESICLES

C. Geoffrey Davis<sup>\*</sup>, Shaul Hestrin<sup>+</sup>, Herbert Landahl<sup>‡</sup>,  
Adrienne S. Gordon<sup>\*</sup>, Ivan Diamond<sup>\*</sup>, and Juan I. Korenbrot<sup>‡+</sup>

Departments of Neurology<sup>\*</sup>, Pharmacology<sup>\*</sup>, Physiology<sup>+</sup>, and Biochemistry<sup>‡</sup>

University of California, School of Medicine  
San Francisco, California 94143

Address correspondence to:

Dr. Juan I. Korenbrot  
Department of Physiology  
Room S-762  
University of California, School of Medicine  
San Francisco, CA 94143

Telephone: (415) 666-1652

In the continued presence of cholinergic ligands, the acetylcholine receptor-channel complex (AChR) in postsynaptic membranes undergoes a sequence of conformational changes. Following the addition of the ligand, the receptor rapidly changes from a closed channel to an open channel conformation<sup>1</sup>. This is followed by a slow change to a nonconducting state which has been termed desensitization<sup>2</sup>. The process of desensitization has recently been resolved into two components, one with a time course of hundreds of milliseconds and one with a time course of seconds<sup>3</sup>. The lifetime of the open channel conformation<sup>4</sup> and the rate of desensitization<sup>5</sup> are both dependent on the magnitude of the membrane potential. Such dependence suggests that the ligand-induced conformational changes in AChR may involve the movement of electrical charges within the membrane<sup>6,7</sup>. Measurements of charge redistribution in AChR membranes following ligand binding have not been reported. Recently, measurements of changes in the membrane partition coefficient of hydrophobic ions have been used as a probe to detect electrostatic changes in both biological<sup>8</sup> and model<sup>9,10</sup> membranes. We report here that cholinergic ligands induce changes in the partition coefficient of the hydrophobic cation tetraphenylphosphonium (TPP) into AChR-enriched membranes. The time course and the stoichiometry of these TPP partition changes are accounted for in a kinetic model. The ion movement is a monitor of a molecular event which may be associated with the slow component of AChR desensitization.

AChR-enriched membrane vesicles were prepared from the electric organ of T. californica<sup>11</sup>. The AChR constitutes approximately 50% of the total protein in this preparation. The AChR specific activity in the membranes was about 3.5

nmole  $\alpha$ -bungarotoxin ( $\alpha$ BTx) binding sites/mg protein. The purified AChR-enriched membrane vesicles were washed in an electrolyte solution (see text Fig. 1) and resuspended in the same solution at a concentration of 6.5 - 7.0  $\mu$ M  $\alpha$ BTx binding sites. 150  $\mu$ l of the vesicle suspension containing 2  $\mu$ M TPP were placed in a recording chamber which permitted rapid stirring and continuous measurement of the concentration of free TPP in the suspending medium. Free TPP was measured with a TPP-selective electrode (Fig. 1). The AChR-enriched membrane vesicles steadily took up the free TPP from the medium over the first several minutes until the free TPP concentration attained a constant value. The sudden addition of cholinergic agonists resulted in a further rapid decrease of the free TPP concentration (Fig. 1B).

The time course of the ligand-induced TPP concentration decrease could be fit by a single exponential function. The value of the rate constant ( $k_{app}$ ) of this function is dependent upon both the choice of ligand and its concentration (Fig. 2A). The  $k_{app}$  increases as the ligand concentration increases up to a limiting value. The limiting value for acetylcholine (ACh) and carbachol is  $.42 \pm .06$  (mean  $\pm$ S.D.)  $\text{sec}^{-1}$ . For choline, the  $k_{app}$  is  $.160 \pm .052 \text{ sec}^{-1}$  at 10  $\mu$ M, the highest concentration tested. The  $k_{app}$  for the antagonist tubocurare is much smaller and reaches a limiting value of  $.032 \pm .010 \text{ sec}^{-1}$ . The extent of the decrease in free TPP concentration is also proportional to agonist concentration (fig. 2B). However, the limiting value of the concentration decrease was the same,  $1 \pm .05 \mu$ M TPP, for all agonists tested and  $0.49 \pm .06 \mu$ M for the antagonist tubocurare. The concentrations of ACh, carbachol, choline, and tubocurare producing half-maximal TPP decrease were determined to be 2.5, 3.5, 300, and 4.5  $\mu$ M, respectively.

The distribution of TPP across membrane vesicles has been extensively used in the past as a probe of the membrane potential due to the unequal free concentrations of permeant ions between the inside and the outside of vesicles<sup>12,13,14</sup>. However, the distribution of TPP, as that of other hydrophobic ions, might also reflect hydrophobic or electrical interaction of the ion with the membrane itself. For example, the membrane surface potential and the membrane boundary potential have been shown to affect the partition of hydrophobic ions into membranes<sup>6,9</sup>. In the experimental system we describe here the ionic transmembrane potential should be 0 mV since the ionic solutions across the membrane are symmetric. Moreover, addition of 0.1% digitonin, a detergent concentration which permeabilizes AChR-enriched membranes to small ions (unpublished observations), has no quantitative effect on the ligand-induced TPP concentration decrease. Therefore, the TPP concentration decrease we report reflects the uptake of TPP by the membrane vesicles as a result of direct interaction of the hydrophobic ion with the membrane itself and not as a result of changes in the macroscopic transmembrane potential.

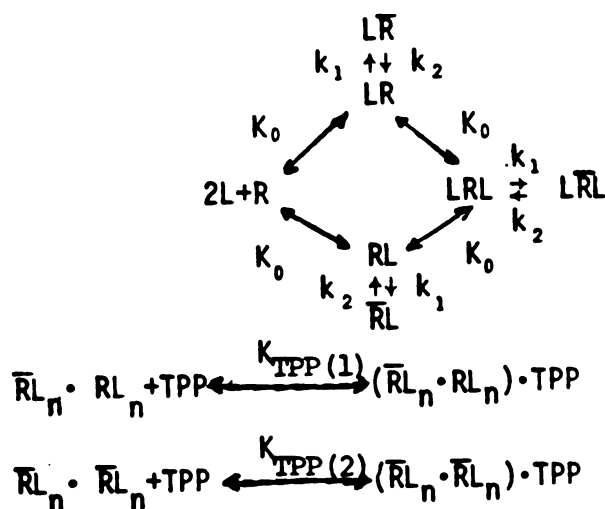
Since the effects of cholinergic ligands could arise from their interaction with either the AChR or membrane-bound acetylcholinesterase, we tested the effect of carbachol on the partition of TPP into red cell ghosts and Torpedo electroplax membranes containing only 0.5-1.0 nmole AChR/mg protein<sup>15</sup>. Red cell membranes contain acetylcholinesterase but not AChR<sup>16</sup>. Addition of 25-250  $\mu$ M carbachol to red cell ghosts at concentrations of either 2 or 4 mg. protein/ml had no effect on the free TPP concentration. The Torpedo membrane vesicles used for these control experiments also contained acetylcholinesterase but only 10-20% as much AChR as the membranes used in our standard assay. Addition of



100  $\mu\text{M}$  carbachol to these crude membranes suspended at 2 mg protein/ml induced an uptake of only 0.1  $\mu\text{M}$  TPP, approximately 10% of that measured in our typical experiment. These results indicate that the ligand-induced uptake of TPP into post-synaptic membranes is a result of ligand interaction with AChR.

If the TPP uptake is in fact a result of ligand binding to the AChR, it follows that it should be blocked by  $\alpha\text{BTx}$ , a highly specific inhibitor of AChR. Additions of  $\alpha\text{BTx}$  alone did not result in any TPP uptake. Figure 3 illustrates the extent of TPP uptake induced by a constant amount of carbachol added to membrane vesicles preincubated with various amounts of  $\alpha\text{BTx}$ . TPP uptake decreased with increasing amounts of  $\alpha\text{BTx}$ . The data of Figure 3 indicate that the extent of ligand-induced TPP uptake is dependent on the fraction of sites available for ligand binding. The ligand-induced TPP uptake is fully reversible; addition of a 25 molar excess of  $\alpha\text{BTx}$  to membranes first exposed to 100  $\mu\text{M}$  carbachol in the presence of TPP results in the release of the TPP specifically taken up. The  $\alpha\text{BTx}$ -induced TPP release occurs over several minutes, but the kinetics of this process was not studied in detail. Thus, the ligand-induced TPP uptake is a fully reversible process which arises specifically from the excitation of the AChR molecule.

To further analyze our data, we developed the following model. This model fits both the kinetic and steady-state data we have obtained.



The model consists of three sequential reactions. In the first reaction, the receptor, R, binds ligand, L, to either of two equivalent sites. The formation of this ligand-receptor complex has an equilibrium constant  $K_0$ . The ligand-receptor complex then spontaneously converts in a second reaction from the original state, R, to a new state,  $\bar{R}$ , with forward and backward rates  $k_1$  and  $k_2$ . It is the formation of the  $\bar{R}$  state that leads to the TPP uptake. However, in the model we consider the receptor molecules to exist as dimers in the membrane (see below), and the conversion of either of the monomers in the pair into the  $\bar{R}$  state is sufficient to develop the increased affinity for TPP. The interaction between the  $\bar{R}$  state and TPP, which leads to TPP uptake, is modeled to be a first order reaction with equilibrium constant  $K_{TPP}$ . We allowed the possibility that the TPP uptake resulting from only one monomer existing as  $\bar{R}$  and the uptake resulting from both monomers existing in the  $\bar{R}$  state may have different equilibrium constants,  $K_{TPP(1)}$  and  $K_{TPP(2)}$ .

In our experiments, the measured  $k_{app}$  defines the rate-limiting step in the sequence of reactions described above. We assume the rate-limiting step in the model to be the formation of the  $\bar{R}$  state. This assumption is justified by the fact that: 1) the rate of formation of RL has been measured by others to be diffusion limited<sup>17</sup> and 2) the rate of TPP uptake induced by the  $\bar{R}$  state is fast compared with the  $k_{app}$  measured for the same ligand at the same concentration. This uptake rate was determined by measuring the kinetics of TPP uptake following the sudden addition of the ion to vesicles preincubated with the ligand for one minute. The assumption in the model that TPP uptake is related

to the activation of receptor dimers is justified by the experimental fact that the stoichiometry of TPP uptake/ AChR activated had a limiting value of 0.5. This value was determined by titrating the TPP uptake with TPP (see Fig. 4). In this experiment, the concentration of AChR (6.5-7.0  $\alpha$ BTx sites) and carbachol (100  $\mu$ M) were held constant. The results were analyzed as a first-order reaction and the plateau value for TPP uptake was determined to be 1.6  $\mu$ M. Others have already suggested that AChR molecules may exist in the synaptic membrane as disulphide-linked dimers<sup>18,19</sup>. The model assumes that the transformation into an  $\bar{R}$  state of only one or of both of the elements of the dimer is sufficient to lead to TPP uptake. This assumption was necessary because models in which either both monomers or one monomer exclusively must convert to the  $\bar{R}$  state to induce TPP uptake generated solutions that did not fit the data.

The solution of the kinetic equations generated by the model above were fit to our experimental data by a least square regression routine to obtain estimates of the values of the kinetic parameters  $K_0$ ,  $k_1$ , and  $k_2$  for each of the agonists tested. The fit was made to six measurements of TPP uptake from .5 to 10 seconds as well as to the steady state value for each ligand concentration. Therefore, the total number of data points fit was 35 for carbachol and 28 for each of the other three ligands. The value of  $K_{TPP(2)}$  was experimentally determined to be 0.4  $\mu$ M from the data shown in Fig. 4. The best fit to the data was obtained under the assumption  $K_{TPP(1)} = K_{TPP(2)}$ , indicating that dimers with either one or two receptors in the  $\bar{R}$  state are equally effective in taking up TPP. (Setting  $K_{TPP(1)} = 0.8 \mu$ M increased the variance of the fit by 34%.) The

solutions predicted by the kinetic scheme are shown as continuous lines in Fig. 2A and 2B. Also shown are the experimental data. The values of the kinetic parameters used in the fits are shown in table 1 for the four ligands tested. The error of the fit is also shown in the table. It is particularly noteworthy that the values of the binding constant ( $K_0$ ) for all four ligands determined by fitting the TPP data are within the range of values reported for this constant by direct measurements of others<sup>20,21</sup>. The value of  $k_1$  is similar to that reported for other slow processes associated with the AChR including changes in the binding constant for toxin<sup>22,23</sup>, changes in intrinsic membrane fluorescence<sup>24</sup>, changes in fluorescence of agonist probes<sup>25</sup>, and the slow component of desensitization<sup>3</sup>.

An important question to be addressed in our results is whether the TPP ions are being bound by a component of the membrane such that their freedom of motion is restricted or partition into a motionally free pool, perhaps the same pool in which they reside prior to AChR activation. In collaboration with D. Cafiso and W. Hubbell, we have investigated this question with the use of a nitroxide labeled TPP analog (their spin label I). Cafiso and Hubbell have shown that the electron spin resonance (esr) spectrum of this molecule can identify motionally free and motionally restricted compartments in the membrane<sup>9</sup>. We found (not shown) that the esr spectrum of the TPP analog in AChR-enriched membranes exhibited the line shape characteristic of these molecules when they reside in a motionally free space of a model lipid bilayer, with only a very small fraction in a motionally restricted state. The esr spectrum confirmed that addition of agonist caused the partition of the TPP analog into the membrane and that the added TPP resided in the motionally free

pool. That is, the added TPP in the membrane is apparently not strongly bound by the AChR dimer.

The partition coefficient of TPP ions into a membrane, as any other ion, is a function of the difference in free energies in the aqueous and the membrane phases. The free energy of hydrophobic ions consists of terms that arise from both their electrostatic and their hydrophobic interactions with the solvating medium. The physical nature of the TPP uptake reported here remains to be precisely determined. However, since the slow component of AChR desensitization is a voltage dependent process that occurs on a time scale commensurate with the measured rates of the TPP uptake we observe, it may be that the hydrophobic cation partition we have reported here reflects a change of electronegativity in the membrane associated with AChR desensitization.

We are grateful to Ms. T. Thomas for excellent technical assistance. This work was supported by NIH grants NS 14742, EY 01586, and GM 27957, NSF grant BNS80-13074, and a grant and a fellowship (to S.H.) from the Muscular Dystrophy Association.

1. Katz, B. and Miledi, R., *Nature* 226, 962-963 (1970).
2. Katz, B. and Thesleff, S., *J. Physiol.* 138, 63-80 (1957).
3. Sakmann, B., Patlak, J. and Neher, E., *Nature* 28, 71-73 (1980).
4. Magleby, K.L. and Stevens, C.F., *J. Physiol.*, 223, 151-171 (1972).
5. Scubon-Muliere, B. and Parsons, R.L., *J. gen. Physiol.*, 71, 285-299 (1978).
6. Hodgkin, A.L. and Huxley, A.F., *J. Physiol.*, 117, 500-544 (1952).
7. Stevens, C.F., *Biophys. J.*, 22, 295-306 (1978).
8. Cafiso, D.S. and Hubbell, W.L., *Biophys. J.*, 30, 243-264 (1980).
9. Cafiso, D.S. and Hubbell, W.L., *Biochemistry*, 17, 187-195 (1978).
10. Andersen, O.J., Feldberg, S., Nakadomari, H., Levy, S., and McLaughlin, S., *Biophys. J.*, 21, 35-70 (1978).
11. Gordon, A.S., Davis, C.G., and Diamond, I., *Proc. natn. Acad. Sci. USA*, 74, 263-267 (1977).
12. Grinius, L.L., Jasaitis, A.A., Kadzouskas, Y.P., Lieberman, F.A., Skulachev, V.P. Topali, V.P., Tsofina, L.M., and Vladimirova, M.A., *Biochim. biophys. Acta*, 216, 1-12 (1970).
13. Ketterer, B., Neumcke, B., and Lauger, P., *J. Membrane Biol.*, 5, 225-245 (1971).
14. Schuldiner, D. and Kaback, H.R., *Biochemistry*, 14, 5451-5461 (1975).
15. Hartig, P.R. and Raftery, M.A., *Biochemistry* 18, 1146-1150 (1979).
16. Alles, G.A. and Howes, R.C., *J. biol. Chem.*, 133, 375-390 (1940).
17. Boyd, N.D. and Cohen, J.B., *Biochemistry*, 19, 5353-5358 (1980).
18. Chang, H.W. and Bock, E., *Biochemistry* 16, 4513-4520 (1977).
19. Hamilton, S.L., McLaughlin, M., and Karlin, A., *Biochemistry* 18, 155-163 (1979).
20. Boyd, N.D. and Cohen, J.B., *Biochemistry*, 19, 5344-5353 (1980).
21. Kasai, M. and Changeux, J-P., *J. Membrane Biol.*, 6, 1-23 (1971).
22. Quast, U., Schimerlik, M., Lee, T., Witzemann, V., Blanchard, S., and Raftery, M.A., *Biochemistry*, 17, 2405-2415 (1978).
23. Weber, M., David-Pfeuty, T. and Changeux, J.-P., *Proc. natn. Acad. Sci. USA*, 72, 3443-3447 (1975).

24. Bonner, R., Barrantes, F.J., and Jovin, T.M., *Nature*, 263, 429-431 (1976).
25. Heidmann, T. and Changeux, J.-P., *Eur. J. Biochem.*, 94, 255-279.
26. Shimbo, T., Kamo, N., Karihara, K., Kobatake Y., *Arch. Bioch. Biophys.* 187, 414-422 (1978).
27. Gold, G.H. and Korenbrot, J.I., *Proc. natn. Acad. Sci. USA*, 77, 5557-5561 (1980).
28. Moody, G.J., Oke, R.B., Thomas, J.D.R., *Analyst*, 95, 910-918 (1970).

Fig. 1 (A). Diagram of the TPP-selective membrane electrode, recording chamber and electrical configuration used to measure the concentration of TPP ions in the medium: The membrane electrode was prepared by incorporating a mixture of TPP and tetraphenyl boron (TPB) ions into a plasticized polyvinylchloride (PVC) matrix. 50 ml of 10  $\mu$ M TPP aqueous solution and 50 ml of 10  $\mu$ M TPB aqueous solution were mixed and extracted overnight into 100 ml of dichloroethane. Dichloroethane was then allowed to separate from the aqueous phase and rotoevaporated<sup>26</sup>. The remaining powder was dissolved in 50 ml of peroxide-free tetrahydrofuran<sup>27</sup>. 3 ml of this solution was mixed with 0.4 g of PVC, 1.5 ml of dioctyl adipate, and 10 ml of tetrahydrofuran. The resulting solution was poured over a 60 cm<sup>2</sup> glass surface. After solvent evaporation, a thin (approximately 100  $\mu$ m) TPP-selective membrane electrode film was obtained. Small (1.2 cm diameter) circles of membrane electrode were cut and glued onto a cylindrical support machined from PVC (dark cylinder in diagram). An acrylic cylinder (shaded cylinder in diagram) was glued on top of the PVC cylinder. A cylindrical chamber of 300  $\mu$ l volume was thus created, the floor of which was the membrane electrode. A motor-driven stirrer was used to minimize diffusion delays in the system. The recording chamber was mounted on the end of a U-shaped acrylic tube which contained a reference solution with a fixed concentration of TPP. Electrical recordings of the potential across the TPP membrane electrode utilized a high input impedance (1000 Mohms), low noise differential amplifier with a recording bandwidth of DC to 100 Hz (PARC, Model 113). The half-time of response of the electrode to a step change in TPP concentration was 150-300 msec. The selectivity of the electrode, measured by the mixed solution technique<sup>28</sup>, had the following values:  $K_{TPP/K^+} > 7.3 \times 10^{-7}$ ,



(B). Maximal TPP uptake: The points represent the average value of maximal TPP uptake at each ligand concentration. Symbols for the different ligands are the same as in 2A. In general, the range of the values measured is within 5% of the average. The lines represent solutions of the model given in the text.

Fig. 3. Effect of partial receptor blockade on carbachol-induced uptake of TPP: In four different experiments ( $\bullet, \circ, \blacktriangle, \triangle$ ), membranes were preincubated with various amounts of  $\alpha$ BTx for 60 minutes at 4<sup>o</sup>. Maximal TPP uptake (ordinate) in response to 100  $\mu$ M carbachol was then measured. In the graph, the amount of TPP uptake is shown as a function of free binding sites remaining after  $\alpha$ BTx treatment (abscissa). The number of free sites was measured by an <sup>125</sup>I- $\alpha$ BTx binding assay.

Fig. 4. Dependence of TPP uptake on TPP concentration: Membranes were equilibrated on the electrode with 2,4,6, or 8  $\mu$ M TPP. 100  $\mu$ M carbachol was then added and the maximal uptake of TPP was measured. Maximal TPP uptake (ordinate) is plotted versus the concentration of free TPP (abscissa).

Table 1. Parameters derived from TPP uptake using the sequential scheme described in the text.

\* Root mean deviation of the difference between calculated and observed values.

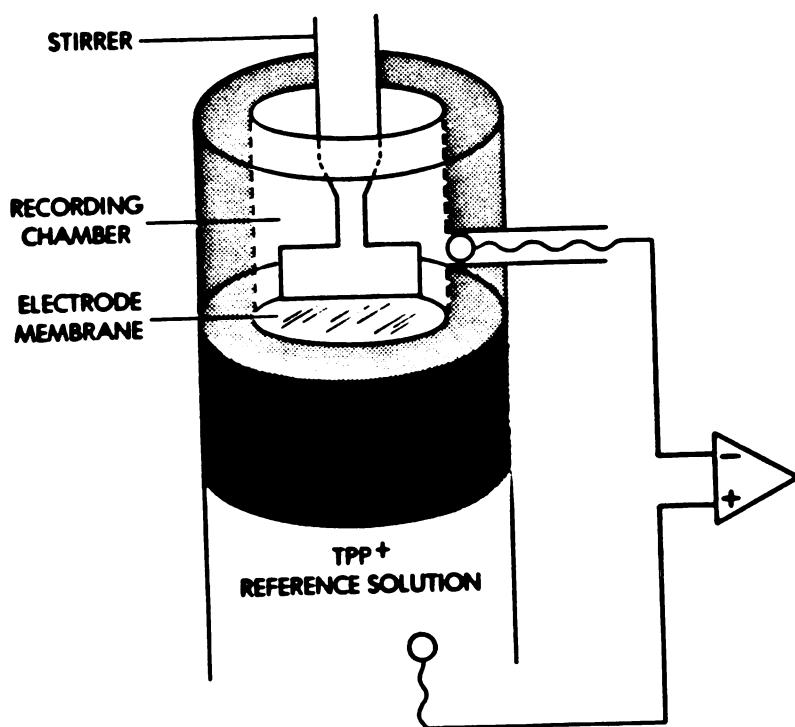




Fig. 1(B)

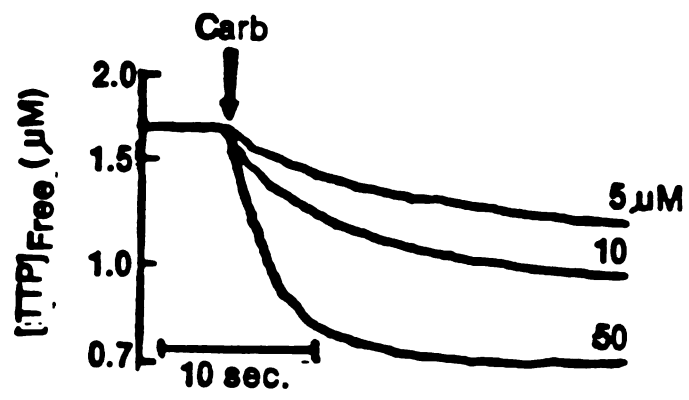


Fig. 2A

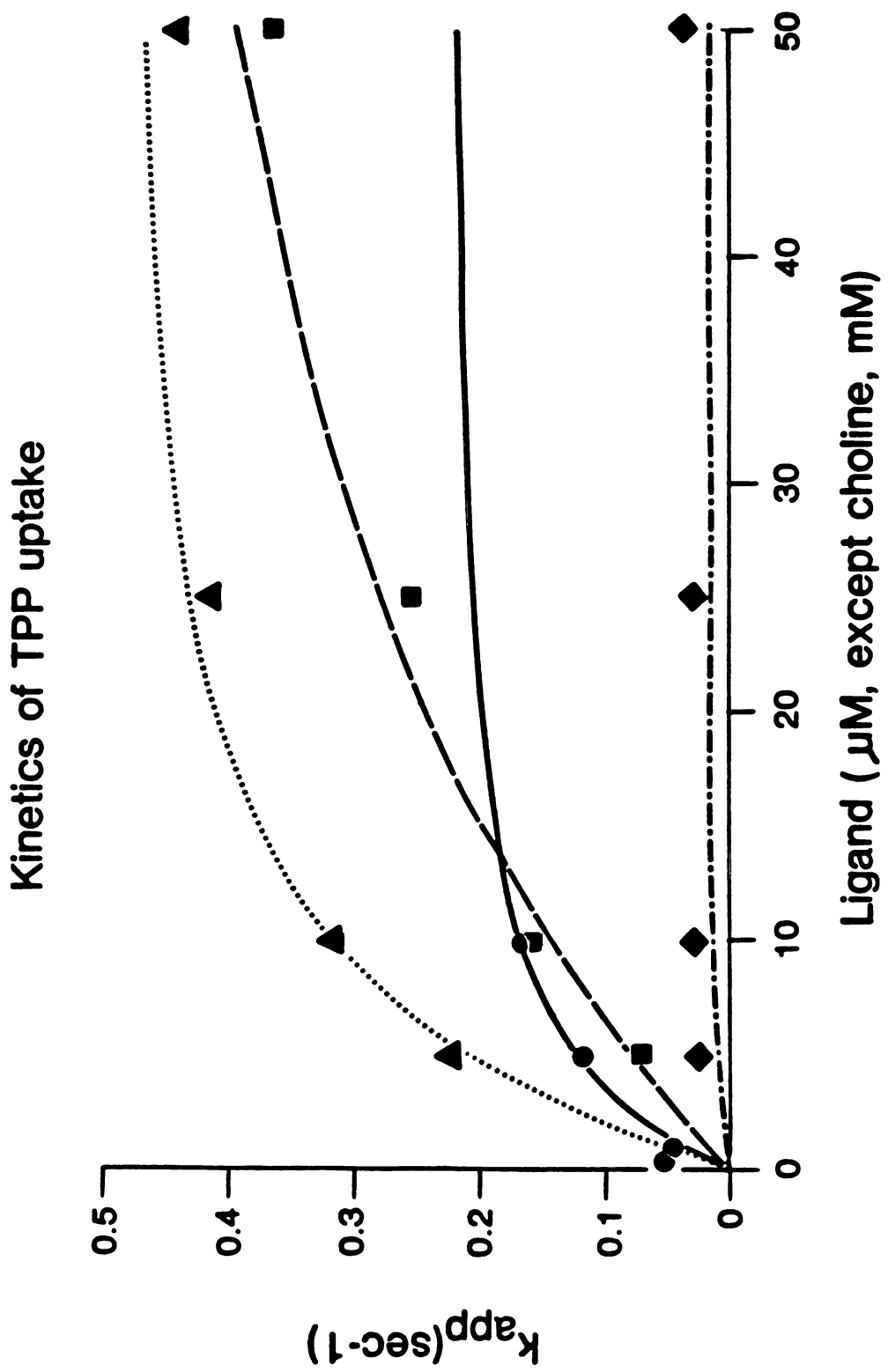
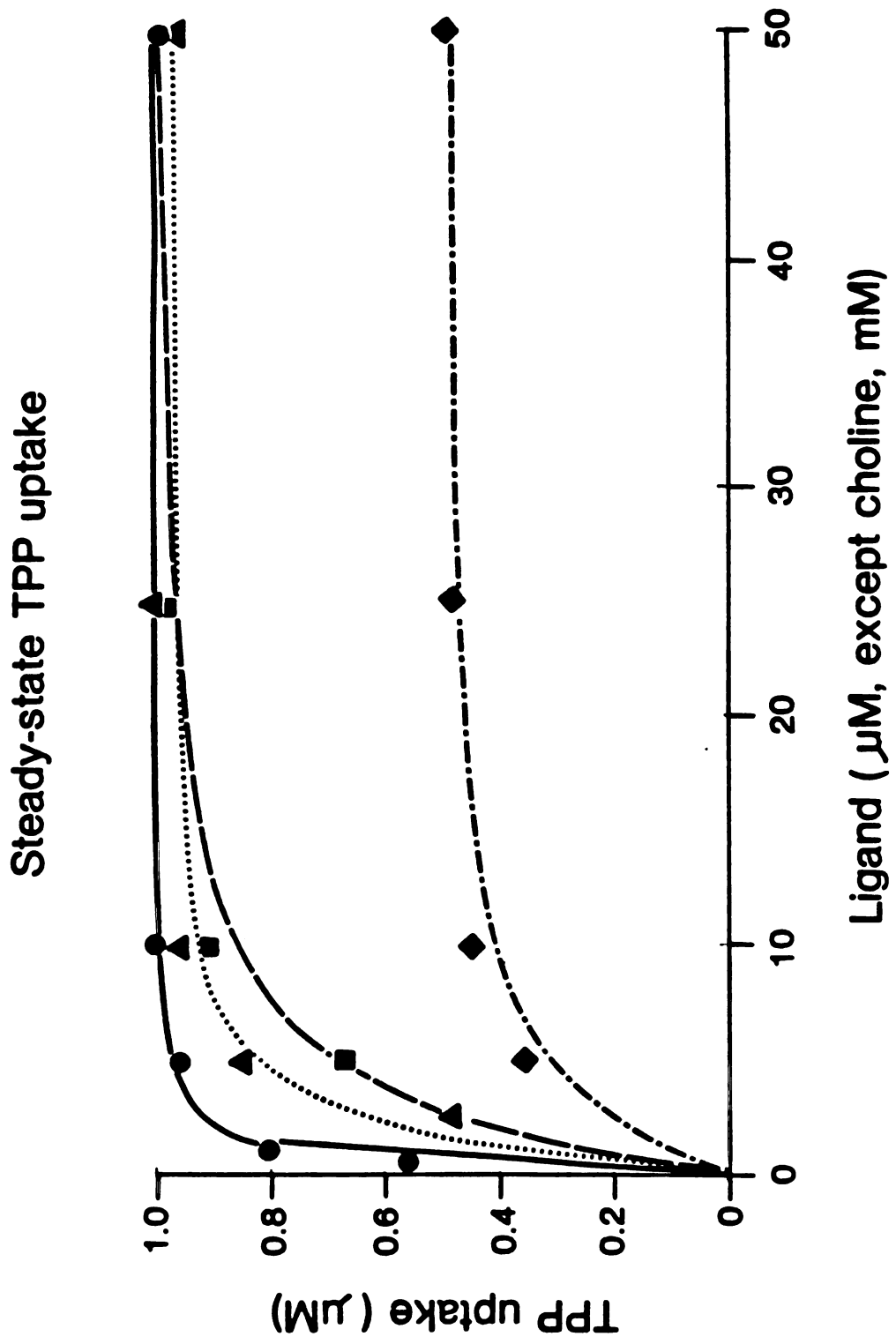
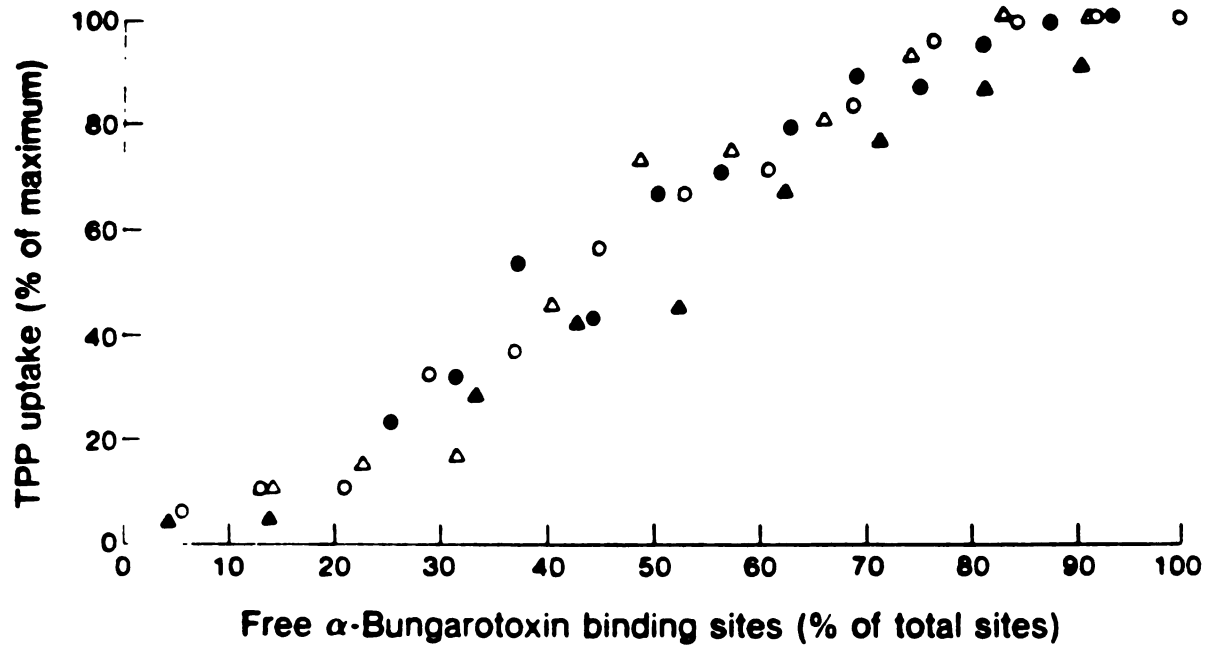
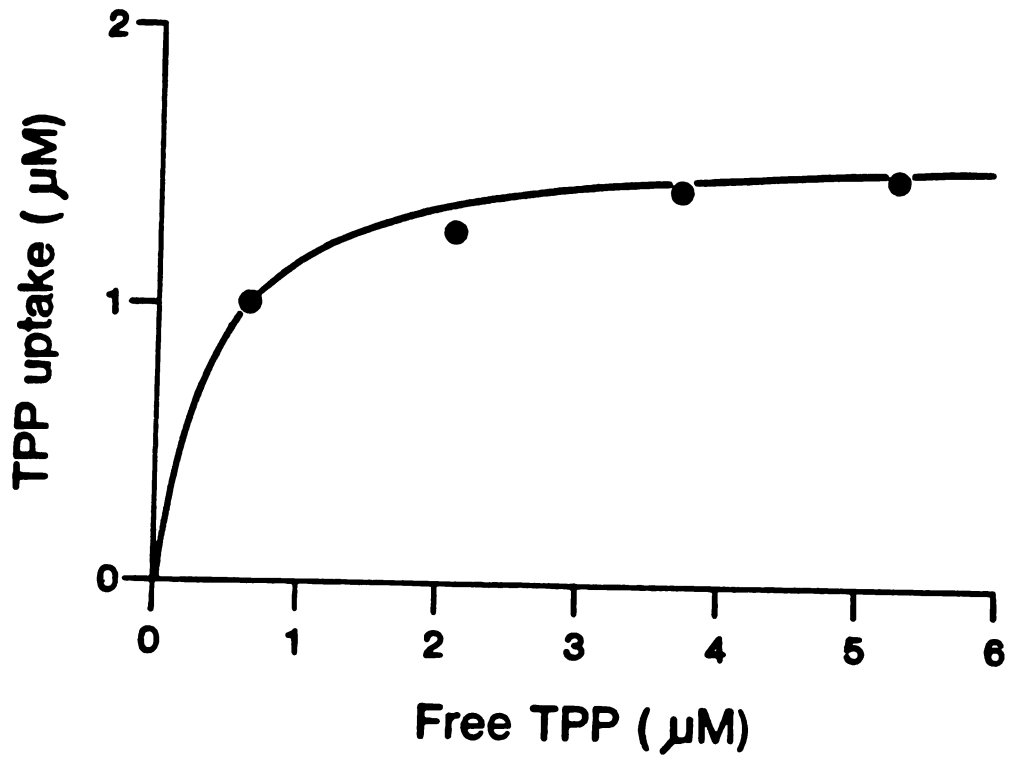


Fig. 2B









	$K_0$ ( $\mu\text{M}$ )	$k_1$ ( $\text{sec}^{-1}$ )	$k_2$ ( $\text{sec}^{-1}$ )
Carb	$55.7 \pm 4.5$	$0.201 \pm .006$	$0.042 \pm .003$
ACh	$10.4 \pm 1.7$	$0.176 \pm .009$	$0.077 \pm .008$
Choline	$10243 \pm 1067$	$0.081 \pm .004$	$0.020 \pm .001$
Curare	$3.2 \pm .2$	$0.006 \pm .0001$	$0.020 \pm .0004$

## Appendix B

### CALCULATIONS FOR TABLE 6

#### (1) One-Compartment Model

All cell-associated TPP is assumed to be potential dependent.

$$[\text{TPP}]_e = 25 \text{ uM} = 515 \text{ cpm/ul}$$

$$\text{TPP}_{\text{cell}} = 6122 \text{ cpm}$$

$$\text{total cell volume} = 0.29 \text{ ul}$$

$$[\text{TPP}]_i = 1029 \text{ uM}$$

$$E_m = -60 \log \frac{1029}{25} = -97 \text{ mV}$$

#### (2) Two-Compartment Model (High Potassium)

TPP partitioning into cell membranes is assumed to be potential-independent and to be equal to the amount of TPP taken up by cells suspended in 140 mM K.

$$\text{TPP}_{\text{cell}} = 6122 \text{ cpm} - 2040 \text{ cpm} = 4082 \text{ cpm}$$

$$[\text{TPP}]_i = 683 \text{ uM}$$

$$E_m = -60 \log \frac{683}{25} = -86 \text{ mV}$$

#### (3) Two-Compartment Model (High K/Valinomycin)

TPP partitioning into cell membranes is assumed to be potential-independent and to be equal to the amount of TPP taken up by cells suspended in 140 mM K + 2.2 uM valinomycin.

$$\text{TPP}_{\text{cell}} = 6122 \text{ cpm} - 829 \text{ cpm} = 5293 \text{ cpm}$$

$$[\text{TPP}]_i = 886 \text{ uM}$$

$$E_m = -60 \log \frac{886}{25} = -93 \text{ mV}$$

#### (4) Exponential Mean Model

This model takes into account the fact that TPP partitioning into the plasma membrane will be influenced by both the extracellular and intracellular TPP concentrations. If a linear potential drop across the membrane and a constant partition coefficient for TPP are assumed, then the mean TPP concentration in the plasma membrane is equal to the exponential mean of the internal and external concentrations,  $\bar{C} = ([\text{TPP}]_i - [\text{TPP}]_e) / \ln([\text{TPP}]_i / [\text{TPP}]_e)$ . Calculation of  $E_m$  by this method requires an iterative procedure described in detail in reference (137).

#### (5) Simultaneous Equations Model (High K)

TPP uptake is measured under physiological conditions and under conditions where the potential across the plasma membrane is equal to 0. Membrane potentials of intracellular compartments are assumed to remain constant. If the experi-

ment is set up such that the difference in  $[TPP]_e$  under the two conditions is negligible, then

$$E_m = -60 \log \frac{[TPP]_{i, \psi=E_m}}{[TPP]_{i, \psi=0}}$$

See Appendix of reference (145) for derivation of this model.

$$[TPP]_{i, \psi=0} = 1029 \text{ uM}$$

$$[TPP]_{i, \psi=E_m} = 341 \text{ uM}$$

$$E_m = -60 \log \frac{1029}{341} = -29 \text{ mV}$$

#### (6) Simultaneous Equations Model (High K/Valinomycin)

The same as model (5) except that the membrane potential is assumed to equal 0 when cells are suspended in 140 mM K + 2.2 uM valinomycin.

$$[TPP]_{i, \psi=0} = 1029 \text{ uM}$$

$$[TPP]_{i, \psi=E_m} = 139 \text{ uM}$$

$$E_m = -60 \log \frac{1029}{139} = -52 \text{ mV}$$



